The Texas Medical Center Library

DigitalCommons@TMC

The University of Texas MD Anderson Cancer Center UTHealth Graduate School of Biomedical Sciences Dissertations and Theses (Open Access)

The University of Texas MD Anderson Cancer Center UTHealth Graduate School of Biomedical Sciences

5-2015

INFLUX AND EFFLUX OF ADENINE NUCLEOTIDES FROM ERYTHROCYTES REGULATE OXYGEN TRANSPORT AND SYSTEMIC METABOLISM

William G. O'Brien III

Follow this and additional works at: https://digitalcommons.library.tmc.edu/utgsbs_dissertations

 Part of the Medicine and Health Sciences Commons

Recommended Citation

O'Brien, William G. III, "INFLUX AND EFFLUX OF ADENINE NUCLEOTIDES FROM ERYTHROCYTES REGULATE OXYGEN TRANSPORT AND SYSTEMIC METABOLISM" (2015). *The University of Texas MD Anderson Cancer Center UTHealth Graduate School of Biomedical Sciences Dissertations and Theses (Open Access)*. 559.
https://digitalcommons.library.tmc.edu/utgsbs_dissertations/559

This Dissertation (PhD) is brought to you for free and open access by the The University of Texas MD Anderson Cancer Center UTHealth Graduate School of Biomedical Sciences at DigitalCommons@TMC. It has been accepted for inclusion in The University of Texas MD Anderson Cancer Center UTHealth Graduate School of Biomedical Sciences Dissertations and Theses (Open Access) by an authorized administrator of DigitalCommons@TMC. For more information, please contact digitalcommons@library.tmc.edu.

The TMC LIBRARY Health Sciences Resource Center

INFLUX AND EFFLUX OF ADENINE NUCLEOTIDES FROM ERYTHROCYTES REGULATE OXYGEN TRANSPORT AND SYSTEMIC METABOLISM

by

William G. O'Brien III (Tre'), M.S.

APPROVED:

_____
Cheng Chi Lee, Ph.D.

_____
Diane Bick, Ph.D.

_____
Mikhail Bogdanov, Ph.D.

_____
Rodney Kellems, Ph.D.

_____
Richard Kulmacz, Ph.D.

APPROVED:

_____
Dean, The University of Texas
Graduate School of Biomedical Sciences at Houston

INFLUX AND EFFLUX OF ADENINE NUCLEOTIDES FROM ERYTHROCYTES REGULATE OXYGEN TRANSPORT AND SYSTEMIC METABOLISM

A

DISSERTATION

Presented to the Faculty of

The University of Texas

Health Science Center at Houston

and

The University of Texas

MD Anderson Cancer Center

Graduate School of Biomedical Sciences

in Partial Fulfillment

of the Requirements

for the Degree of

DOCTOR OF PHILOSOPHY

by

William G. O'Brien III (Tre'), M.S.

Houston, Texas

May, 2015

Dedication

I would like to dedicate this piece of work to my friends and family as without them, none of this is possible:

First and foremost, my parents, Gerry O'Brien and Patty Jackson for everything you have done and continue to do. I could easily write a dissertation on the ways each of you have impacted my life. Truly, the BEST parents a person could ever ask for (no hyperbole needed). Thank you so very much! I love you!

Next, my brother, Sean O'Brien. I am forever in your debt for the many years of extremely generous hospitality and amazing friendship/brotherhood you have showed me since I returned from university. Growing up, I never expected for my brothers to be also considered best friends as we didn't always get along when we were younger (boys will be boys). I have never been happier to have been proven wrong.

Next, my younger brother, Jeffrey O'Brien. Thank you for supporting me throughout all this time spent in graduate school and being my occasional sounding board. It has been a pleasure watching you grow into the man you are today. I am incredibly proud to be the older brother of such a talented man.

Lastly, my incredibly amazing group of friends that gave me the love and support needed for this grueling task of completing the Ph.D. Rassul Zarinfar, Christopher Dodd, Lindsey Bigelow, Todd Albrecht, Rita Sirrieh, Drew Dolino, Tikeshlia Williams, etc. Once again, I could easily write a dissertation devoted to all the people that have kept me afloat throughout this entire grueling process – but I am limited to a page.

I am an extremely lucky person to have everyone above's (and more) love and support and for that, I dedicate the past 5^{+} years of my life's work.

ACKNOWLEDGEMENTS

First and foremost, I would like to thank my boss, Dr. Cheng Chi Lee, for being absolutely fantastic as a mentor, boss, and friend. I was extremely lucky to have found such an understanding and dedicated scientist and person from which to learn from over the past 7 years as I worked towards my degrees. Thanks to you and the many lessons you taught me, I am a smarter, more developed person as I leave this school.

I would also like to thank my second boss, Dr. Zhaoyang Zhao, for all your help with my training, both in my experimental design and my writing. You have been a constant presence in the lab that I have been able to learn a great deal from and for that I am eternally grateful.

Next I would like to thank all previous and current members of my committees. Drs. Diane Bick, Michael Blackburn, Mikhail Bogdanov, Zheng Chen, Shane Cunha, William Dubinsky, Rodney Kellems, Richard Kulmacz, Ann-Bin Shyu, Henry Strobel, and Eric Wagner. I have been incredibly fortunate to have had the guidance of the brightest, most helpful group of advisors in my time here and without your input to constantly redirect me I would not be here today.

Along those same lines, I have spent a good portion of my time here in other people's labs, using your equipment and expertise to help me answer the questions my project was asking me. I would literally not be graduating without everyone's help and permission to use your specialized machinery. So for that I would like to thank the Blackburn, Bogdanov(Vitrac), Chen, Jayaraman, Jin, Kellems, Kulmacz, Tsai (Berka), Wagner, Xia(Song), and Zhu labs.

I would also like to thank the amazing BMB program/department. Having a home/family away from home helps pass the time and I have been incredibly grateful

for all the distractions provided by all the wonderful people I have had the pleasure to call friends and colleagues over the past 7 years. This includes all the administrators, faculty members, post docs, and especially the students.

Last but not least, I would like to thank the administrators over at GSBS. Past and present, the deans and office personnel have also been extremely helpful and friendly allowing me to take part in student governance and being my guiding lights when there was no apparent answer to the problem at hand.

There have been so many people over the years that have had an impact on my research life and as you can tell above, it takes way more than one person to be successful as a Ph.D. student. For this, I would like to send out the sincerest of thank yous. You are all the best!

INFLUX AND EFFLUX OF ADENINE NUCLEOTIDES FROM ERYTHROCYTES REGULATE OXYGEN TRANSPORT AND SYSTEMIC METABOLISM

William G. O'Brien III (Tre'), M.S.

Advisory Professor: Cheng Chi Lee, Ph.D.

Erythrocytes are responsible for ensuring a sufficient supply of oxygen to meet activity demands. The mammalian erythrocytes primarily modulate their oxygen-carrying capacity by varying the levels of organic phosphates, such as 2,3-BPG. In other organisms, such as fish, ATP instead of 2,3-BPG is used to modulate their erythrocyte's oxygen binding ability. Here, using a series of genetically modified mice, we investigated a previously unrecognized pathway of adenine nucleotide influx and efflux that modulates erythrocyte's oxygen binding ability and controls systemic metabolism. Our studies show that the loss of AMPD3 and CD73, two important enzymes in regulating AMP levels intra- and extra-cellularly, respectively, allows for an increase in sustained metabolic activity. We show that this increase in work capacity is linked to an increase in erythrocyte's intracellular ATP levels which modulates hemoglobin affinity for oxygen directly. Pharmacologically, we show that *Ampd3*$^{-/-}$*/Cd73*$^{-/-}$ mice display an enhanced hypometabolic phenotype in response to AMP administration. Our studies reveal that the hypometabolism is associated with a severe reduction in oxygen binding affinity that results from erythrocyte's uptake of AMP.

Table of contents

List of Illustrations

List of Tables

List of Abbreviations

2,3-BPG	2,3 Bisphosphoglycerate
A1a	Adenosine receptor isoform A
ADA	Adenosine deaminase
Ado	Adenosine
ADP	Adenosine diphosphate
AIHM	AMP-induced hypometabolism
AMP	Adenosine monophosphate
AMPD	AMP deaminase
AMPK	5’ AMP-activated protein kinase
ANT	Adenine nucleotide translocase
ATP	Adenosine triphosphate
BA	Bongkrekic acid
BSA	Bovine serum albumin
cAMP	5’-3’-cyclic AMP
CAT	Carboxyatractyloside
CBX	Carbenoxolone
CD39	Extracellular ATPase
CD73	5’-ectonucleotidase
CMP	Cytidine monophosphate
DMSO	Dimethyl sulfoxide
ENT	Equilibrative nucleoside transporter
GMP	Guanosine monophosphate
H_2S	Hydrogen sulfide

Hb	Hemoglobin
HPLC	High-pressure liquie chromatography
IMP	Inosine monophosphate
IP	Intraperitoneal
mTOR	Mammalian target of rapamycin
NO	Nitric Oxide
P2Y	Purinergic G protein-coupled receptor family
p50	pressure of oxygen with 50% hemoglobin oxygen saturation
pANT	Peroxisomal ANT
PBS	Phosphate buffered saline
PNX1	Pannexin 1
PI3K/AKT	Phosphatidylinositol 3-kinase/protein kinase-B
REM	Rapid eye movement
rpm	revolutions per minute
T_1AM	3-Iodothyronamine
T_a	Ambient temperature
T_b	Core body temperature
TAN	Tannic Acid
TBAP	Tetrabutylammonium phosphate
TCA	Tricarboxylic acid cycle (Krebs Cycle or citric acid cycle)
TCA	Trichloroacetic acid
TLC	Thin-layer chromatography
VDAC	Voltage gated anion channel
VO_2	Volume of oxygen consumed

1. Introduction

1.1. Metabolism and Metabolic Rate

An organism's metabolic control is a key factor in ensuring survival; therefore, metabolism is highly regulated both on a systemic level and a cellular level to ensure optimal utilization of energy. The main regulation of systemic metabolism is believed to be controlled by the central nervous system, with a majority of this control coming from the peripheral signals interacting with the hypothalamus (Nasrallah and Horvath, 2014, Williams and Elmquist, 2012, Levin and Sherwin, 2011, Pocai et al., 2005). On the cellular level, there are numerous pathways (ex. AMPK, mTOR and PI3K/AKT, etc.) that are tightly regulated depending on the energy status and metabolic demand of the individual cell (Albert and Hall, 2014, Wullschleger et al., 2006, Gomes and Blenis 2015). With these various levels of regulation, each individual maintains a basal metabolism or resting metabolic rate, which determines how quickly an individual uses energy supplies to sustain basic functions. For example, during exercise, muscle cells need two main components in order to maintain the high energy demand: more fuel substrates and more oxygen for the cells to increasingly produce more ATP (Felig and Wahren, 1975). This change in supply is mediated by a vascular signal to dilate the vessels upstream of the site of demand (Goldman et al., 2012). By contrast, during the basal metabolism, an individual can experience a drop in metabolic rate either transiently, such as during rest (Heldmaier et al., 2004), or for an extended period of time, as is the case in animals that undergo hibernation or daily torpor, two forms of hypometabolism observed in nature (Heldmaier and Ruf, 1992).

1.2. Natural Hypometabolism

Natural hypometabolism is a physiological response that occurs in both endo- and ectotherms. However, since endotherms maintain their core body temperature at about 37°C, the energy demand of a similarly sized endotherm is at least eight times higher than that of an ectotherm (Else and Hulbert 1981). Hence under metabolic stress, the potential benefit an endotherm could receive from entering hypometabolism is significantly greater than for an ectotherm whose body readily adapts to ambient temperatures. As illustrated in Figure 1, deep hypometabolism has been observed in many different orders of mammals, including some primates.

Among mammals, hypometabolism is generally classified into two categories, hibernation and daily torpor, based on the severity and length of hypometabolism (Heldmaier et al., 2004). Both hibernation and daily torpor are characterized by four stages (Figure 2): entrance, maintenance, arousal, and euthermia (Heldmaier et al., 2004). Entrance is characterized by a sharp drop in metabolic rate that is followed by a gradual decline in core body temperature. Once the metabolic rate and body temperature have reached a nadir, the animal is considered to have entered the maintenance stage. The maintenance stage can last from many days to weeks for various cases of hibernation but only lasts hours for daily torpor. Typically, hibernators achieve greater drops in metabolic rate with lower core body temperatures than animals undergoing daily torpor (Geisner and Ruf 1995, Lovegrove et al., 1999, Wilz and Heldmaier 2000). In the maintenance phase, each animal species has an optimal range of ambient temperatures that allow for the most efficient metabolism during a hypometabolic bout (Figure 3). Lowering of T_b beyond optimal range can increase metabolic rate. At the end of the maintenance phase, the animals enter the arousal phase where a sharp rise in metabolic rate is followed by an

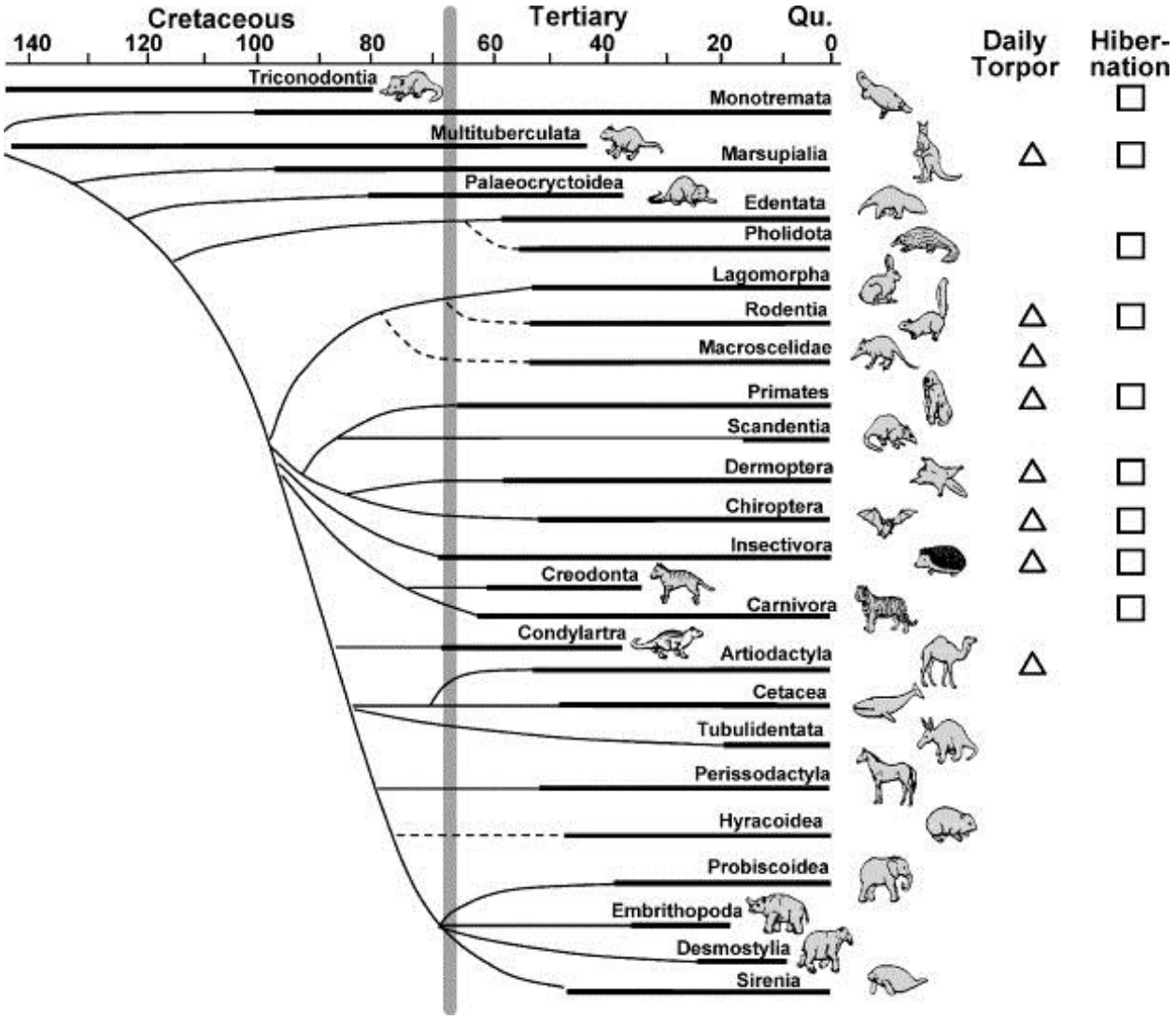

Figure 1. Daily torpor and/or hibernation among mammalian orders. Figure originally published by Heldmaier G, Ortmann S, Elvert R. Natural hypometabolism during hibernation and daily torpor in mammals. *Respir Physiol Neurobiol*. Aug 12;141(3):317-29 (2004) and reprinted with permission from Elsevier.

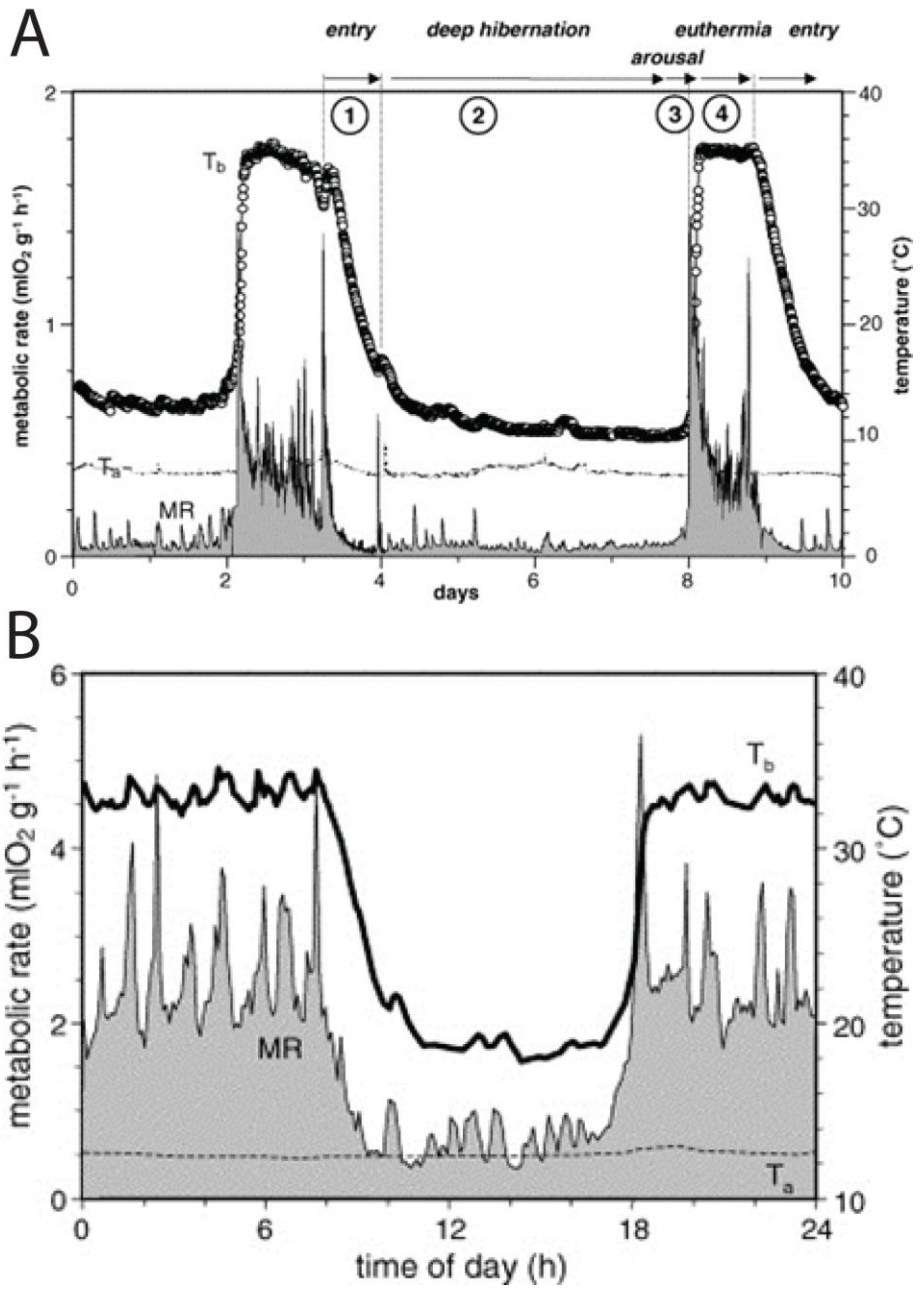

Figure 2. Variations in metabolic rate and body temperature (Tb) during hibernation in an Alpine marmot (A) and daily torpor in a Djungarian hamster (B). The four stages (entrance, maintenance, arousal, and euthermia) are labeled in A) and are clearly apparent in B). Figures originally published by Heldmaier G, Ortmann S, Elvert R. Natural hypometabolism during hibernation and daily torpor in mammals. *Respir Physiol Neurobiol*. Aug 12;141(3):317-29 (2004) and reprinted with permission from Elsevier.

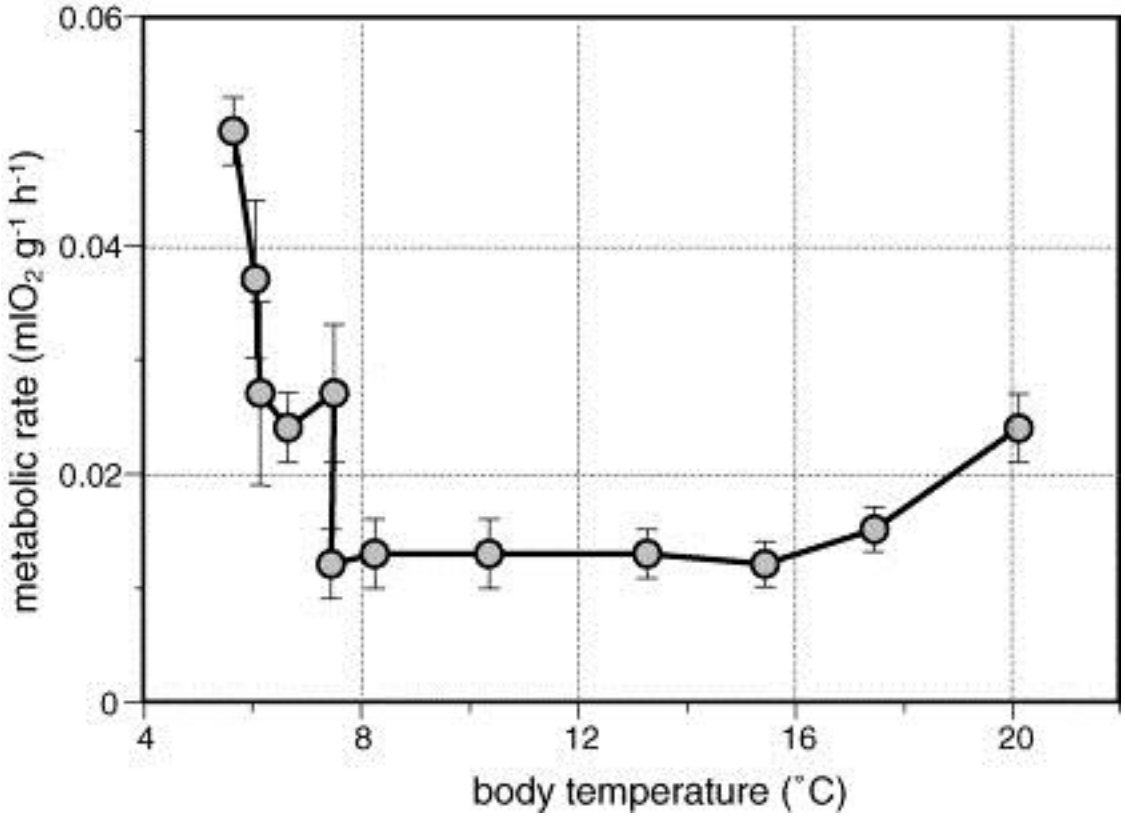

Figure 3. Effect of environmental temperature on metabolic rate in a hibernating marmot showing a range of optimal hibernating temperature. Originally published by Heldmaier G, Ortmann S, Elvert R. Natural hypometabolism during hibernation and daily torpor in mammals. *Respir Physiol Neurobiol*. Aug 12;141(3):317-29 (2004) and reprinted with permission from Elsevier.

increase in core body temperature (Heldmaier et al., 2004). Upon returning to an euthermic temperature, the animal enters the fourth stage, euthermia, where the animal maintains normal euthermic functions either for a day or two (hibernators) or many hours (daily torpor) before beginning the next hypometabolic bout. These arousals from hibernation are very taxing on the energetic reserves of the animal; it has been estimated that ~70% of the energy used during a hibernation season is spent on the arousal and euthermic phases (Heldmaier et al., 1993). While the need for arousal can be eliminated when hibernators are kept at warm (>30°C) ambient temperatures (Dausmann et al., 2005), some investigators believe arousal is a necessary phase of a hibernation bout (Humphries et al., 2003, Carey et al., 2003). There are many hypotheses to explain these energetically costly arousal bouts: from a need to get REM sleep (Daan et al., 1991), to preventing damage to the central nervous system (Strijkstra et al., 2003), and replenishing depleted energy storage (glycogen) and some proteins of the mitochondrial electron transport chain (Carey et al., 2003).

It has been hypothesized that the initiation of a torpor bout is the result of a suppression of the metabolic rate, and that the drop of the core body temperature is a result of a change in the body's thermostat set point, with no change in the organism's thermoregulation (Heller et al., 1977). This active suppression of the metabolic rate is of particular interest as it was postulated to be the trigger for natural hypometabolism, but the underlying mechanism is unknown (Heldmaier et al., 2004). It has been proposed that metabolic suppression could be achieved via two mechanisms that are not mutually exclusive: a decrease in ATP creating processes and a down regulation of ATP consuming pathways (Heldmaier et al., 2004).

There are examples of animals in hypometabolism of a shift in fuel utilization from carbohydrates to lipids (Andrews et al., 1998), of a general decrease in glycolysis and oxidative phosphorylation (Heldmaier et al., 1999, Martin et al., 1993), as well as decreases in gene transcription and protein translation (Heldmaier et al., 2004). This decrease in cellular processes would only account for ~30% of the reduced energy savings seen in hypometabolism (Buttgereit and Brand, 1995). Thus, it has been postulated that other, as yet unknown, mechanisms of energy saving are in play during hypometabolism. One hypothesis is that AMPK activation is a signal that coordinates the reductions in ATP consuming processes (Horman et al., 2005). AMPK is a conserved eukaryotic energy sensor that regulates ATP producing and utilizing pathways (Hardie et al., 1998). However, during hypometabolism AMPK activity increases in white adipose tissue but decreases in the liver (Horman et al., 2005), so a change in AMPK activity most likely does not cause the suppression of metabolic rate that induces hypometabolism.

1.3. Pharmacological Hypometabolism

Natural hypometabolism is accompanied by reductions in heart rate, metabolic rate, breathing rate, and core body temperature (Heldmaier et al., 2004). Table 1 lists compounds currently known to induce hypometabolism, and thus could potentially be useful in treating heart attacks and stroke, surgeries, improving organ transplantation viability (Bouma et al., 2011). Currently, three molecules have been widely studied for pharmaceutically induced hypometabolism: hydrogen sulfide gas (H_2S), 3-iodothyronamine (T_1AM), and 5’-adenosine monophosphate (AMP).

Table 1. Naturally occurring compounds that induce hypothermia in mice

Compound	Structure	M.W. (Daltons)
3-iodothyronamine (T_1AM)	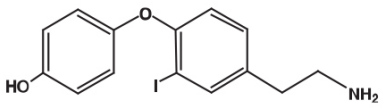	355.17
5′-adenosine monophosphate (5′-AMP)	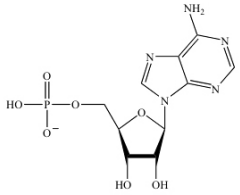	345.21
hydrogen sulfide gas (H_2S)	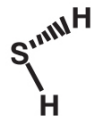	34.08

Table 1. Summary of known natural compounds that can be used to induce hypothermia in mice. Modified from Andrews MT. Advances in molecular biology of hibernation in mammals. *Bioessays.* May;29(5):431-40 (2007) and reprinted with permission from John Wiley and Sons.

H_2S is produced naturally in the body in minute quantities as an antioxidant and anti-apoptotic signaling molecule (Gadalla and Snyder, 2010, Calvert et al., 2010). H_2S is known to be a potent inhibitor of the electron transport chain (complex IV), which is thought to account for the observed reduction in metabolic rate, oxygen consumption, and the resulting reduction in core body temperature (Aslami et al., 2009, Blackstone, 2005). However, an earlier study has demonstrated that inhaled H_2S is rapidly taken up by erythrocytes, leading to an increased production of deoxygenated hemoglobin (Evans, 1967). It has been proposed that the primary effect of H_2S poisoning is the disruption of the erythrocytes' ability to transport oxygen (Evans, 1967). Studies using H_2S in larger mammals (Bouma et al., 2011) consistently demonstrated anti-apoptotic effects but H_2S did not induce hypometabolism, unlike the situation in small rodents. The mechanism underlying H_2S induction of hypometabolism remains poorly understood.

Another molecule of interest, T_1AM, is produced naturally in the thyroid and has been shown to reduce metabolic rate when introduced exogenously (Braulke et al., 2008). It is thought that T_1AM is an agonist for the trace amine-associated receptor (TAAR1) (Panas et al., 2010). Compared to natural hypometabolism the duration of metabolic depression by T_1AM is relatively short and the arousal phase is relatively prolonged (Braulke et al., 2008; Panas et al., 2010). Furthermore, the T_b drop induced by T_1AM is relatively shallow, only several degrees below euthermia. The mechanisms of T_1AM action leading to reduced T_b are not well understood.

The third molecule, AMP, has been shown to consistently induce hypometabolism in mice with a T_b maintained 1 or 2 °C above ambient temperature (Daniels et al., 2010). This study also demonstrated that AMP can induce

hypometabolism of dogs, suggesting a conserved pathway. Our previous studies implicated an interaction between AMP and erythrocytes in this process (Daniels et al., 2010). Additional insights on the AMP induced hypometabolism will be discussed in the "Previous Studies" section.

1.4. Oxygen Consumption/Delivery Control

Metabolism and oxygen utilization have been intimately linked for almost a century, since scientists devised a model that suggested that the body needed tight coordination between the tissues that needed oxygen and the supply of oxygen delivered the oxygen sensing/delivery pathway (Krogh, 1919). Investigators have proposed and tested many hypotheses regarding a mechanism for such coordination. These ideas ranged from the endothelial cells themselves regulating the oxygen flow upon sensing tissue need (Pittman and Duling, 1973, Duling, 1974, Jackson, 1987), to signaling metabolites diffusing through the cells of the vessel walls (Hester 1993), to the smooth muscle around the endothelium being in control of the vasculature's response to surrounding signals (Ellworth et al., 1994, Ellworth and Pittman, 1990). Each theory had some supportive data; however, no scenario could completely explain the vascular response in regulating oxygen supply and demand. Studies have shown that the erythrocytes' maintenance of oxygen supply was based on oxygen content (amount of oxygen molecules within the erythrocytes) and not oxygen tension (pressure of oxygen in the vasculature) as previously hypothesized (Jagger et al., 2001). It was further hypothesized that the erythrocytes could be regulating oxygen supply and demand (Stein and Ellsworth 1993). Independent studies have found that erythrocytes release ATP, which can activate nearby purinergic receptors of activated endothelial cells releasing vasodilators, such as nitric oxide (NO) (Houston et al., 1987,

Motte et al., 1993, Kennedy et al., 1985). Given the abundance of nucleotidases in circulation, it was postulated that the ATP target must be extremely close to the ATP release site (Meghji et al., 1995). If the erythrocytes are the source of the extracellular ATP, it appeared logical that this ATP release mainly occurs in the capillaries, where erythrocytes change shape as they pass through the narrow capillaries (Pries et al., 1996). To examine the feasibility of this mechanism, it was shown that the amount of ATP released by the erythrocytes quickly causes vasodilation prior to the site of ATP release (Sprague et al., 2007, Bergfeld and Forrester 1992). Other studies have demonstrated that the ATP signal not only results in the endothelial cells increasing the oxygen tension for surrounding tissues, but it also increases the diameter of the vessels, allowing for an increase in the number of erythrocytes that can flow to the area (Ellsworth, 2000). These studies have supported the hypothesized role of the erythrocyte as the cellular mediator that senses the local demand for oxygen and increases local oxygen delivery.

1.5. Hemoglobin

Hemoglobin, the predominant protein in erythrocytes, is responsible for the characteristic red color of erythrocytes, and determines the erythrocytes' interactions with oxygen and other gas ligands (e.g., CO_2, NO, CO, and H_2S). On one level, the body controls the amount of oxygen that can be delivered to the peripheral organs by regulating the number of erythrocytes that are created (erythropoiesis) and destroyed (eryptosis) (Lang et al., 2012). This balance is tightly regulated; too few erythrocytes in circulation can cause anemia, too many and the blood becomes viscous, which can lead to seizures, heart attacks, or thrombosis (Jelkmann, 2012).

Beyond the number of erythrocytes, the hemoglobin within erythrocytes is the major regulator of oxygen availability. Hemoglobin is a tetramer of two alpha and two beta globins, each containing a heme group that binds oxygen (Adair 1925). These four binding pockets exhibit cooperative behavior and investigators have devised binding models to explain the sigmoidal shape of hemoglobin's oxygen binding curve (Yonetani and Kanaori, 2013). The binding pocket of each heme group can either be oxygen-bound (relaxed or R state) or deoxygenated (tense or T state) (Yonetani and Kanaori, 2013). It had long been expected that the change from the R to T state was due to a change in the structure of the binding pocket because modulators affecting oxygen affinity were only thought to bind to the T state (Perutz, 1970, Yonetani and Kanaori, 2013). However it has been found recently that modulators, or allosteric effectors, are able to bind to both the R and T states (Yonetani and Kanaori, 2013). They also showed that the oxygen affinity parameters (p50, K_{low}, etc.) of hemoglobin did not change between the T and R states. Rather, the adjustment of these parameters for a given binding state is through the binding of allosteric effectors, which do not alter the quaternary or tertiary structure of the hemoglobin (Yonetani and Kanaori, 2013). These effectors are organic phosphates, chloride ions, hydrogen ions (Bohr effect), and temperature (Weber and Campbell, 2011). Whereas temperature is a global effector, the three molecular effectors work by binding to various, specific sites on hemoglobin: organic phosphates bind to the beta chain at one of four amino acid sites (residues: 1, 2, 82 and 143); chloride ions bind in a general area on either alpha or beta chains, and hydrogen ions bind solely to amino acid position 146 on the beta chain (Weber and Campbell, 2011). The binding of these effectors has a diverse set of effects, which is

the basis for physiological modulation of hemoglobin's oxygen transport abilities (Yonetani and Kanaori, 2013).

Knowing that the effectors are changing oxygen affinity but are not altering the protein structure, the obvious question that follows is: how do the modulators affect the oxygen affinity? It was discovered that effectors alter residues on the distal side of the heme binding pocket, which generates "dynamic fluctuations" (Kanaori et al., 2011). It had been recently proposed that these dynamic fluctuations would alter the ease of gas ligand (O_2, CO_2, NO) escape from the ligand-hemoglobin complex (Yonetani and Kanaori, 2013). As illustrated in Figure 4, this working model states that different effectors alter the gating of hemoglobin, allowing the ligand to leave at different rates due to a regulation of the thermal fluctuations. For instance, it has been shown that 2,3-BPG, an organic phosphate allosteric effector of hemoglobin, acts by increasing the rate of dissociation of oxygen, which would increase its ability to completely separate from the heme pocket (Salhany et al., 1970). It has also been shown that the reason T state hemoglobin is deoxygenated is the greater thermal fluctuation in that state allowing the ligands to more readily escape compared to the R state (Kanaori et al., 2011).

Some investigators sought to understand the differences among animals in their responses to the same effectors. For instance, fish hemoglobin is influenced by the binding of ATP rather than binding 2,3-BPG as in mammals (Weber and Campbell, 2011). These various animals' hemoglobin structures have been evaluated and the resulting alterations shed light on to the differential impact effectors have on particular hemoglobins (Weber and Campbell 2011). Some have changes in amino acid residues affect its affinity for organic phosphates (Weber and Campbell, 2011). Others have a

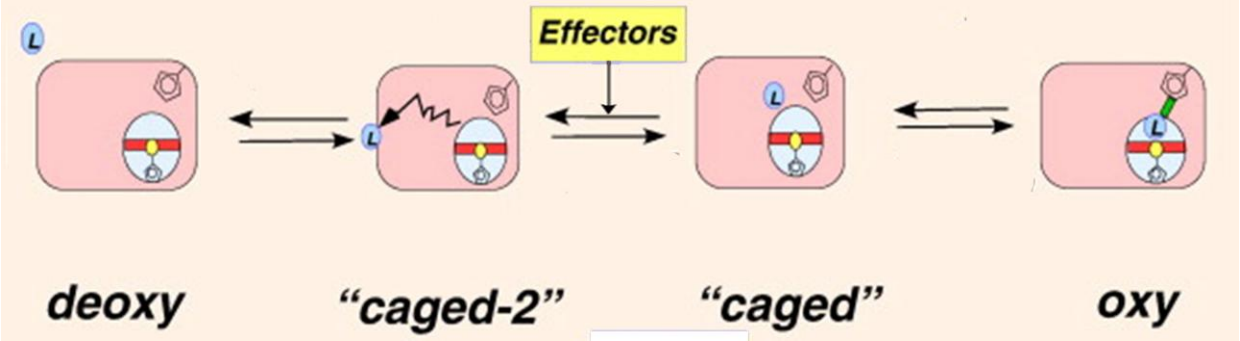

Figure 4. Ligand-hemoglobin binding steps as postulated by Yonetani and Kanaori, 2013. This schematic depicts two additional forms of hemoglobin (caged-2 and caged) between the oxygen-bound (oxy) and the oxygen-free (deoxy) states, with effectors (such as ATP and 2,3-BPG) modulating the central equilibrium. Figure adapted from Yonetani T, Kanaori K. How does hemoglobin generate such diverse functionality of physiological relevance? *Biochim Biophys Acta.* Sep;1834(9):1873-84 (2013) and reprinted with permission from Elsevier.

synergistic effect between the binding of the chloride ions and the organic phosphate molecules (Colletta et al., 1994). These genetic variations have shed light on how hemoglobin can operate differently in various species.

Regardless the animal species that hemoglobin is operating in, its major role is the same: it carries oxygen to tissues and removes carbon dioxide from them.

1.6. Adenine Nucleotide Pathways

So far, we have described what is known about the regulation of systemic metabolism, oxygen delivery, and the role played by the erythrocytes and hemoglobin. We now turn to the modulation of erythrocytes' functions by adenine nucleotides.

The absolute and relative intracellular levels of various adenine nucleotides have long been thought to be central to control of carbohydrate metabolism (Hunter and Jefferson, 1969). The levels of ATP, ADP, and AMP are all tightly regulated, inside and outside of the cell (Dzeja and Terzic, 2009). One way this regulation is achieved is through the cell membrane. Due to the negative charge of nucleotides, their ability to passively diffuse across the membrane is extremely limited. For example, an early study (Liebman and Heidelberger, 1955) found that AMP must be degraded to adenosine before being taken up into hepatocytes through the equilibrative nucleoside transporters (ENTs) and subsequently rephosphorylated back into AMP. Once in the cells, AMP has been shown to allosterically modify metabolic enzymes, inhibit nucleotide biosynthesis (Stadtman, 1966) and increase TCA cycle intermediate turnover (Hunter and Jefferson, 1969).

Both extracellular and intracellular levels of adenine nucleotides are tightly regulated by several well studied enzymes. There is an extracellular ATPase (CD39) that converts ATP to ADP and then AMP (Wang and Guidotti, 1996). In addition, an

extracellular ectonucleotidase (CD73) dephosphorylates AMP to adenosine (Thompson et al., 1990). Adenosine is taken up through nucleoside transporters such as ENT1/2, and intracellular adenosine can be phosphorylated by adenosine kinase, forming AMP (Liebman and Heidelberger, 1955). Adenosine is quickly deaminated to inosine by adenosine deaminase (ADA) (Schaedel et al., 1947). AMP can be phosphorylated by adenylate kinase (AK) (with ATP as phosphate donor) to produce ADP (Dzeja and Terzic, 2009). Another fate of intracellular AMP is deamination to inosine monophosphate (IMP) (Hancock et al., 2006). In nucleated cells, IMP can be converted back to AMP by adenylosuccinate synthase and lyase (Hancock et al., 2006).

Unlike nucleated cells, erythrocytes do not carry out de novo purine biosynthesis nor do they have a salvage pathway for IMP. Despite having a regulatory environment for extracellular adenine nucleotides similar to other cell types, erythrocytes seem to have a distinct mechanism to take up extracellular AMP efficiently (Daniels et al., 2010; Mathews et al., 2005). Erythrocyte AMP is mainly catabolized through AMP deaminase 3 (AMPD3), an irreversible reaction due to the erythrocyte's lack of adenylosuccinate synthase and lyase (Baranowska-Bosiacka et al., 2004).

Several nucleotide transporters have been found in the erythrocyte membrane, such as Pannexin (Goldman et al., 2012). Pannexin channels have been proposed to release ATP from erythrocytes in response to decreased oxygen saturation (Goldman et al., 2012).

Interestingly, recent studies of the erythrocyte membrane have found both ANT (ATP/ADP translocase) and VDAC (voltage dependent anion channel) (Bouyer et al., 2011). The erythrocytes' release of ATP could be blunted by TRO19622, a specific VDAC inhibitor (Sridharan et al., 2012). ANT belongs to the SLC25 family; most

members of this family are antiporters that can be inhibited to varying degrees by carboxyatractyloside (CAT), bongrekic acid (BA), and tannic acid (TAN) (Guitierrez-Aguilar and Baines, 2013). VDAC facilitates passive diffusion of many different molecules, regardless of size or charge (Shoshan-Barmatz et al., 2010). VDAC can be modulated by calcium and by adenine nucleotides, as well as by 4,4'-diisothiiocyanostilbene-2-2'-disulfonic acid (DIDS) (Shoshan-Barmatz et al., 2010).

1.7. Previous studies

Our earlier investigations identified AMP as a biomolecule that can induce hypometabolism in mammals (Daniels et al., 2010). We demonstrated the length of AIHM is not dosage dependent. Induction of AIHM is specific to adenine among the nucleotides (Daniels et al., 2010). We and others have shown that AMP induced hypometabolism (AIHM) mimics some of the features observed in natural hibernation. Our observation that circadian control of gene expression during AIHM is largely stalled was also observed in hamsters during natural hibernation (Zhao et al., 2011, Revel et al., 2007). Others have shown that lymphopenia observed in natural hibernators is also observed in mice during AIHM (Bouma et al., 2013). While there are similarities between AIHM and natural torpor, there are also dissimilarities. One of the dissimilarities is that the rate of T_b reduction observed in natural torpor is typically slower than that in AIHM (Strijkstra et al., 2012).

AMP administration leads to rapid slowing of the heart rate, and it has been suggested that adenosine receptor (A1a) mediated bradycardia was the underlying mechanism for AIHM (Swoap et al., 2007). However, we observed that wild type, *A1a*$^{-/-}$, *A2a*$^{-/-}$, *A2b*$^{-/-}$, and *A3a*$^{-/-}$ mice undergo AIHM in a similar fashion (Daniels et al., 2010), demonstrating that the disruption of adenosine receptor function did not alter AIHM.

Interestingly the rapid decline in heart rate in response to AMP seen in wildtype mice was absent in *A1a*$^{-/-}$ mice, suggesting bradycardia is not the cause, but a result of AIHM (Tao et al., 2011). We further investigated if adenosine is needed for the AIHM response by studying the impact of eliminating CD73, the ecto-nucleotidase responsible for dephosphorylating AMP to adenosine extracellularly (Zhang 2010), on AIHM. We observed that *Cd73*$^{-/-}$ mice were more sensitive to lower doses of AMP than wildtype mice (Daniels et al., 2010), suggesting that the deficiency of this nucleotidase enhanced the effect of injected AMP. This finding demonstrated that generation of adenosine via dephosphorylation of AMP by CD73 actually impeded AIHM.

Using radioisotope tracing, we observed that AMP was rapidly taken up into erythrocytes (Daniels et al., 2010). This finding was consistent with an earlier observation that identified erythrocytes as a major cellular target of AMP in a whole body study with radiolabelled AMP (Mathews et al., 2005). Corresponding to AMP uptake, The kinetics of increasing erythrocyte levels of 2,3-BPG, the main hemoglobin modulator, paralleled those of AMP uptake following an AMP injection (Daniels et al., 2010). Serum 2,3-BPG was also significantly elevated during AIHM (Zhao et al., 2014). Given that 2,3-BPG mutase, the key enzyme for 2,3-BPG biosynthesis, is only found in erythrocytes and placenta (Pritlove et al., 2006), these results implicate erythrocytes as the cellular target of AMP (Daniels et al, 2010).

To further characterize the role of the erythrocytes in AIHM, we investigated the effect of altering AMP degradation within erythrocytes. There are two pathways for AMP catabolism: dephosphorylation to adenosine and subsequent conversion to inosine via ADA; and deamination of AMP to inosine monophosphate (IMP) (Figure 5). Given that the K_m of ADA for adenosine is two orders of magnitude larger than that of

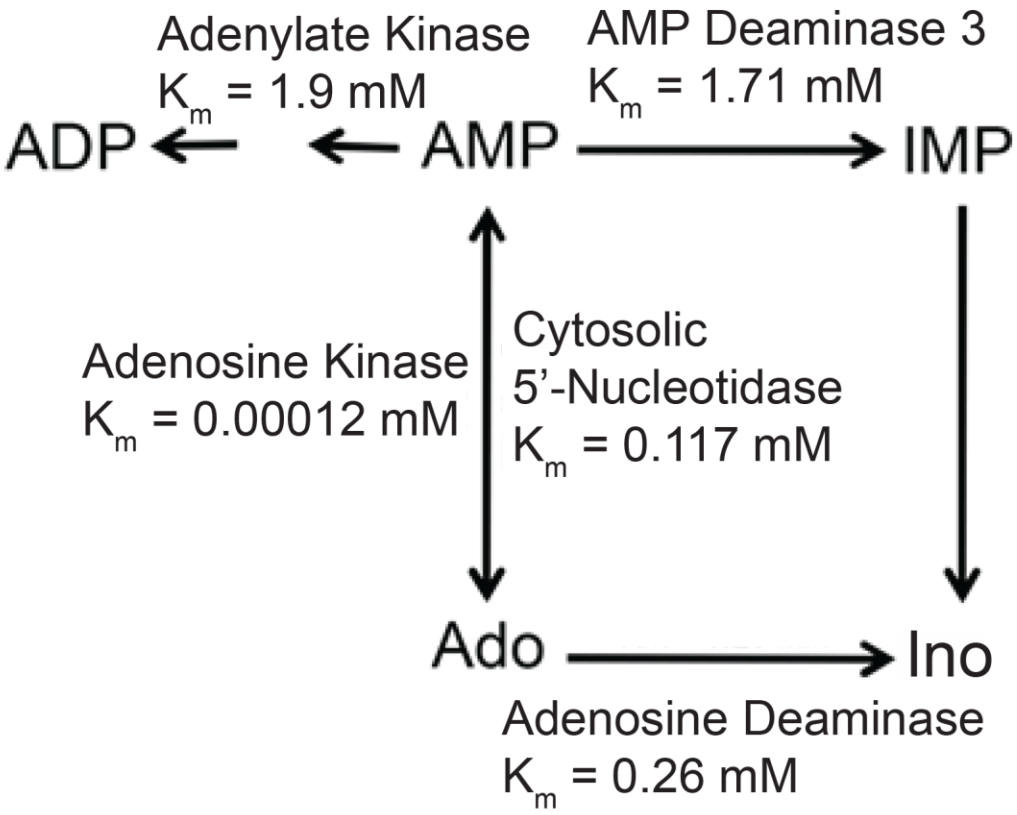

Figure 5. Km values of various enzymes relating to intracellular catabolism of AMP in erythrocytes.

adenosine kinase, we reasoned that the majority of AMP catabolism must be via its deamination to IMP. Since erythrocytes do not have a salvage pathway for converting IMP back to AMP (Baranowska-Bosiacka et al., 2004), the catabolism of AMP by AMP deaminase (AMPD) would be irreversible. We sought to disrupt AMP degradation in erythrocytes by mutating the gene for AMPD3, the enzyme isoform responsible for AMP deamination in erythrocytes (Daniels et al., 2013). Thus, we created a strain of mouse deficient in AMPD3, the *AMPD3*$^{-/-}$ model. We expected that elimination of this pathway would drastically increase intracellular AMP levels. However, we observed that erythrocyte AMP levels did not change significantly in the *AMPD3*$^{-/-}$ model (Daniels et al., 2013). Instead, both ATP and ADP levels increased about 3-fold. Additionally, we observed that *Ampd3*$^{-/-}$ mice, like the *Cd73*$^{-/-}$ mice, were more prone to AIHM than wild type mice. These results with single knockout models indicated that CD73 and AMPD3 each modulate AIHM, and they further indicate that erythrocytes have a major role in mediating AIHM. These observations led to several important questions that are central to my thesis studies:

1. What is the physiological importance of CD73 and AMPD3 to mammalian metabolism?

2. Does alteration of AMP catabolism affect the physiological functions of erythrocytes, particularly oxygen transport?

3. Can CD73 and AMPD3 deficiency models help elucidate the mechanism of AIHM?

4. How is the erythrocytes' oxygen transport affected when exposed to non-physiological levels of AMP, such as in AIHM?

5. In contrast to nucleated cells, erythrocytes are capable of AMP uptake. Is there a functional significance of this capability?

2. Materials & Methods

Materials: Radiolabelled nucleotides were acquired from Moravek Biochemicals. Solutions for the Hemox-Analyzer were acquired from TCS Scientific Corporation. Phosphate Buffered Saline (BP399-1, 10X PBS solution diluted to 1X prior to use with final concentrations of 11.9 mM Phosphates, 137 mM Sodium Chloride, and 2.7 mM Potassium Chloride) was acquired from Fisher Scientific. TRO19622 was acquired from Tocris Bioscience (Bristol, United Kingdom). All other chemicals and reagents were acquired from Sigma.

Mouse housing/husbandry/protocols: All animal studies were carried out in the institutional animal facility by trained personnel under protocols HSC-AWC-13-012 and HSC-AWC-12-079 approved by the Animal Welfare Committee (AWC), the institutional animal care and use committee (IACUC) at UTHSC-Houston. Wild type mice were ordered from Jackson Laboratory (Bar Harbor, Maine). The *Cd73*$^{-/-}$ mice were obtained from Dr. L. Thompson (Thompson et al., 2004). The *Ampd3*$^{-/-}$ mice were generated as previously reported (Daniels et al., 2013). The *Cd73*$^{-/-}$*/Ampd3*$^{-/-}$ mouse was generated from breeding the *Cd73*$^{-/-}$ with the *Ampd3*$^{-/-}$, followed by backcrossing the F1. Mice were maintained in the animal facilities with a 12h:12h light:dark cycle at an ambient temperature of ~23°C. Mice had access to standard rodent chow and water ad libitum and their cages were changed twice a week.

Wheel running experiments: Mice were placed in individual cages with a running wheel within a circadian chamber and provided with food and water ad libitum as previously described (Miki et al., 2013, Siepka and Takahashi, 2005). Briefly, wheel-running activity was measured continuously using Actiview Software. For each genotype, both male and female mice (n=4) of similar age (14-18 weeks) were used.

Mice were kept in a 12h:12h light:dark (LD) cycle for 2 weeks. The quantification of total wheel revolutions in zeitgeber time (ZT) was determined using Actiview software.

Metabolic chamber experiments: A Comprehensive Lab Animal Monitoring System (CLAMS, Columbus Instruments, Columbus, OH) was used to measure animal metabolic rate as previously described (Daniels et al., 2010). Briefly, each chamber contained an individual mouse with free access to food and water. The O_2 consumption and CO_2 production of each mouse were monitored and recorded with the OxyMax System from Columbus Instruments. Each chamber has the option of wheel addition for running. The chamber was maintained at normal husbandry conditions at 23°C under a 12h:12h LD cycle.

Erythrocyte isolation: Whole blood was collected from a tail clip and allowed to drip into a heparinized Eppendorf tube. The whole blood was then centrifuged at 4°C at 3000 rpm for one minute. The plasma was then removed and the erythrocytes were washed 3X by resuspension in a 10X volume of ice-cold phosphate buffered saline (PBS) and centrifugation was repeated. After a final wash, the resulting erythrocyte pellet was resuspended with a small volume of PBS to about the original whole blood volume. The resulting suspension was counted on a hemacytometer for the number of erythrocytes after two serial 1:100 dilutions. Based on the cell count, the isolated erythrocytes were then diluted with PBS to obtain about 10^6 cells/µL. For oxygen saturation experiments, TLC experiments, AMP uptake experiments, and ATP release experiments, 10 µL of 10^6 cells/µL were used; for adenine nucleotide extraction experiments, 75 µL of 10^6 cells/µL were used**.** Erythrocytes from mice of all the genotypes were prepared in a similar manner.

Blood Oxygen Saturation experiments: All blood oxygen saturation experiments were measured with a Hemox Analyzer from TCS Scientific Corporation as described by Guarnone et al. (1995). Solutions for the Hemox Analyzer were also acquired from TCS Scientific Corporation. Briefly, 10 µL of 10^6/µL of erythrocytes were incubated in 4 mL of Hemox buffer, 10 µL anti-foaming agent (AFA-25, TCS Scientific Corporation) and 0.1% BSA and equilibrated at 37°C. In experiments where lysate was used, the 10 µL of 10^6/µL of erythrocytes were treated by freeze-thawing twice to generate the lysate. Once the sample in the Hemox Analyzer had equilibrated to a pO_2 of 150 mmHg and a temperature >36.7°C, measurement of oxygen saturation was initiated by perfusing the sample with nitrogen gas to deoxygenate the hemoglobin. The analysis of p50 was complete once the pO_2 was below 2 mmHg.

2,3-BPG Quantification: The quantification of erythrocytes' 2,3-BPG was carried out as described by Rumi et al. (2009). Briefly, erythrocytes were isolated as described above and then, as per the kit manufacturer's instructions, they were neutralized and processed to quantify the amount of 2,3-BPG in the sample (Roche Lifescience). In parallel, the concentration of erythrocyte protein was quantified using a BCA Assay kit (Pierce). The level of 2,3-BPG was then normalized to the level of total protein.

Adenine Nucleotides Measurements: Adenine nucleotide measurements were carried out as described by Stocchi et al. (1985). Briefly, 2 volumes of 7.5% perchloric acid were added to isolated erythrocytes, mixed by vortexing, and then centrifuged for 10 min at 4°C at 13,000g. The supernatant was neutralized with an equal volume of 0.75 M K_2CO_3. After neutralization, the reaction mixture was centrifuged at 4°C for 10 min at 13,000 x g and the resulting supernatant was injected on a pre-equilibrated HPLC C-18 column. The HPLC elution gradient was as described by Bhatt et al.

(2012). Buffer A: 30 mM KH_2PO_4 + 0.8 mM TBAP (tetrabutylammonium phosphate) pH 5.45. Buffer B: 50% (v/v) acetonitrile in 30 mM KH_2PO_4 + 0.8 mM TBAP, pH 7.0. After each run, a 20 minute flush with Buffer A was carried out to re-equilibrate the column.

Preparation of Hemoglobin: Lyophilized human Hemoglobin (Sigma #H7379) was dissolved in 50 mM HEPES buffer, pH 7.4 (final concentration of Hb was calculated to be about 2mM in a volume of 0.5mL) and reduced with powder of sodium hydrosulfite (3-5 crystals) (Sigma #157953). Reduced hemoglobin was passed through an Econo-Pac 10 DG Desalting column (Bio-Rad), pre-equilibrated with aerobic HEPES buffer, to remove excess sodium hydrosulfite and form oxyhemoglobin. Electronic absorption spectra of oxyhemoglobin were recorded using a Hewlett-Packard 8452A diode-array spectrophotometer. The concentration of oxyhemoglobin was calculated using an extinction coefficient of 128 $(mM\ heme)^{-1}cm^{-1}$ at 415 nm (Antonini and Brunori, 1971).

Injection of AMP in mice: Mice were fasted overnight and an intraperitoneal injection with the desired dose of 5'-AMP in sterile saline was given early in the morning to induce the 5'-AMP Induced Deep Hypometabolic (AIHM) state. The metabolic chamber is maintained at ~15°C during these experiments in order to facilitate the induction and maintenance of the AIHM state. The animals were monitored via the CLAMS computer readout and were removed from the metabolic chamber and placed in their room temperature cage upon arousal from the AIHM state. We defined the AIHM state as a VO_2 below 1200 mL/kg/h. We have observed that most mice would begin arousal and rapid re-warming not long after reaching a VO_2 of 1500 mL/kg/h.

Incubation of erythrocytes with adenosine/AMP/other nucleotides: Adenosine (Ado) was dissolved in DMSO to make a stock of 200mM, which was then diluted to the appropriate concentration with PBS. Solutions of the other nucleotides were prepared similarly. After addition of nucleotide, the erythrocyte suspension was shaken at 37°C at 750 rpm in a thermomixer. At the desired time, the erythrocytes suspension was removed and processed according to the experimental protocol.

TLC of Radiolabelled ADP/AMP: Isolated erythrocytes (13 µL cells) were incubated at 37°C with 2 µL of stock [^{14}C]-AMP or [^{14}C]-ADP for the desired time and then centrifuged at 4°C for 1 min at 3000g to separate cells from supernatant. The supernatant was removed and saved for future analysis. The cell pellet was washed twice with 1 ml of cold PBS, and the final cell pellet was lysed by mixing rapidly with 15 µL of 5% TCA. The reaction mixture was centrifuge, and final supernatant saved for TLC analysis. Both the initial supernatant and the final supernatant were then spotted (1 µL at a time, with a hairdryer used to speed up drying) on plastic TLC plates coated with silica gel 60 and F254 fluor (Merck). The TLC plates were developed with butanol / methanol / water / ammonium hydroxide (60:20:20:1). The TLC plate was then air dried and the radioactive bands visualized by exposure to X-ray film at -80°C.

Uptake of AMP using ^{14}C-AMP: Isolated erythrocytes were incubated at 37°C with various concentrations of AMP with constant specific activity. After 45 min incubation at 37°C, all reactions were centrifuged to separate cells from supernatant. The supernatant was removed and kept for further analysis. The cell fraction was washed twice with 1 ml cold PBS, and the final cell pellet was lysed by mixing with 15 µL of 5% TCA. The amount of radioactivity in the supernatant and cell fractions were determined by adding 10 mL of ScentiSafe Econo 2 scintillation cocktail (Fisher) and

vials were counted for 5 min each using a scintillation machine [Pharmacia Rackbeta #1209-015]. In experiments where an inhibitor was used, the inhibitor was pre-incubated with the erythrocytes for 5 minutes prior to addition of AMP. In competition experiments with other nucleotides/metabolites, each competitor was added at the same time as AMP.

ATP release: ATP released by erythrocytes was measured using a Perkin Elmer ATP luciferase kit following the manufacturer's instruction. Initial experiments were recorded using a 96-well plate luminometer [Envision Multilabel Reader (Perkin Elmer) #2104-0010] in real time. In the experiments with inhibitors, the erythrocytes were preincubated with inhibitor for 5 minutes before addition of AMP.

Statistics: All values plotted are averages +/- SEM, with the significance of any differences evaluated by either t-test or ANOVA, as appropriate for the data set.

3. CD73 and AMPD3 deficiency enhance metabolic performance via erythrocyte ATP that decreases hemoglobin oxygen affinity

3.1. Results

3.1.1. Mice deficient in CD73 and AMPD3 display enhanced levels of locomotor and metabolic activities.

The *Ampd3*$^{-/-}$/*Cd73*$^{-/-}$ mice are fertile and morphologically indistinguishable from wild type mice. In an effort to find possible physiological differences in *Ampd3*$^{-/-}$/*Cd73*$^{-/-}$ mice, we measured their locomotor activity assessed by wheel-running measurements using age and sex matched wild type, *Ampd3*$^{-/-}$, *Cd73*$^{-/-}$, and *Ampd3*$^{-/-}$/*Cd73*$^{-/-}$ mice. The wheel running results revealed that the *Ampd3*$^{-/-}$/*Cd73*$^{-/-}$ mice had enhanced levels of locomotor activity compared with wild type, *Ampd3*$^{-/-}$ or *Cd73*$^{-/-}$ cohorts (Figure 6 A and B). The actograms revealed that wheel running activities for *Ampd3*$^{-/-}$/*Cd73*$^{-/-}$ mice appeared largely continuous during zeitgeber time (ZT) 12-24, unlike the other genotypes, where periods of activity were interrupted by periods of rest. The wheel-running activity between ZT0-ZT12 was low and similar among the four genotypes, indicating that their activities were under circadian regulation. The average daily wheel running activity of an *Ampd3*$^{-/-}$/*Cd73*$^{-/-}$ mouse was about three-fold higher than for a wild type mouse. The average wheel running activity of an average *Ampd3*$^{-/-}$ mouse was moderately, but significantly, elevated compared to wild type. Daily locomotor activity of an average *Cd73*$^{-/-}$ mouse was not significantly different from wild type. Comparing *Ampd3*$^{-/-}$/*Cd73*$^{-/-}$ to *Ampd3*$^{-/-}$ mice shows the latter had significantly less locomotor activity, suggesting that CD73 and AMPD3 are likely additive in regulating the AMP degradation pathway.

Next, we measured metabolic rate based on oxygen consumption (VO_2) of mice

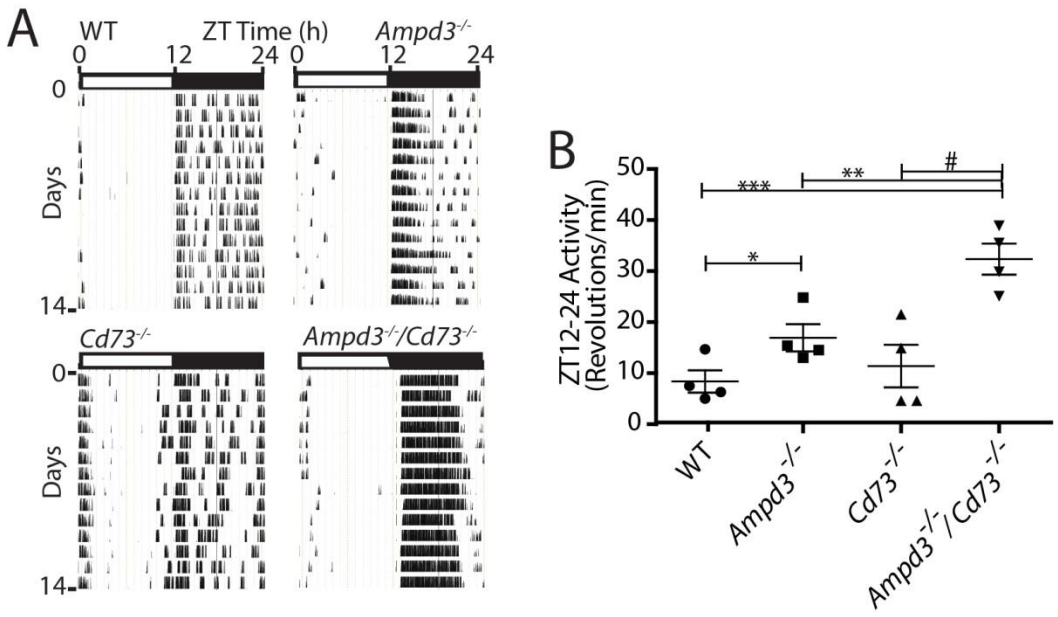

Figure 6. Locomotor activities of wild type, Ampd3$^{-/-}$, Cd73$^{-/-}$, and Ampd3$^{-/-}$/Cd73$^{-/-}$ mice. A) Representative individual wheel running actograms of the four genotypes of mice in a 12:12h Light:Dark (LD) cycle. B) The average wheel running activities between ZT12-ZT24 for the wild type, *Ampd3*$^{-/-}$, *Cd73*$^{-/-}$, and *Ampd3*$^{-/-}$/*Cd73*$^{-/-}$ mice (n=4). P values = * < .05, # < .01, ** < .005, and *** < .0001.

in the presence and absence of running wheels. When a running wheel was not accessible, the metabolic rates of *Ampd3*$^{-/-}$/*Cd73*$^{-/-}$ and wild type mice were comparable (Figure 7 A). When a running wheel was provided, both wild type and *Ampd3*$^{-/-}$/*Cd73*$^{-/-}$ mice displayed enhanced metabolic activities. However, the *Ampd3*$^{-/-}$/*Cd73*$^{-/-}$ mice exhibited significantly elevated average daily VO_2 when compared to wild type (Figure 7 A and B). Providing access to a wheel for *Cd73*$^{-/-}$ or *Ampd3*$^{-/-}$ mice did not significantly enhance their average daily VO_2 levels over wild type (Figure 7 B, D, and E). We further undertook measurement of daily food consumption among the genotypes with access to wheel running. These measurements indicate that the *Ampd3*$^{-/-}$/*Cd73*$^{-/-}$ mice ate significantly more than *Ampd3*$^{-/-}$, *Cd73*$^{-/-}$, or wild type mice when access to wheel running was provided (Figure 7 C). Thus, the metabolic activities of the mice appear to correlate in part with food intake. Together, these observations suggest that loss of AMPD3 and CD73 function has a additive impact on the capacity for metabolic activity and food consumption in mice.

3.1.2. Loss of AMPD3 alters erythrocyte oxygen saturation level.

We suspected that the observed continuous metabolic activity phenotype of *Ampd3*$^{-/-}$/*Cd73*$^{-/-}$ mice (Figure 6) could be linked to changes in the erythrocytes' main function of oxygen transport. Using a Hemox analyzer, we measured the pressure required for 50% oxygen saturation (p50) in isolated erythrocytes from wild type, *Ampd3*$^{-/-}$, *Cd73*$^{-/-}$, and *Ampd3*$^{-/-}$/*Cd73*$^{-/-}$ mice. Strikingly, the p50 value was significantly increased in *Ampd3*$^{-/-}$ erythrocytes, by 4 to 6 mmHg, when compared to erythrocytes from wild type mice (Figure 8 A and B). Relative to wild type, the p50 was also increased by 5 to 9 mmHg in *Ampd3*$^{-/-}$/*Cd73*$^{-/-}$ erythrocytes. The p50 values obtained for erythrocytes from *Cd73*$^{-/-}$ mice were not significantly different from wild type mice.

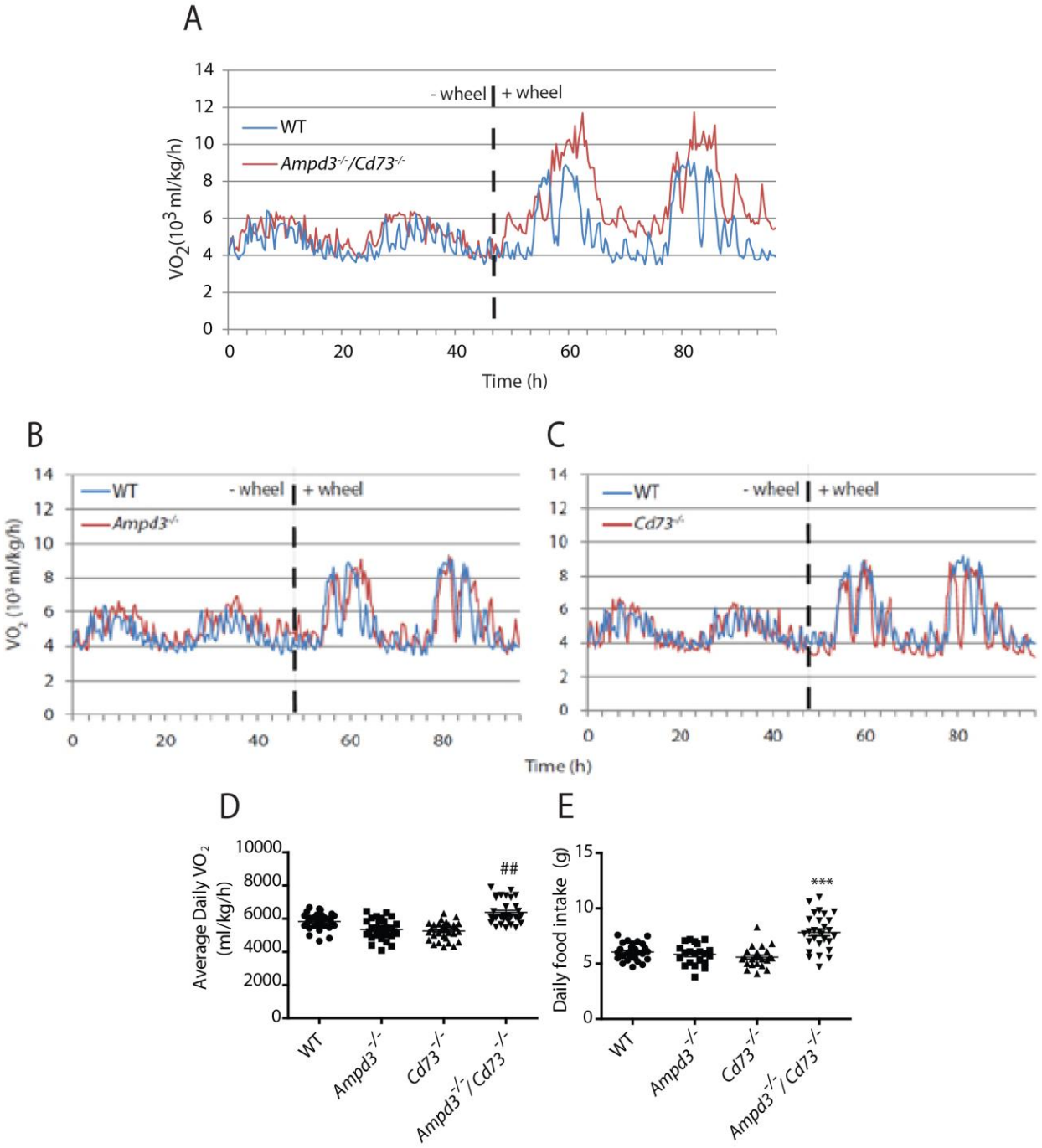

Figure 7. Loss of both CD73 and AMPD3 affects locomotor and metabolic activities of mice. A), B) and C) Representative oxygen consumption (VO_2) readings of a wild type and *Ampd3*$^{-/-}$/*Cd73*$^{-/-}$ (A) *Ampd3*$^{-/-}$ (B) or *Cd73*$^{-/-}$ (C) mouse without and with access to an exercise wheel. D). The daily average metabolic activity with access to a wheel for wild type, *Ampd3*$^{-/-}$, *Cd73*$^{-/-}$, and *Ampd3*$^{-/-}$/*Cd73*$^{-/-}$ (n=4/genotype) mice over a period of seven days. E) The daily food consumption by the mice in D). P values = ## < .0005, and *** < .0001.

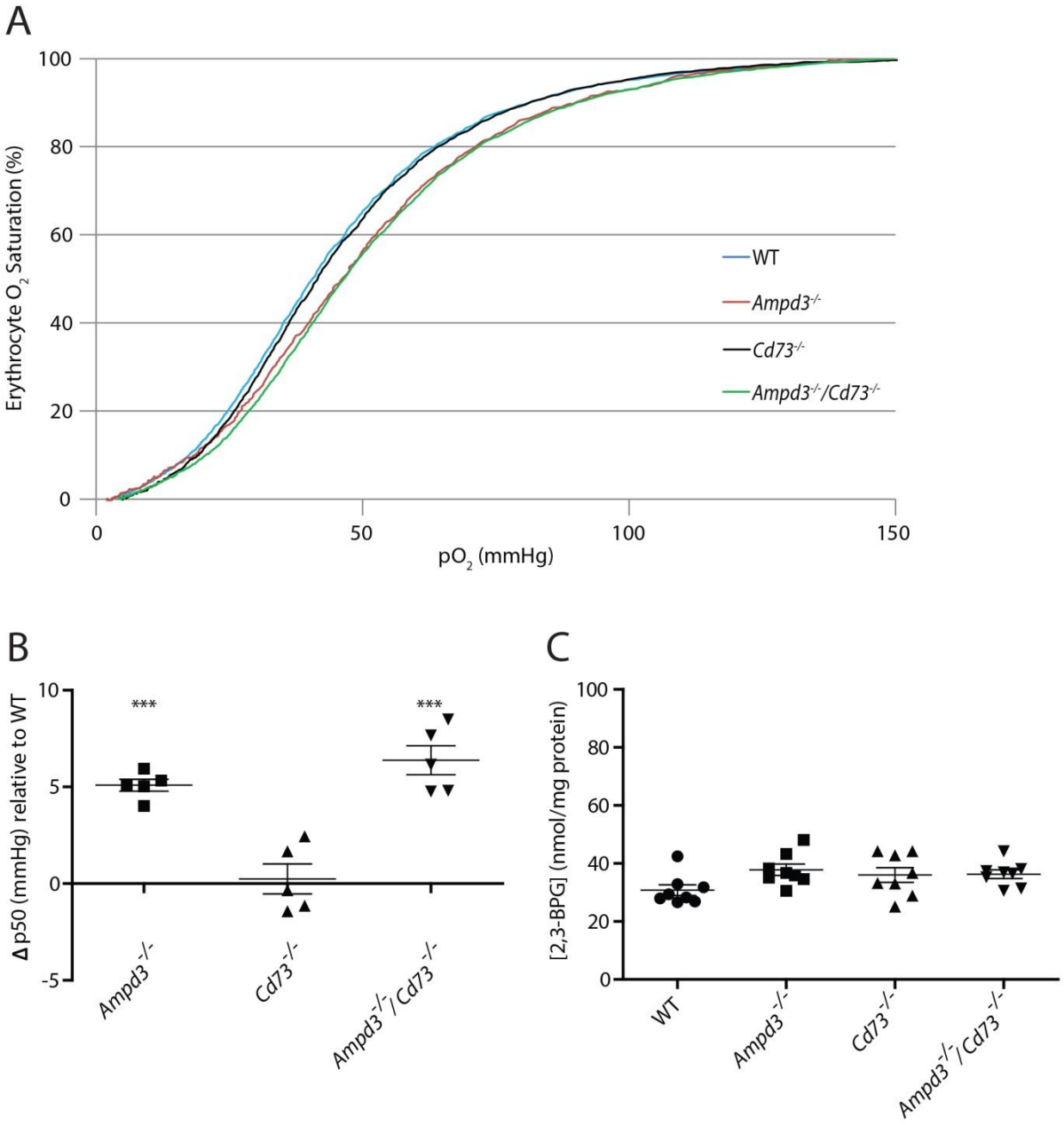

Figure 8. Erythrocytes' p50 and 2,3-BPG values in mice deficient in AMPD3 and/or CD73. A) Representative profiles of oxygen saturation vs oxygen pressure of isolated erythrocytes from wild type, *Ampd3*$^{-/-}$, *Cd73*$^{-/-}$, and *Ampd3*$^{-/-}$/*Cd73*$^{-/-}$ mice. B) Quantitative change in isolated erythrocytes from *Ampd3*$^{-/-}$, *Cd73*$^{-/-}$, and *Ampd3*$^{-/-}$/*Cd73*$^{-/-}$ p50 value with respect to wild type erythrocytes. C) Erythrocyte 2,3-BPG levels in wild type, *Ampd3*$^{-/-}$, *Cd73*$^{-/-}$, and *Ampd3*$^{-/-}$/*Cd73*$^{-/-}$ mice. Each plotted point represents an individual mouse. P values = *** < .0001

The right shift of the p50 value indicates that a higher pressure is required for the erythrocytes to reach 50% oxygen saturation. These data indicate that the erythrocyte's affinity for oxygen is reduced, facilitating the release of oxygen to tissues.

Since 2,3-BPG is known as the main intracellular modulator of Hb's affinity for oxygen (Mulquiney and Kuchel, 1999), and an increase in its concentration shifts the Hb oxygen dissociation curve rightward (Isaacks et al., 1987), we measured 2,3-BPG levels in erythrocytes from all four genotypes. We found no significant difference in 2,3-BPG levels among the erythrocytes of the different genotypes (Figure 8 C). These findings indicate that the increase in p50 value is not due to a rise in intracellular 2,3-BPG levels.

Next we investigated whether a genotype-specific change in erythrocyte pH was involved. Erythrocytes from each of the genotypes in Hemox reaction medium all had an extracellular pH of 7.4, the same as the medium's pH. To measure the erythrocytes' intracellular pH, 100 µL samples of isolated erythrocytes from each genotype were lysed in 0.5 mL of deionized water, and the pH of these lysates was measured at 37°C. The erythrocyte's intracellular pH value was 7.2 for wild type mice, and 7.3 for *Ampd3*$^{-/-}$, *Cd73*$^{-/-}$, and *Ampd3*$^{-/-}$/*Cd73*$^{-/-}$ mice. The values measured were consistent with the physiological pH range of the erythrocyte's cytosol, between pH 7.1-7.3 (Funder and Wieth, 1966). Since the p50 measurements were carried out at 37°C, the effects of temperature on Hb affinity for oxygen could be excluded. Together, it appears that mice deficient in AMPD3 have an elevated erythrocyte p50 value that is not linked to an increase in intracellular 2,3-BPG levels or to a change in intracellular pH.

3.1.3. Elevated adenine nucleotide levels in AMPD3 deficient erythrocytes.

We reasoned that in *Ampd3*$^{-/-}$/*Cd73*$^{-/-}$ mice, the blockade of AMP catabolism in erythrocytes could alter the levels of ATP and ADP, as well as AMP, since ATP and ADP must first be dephosphorylated to AMP before they can be further catabolized (Ataullakhanov and Vitvitsky, 2002). Utilizing HPLC, we measured the levels of adenine nucleotides after perchloric acid extraction of erythrocytes from the four genotypes (Figure 9 A-C). The data showed that total adenine nucleotides were significantly increased in *Ampd3*$^{-/-}$ erythrocytes, largely due to increases in ATP and ADP rather than AMP. AMP levels in *Ampd3*$^{-/-}$ erythrocytes are about two-fold higher than those in *Ampd3*$^{+/+}$ erythrocytes. By contrast, ADP and ATP levels were about three-fold increased in *Ampd3*$^{-/-}$ erythrocytes compared with *Ampd3*$^{+/+}$ erythrocytes. Consistent with previous reports, and irrespective of the mouse genotype, we observed that the ratios of [ATP] to [ADP] and [ATP] to [AMP] were maintained at approximately 10:1 and 100:1, respectively (Benesch and Benesch, 1967, Formato et al., 1990).

ATP comprises the majority of the erythrocyte adenine nucleotide pool in all genotypes of mouse (Figure 9). Comparison of *Ampd3*$^{-/-}$/*Cd73*$^{-/-}$ to *Ampd3*$^{-/-}$ erythrocytes showed that ATP and ADP, but not AMP, were significantly elevated. Relative to wild type erythrocytes, the ATP levels of *Ampd3*$^{-/-}$/*Cd73*$^{-/-}$ and *Ampd3*$^{-/-}$ erythrocytes showed an average increase of 3.2- and 2.8-fold, respectively (Fig 9 B and C). These findings suggest that AMPD3 is the major regulator of the erythrocyte adenine nucleotides pool.

Interestingly, the different adenine nucleotides levels in erythrocytes among the four genotypes (Figure 9) correlate well with their erythrocyte p50 values (Figure 8). This correlation suggests that the observed increase in the *Ampd3*$^{-/-}$ erythrocyte's p50 values are associated with the increased cellular adenine nucleotide levels.

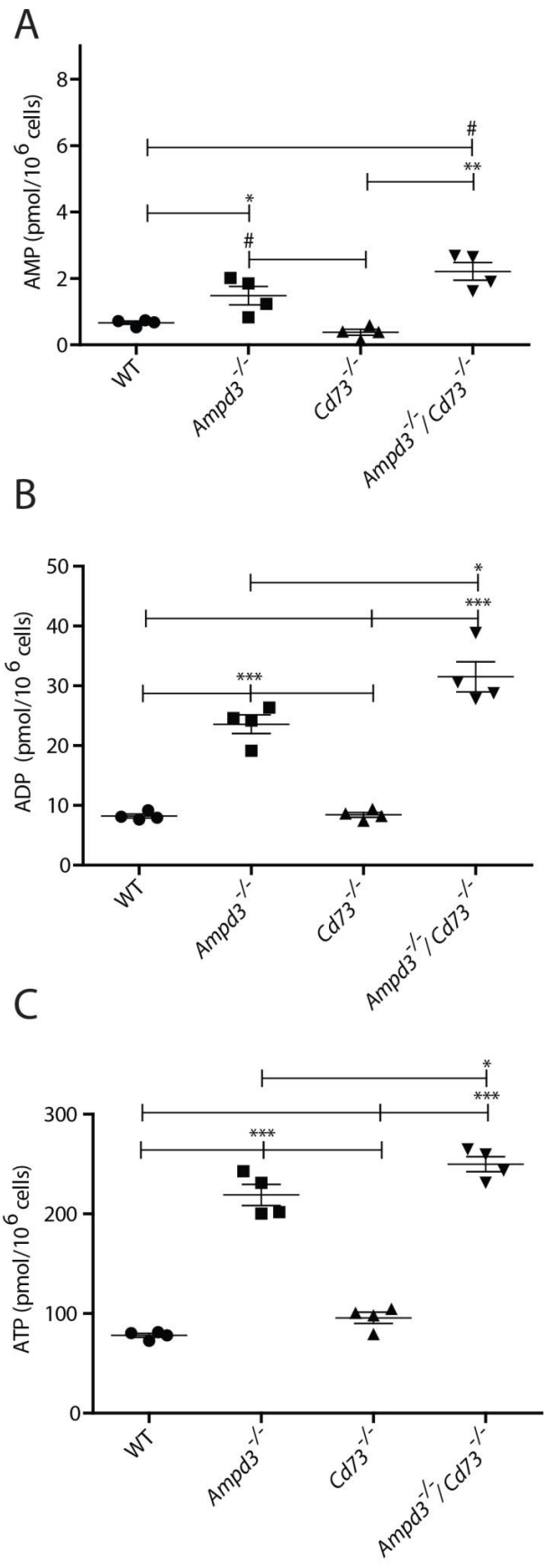

Figure 9. Erythrocyte adenine nucleotide levels in wild type, Ampd3$^{-/-}$, Cd73$^{-/-}$, and Ampd3$^{-/-}$/Cd73$^{-/-}$ mice. Mouse erythrocytes were analyzed for the levels of: A) 5'-AMP, B) ADP and C) ATP. Each plotted point is an individual mouse. P values = * < .05, # < .01, ** < .005, and *** < .0001.

3.1.4. Modulation of hemoglobin's oxygen saturation by ATP.

Previous studies have demonstrated that many organic phosphates can bind to Hb and modulate its affinity for oxygen (Benesch and Benesch, 1967). However, it has been proposed that, except for 2,3-BPG, the physiological concentrations of the majority of these organic phosphates are too low to be effective *in vivo* moderators of Hb affinity for oxygen (Benesch et al., 1968).

In *Ampd3*$^{-/-}$/*Cd73*$^{-/-}$ mice, the endogenous erythrocyte adenine nucleotide levels are ~3-fold higher than those in wild type mice. Therefore, we investigated whether these increased levels of adenine nucleotides are sufficient to alter Hb's affinity for oxygen and thus account for the increase in p50 values. The physiological intracellular concentration of ATP in wild type erythrocytes is estimated to be between 1-2.5 mM, ADP at 0.1-0.25 mM, and AMP at 0.01-0.02 mM (Benesch and Benesch, 1967, Miseta et al., 1993). To measure the effect of adenine nucleotides on p50 values, we titrated purified human adult Hb (Hb-A) with different concentrations of ATP, ADP, and AMP in the presence of physiological (1 mM) 2,3-BPG levels.

We observed that the Hb-A p50 value is weakly affected by AMP (Figure 10 A and B) and, even at 10 mM AMP, the increase in the Hb-A p50 value is only about 1-2 mmHg. Thus, the AMP increase in *AMPD3*$^{-/-}$ erythrocytes (Figure 9) should not alter its p50 value significantly.

The effect of ADP concentration on Hb-A's p50 value was linear up to 10 mM, with a steeper slope than seen for AMP (Figure 10). Nevertheless, based on results in Figures 10D and 9B, the three-fold increase in ADP concentration in *Ampd3*$^{-/-}$ erythrocytes predicts only a 0.2-0.5 mmHg increase in the p50 value of Hb-A. Therefore,

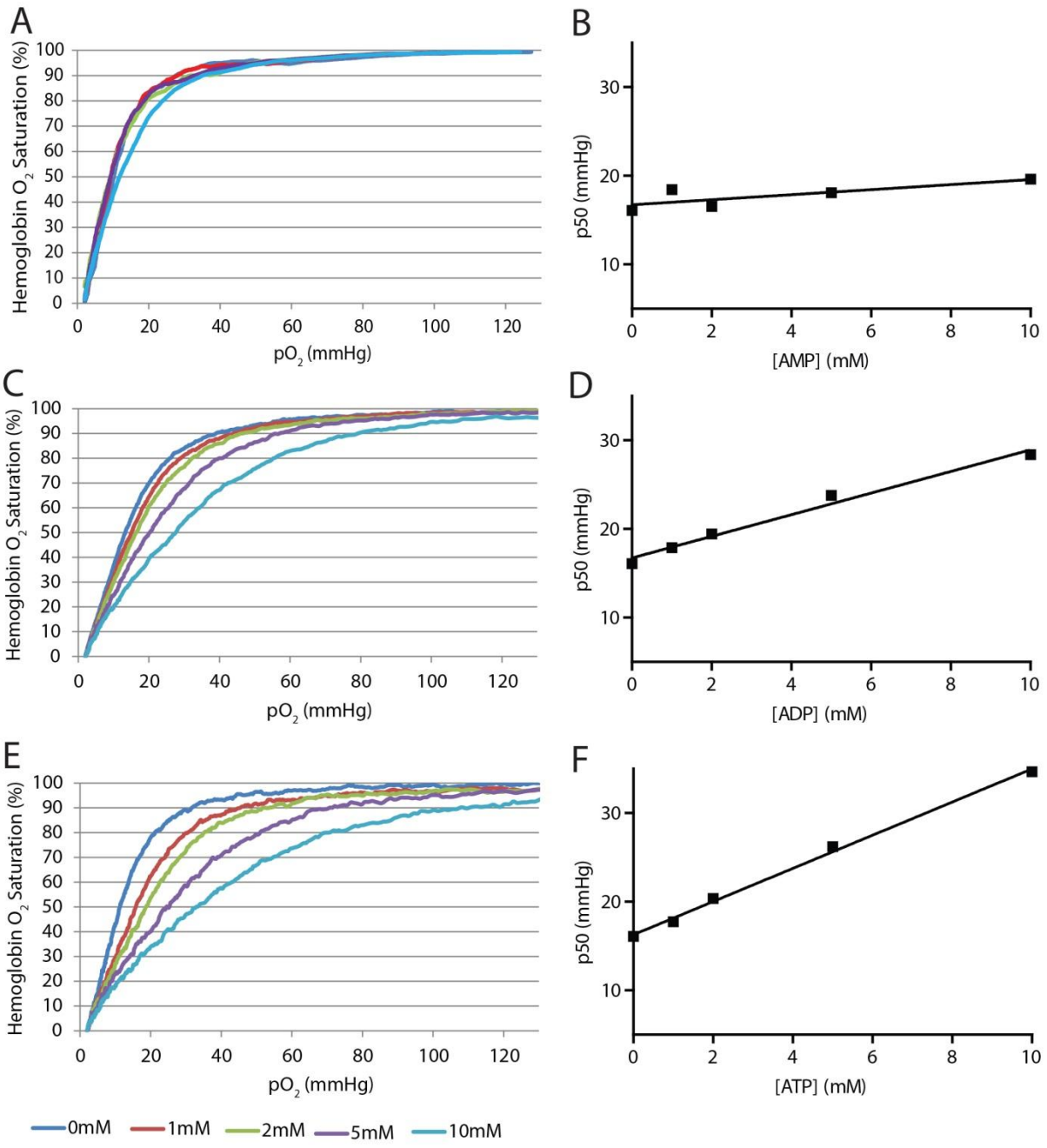

Figure 10. Adenine nucleotides' effects on p50 of hemoglobin. Adenine nucleotide titrations at 37°C against human hemoglobin in the presence of 1 mM 2,3-BPG: A) and B) 5'-AMP, C) and D) ADP, and E) and F) ATP. The left-hand figures show the oxygen saturation curves for the various concentrations and the right-hand figures are plots of the p50 values from the saturation curve plotted against the respective adenine nucleotide concentration.

the increase in intracellular ADP is likely a negligible contributor to the observed rise in *Ampd3*$^{-/-}$ erythrocytes' p50 value.

The effect of ATP concentration on Hb-A's p50 value was linear up to 10 mM, with a steeper slope (1.9 mmHg / mM) than seen for AMP (0.28 mmHg / mM) or ADP 1.2) mmHg / mM) (Figure 10). This difference indicates that ATP is more effective as a modulator of Hb-A p50 than the other two nucleotides. Based on the physiological concentrations of ATP in wild type mammalian erythrocytes of 1.0-2.5 mM, the data from Figures 9C and 10F predict that the 3.2-fold increase in ATP concentration in *Ampd3*$^{-/-}$ (versus wild type erythrocytes) would increase the Hb p50 value by 4-9 mmHg. This value is consistent with the observed average difference in erythrocyte p50 values of about 6 mmHg. These findings suggest that the shift in p50 is primarily caused by the increase in intracellular ATP in the *Ampd3*$^{-/-}$ erythrocytes.

3.2 Discussion

Energy homeostasis in a living organism is maintained by regulation of systemic metabolism (Coll and Yeo, 2013). The role of erythrocytes in the regulation of systemic metabolic control is well recognized, as illustrated by the use of blood doping (artificially boosting the number of erythrocytes in circulation) to enhance athletic performance (Lundby et al., 2012, Vogel et al., 2014), or by the induction of hypothermia through blood loss (Ikeda, 1965, Marion et al., 1996). In our previous reports we have proposed that the erythrocyte adenylate equilibrium was perturbed upon an acute uptake of AMP (Daniels et al., 2010, Daniels et al., 2013), leading to systemic metabolic repression (Ikeda, 1965). These observations raised the question of how erythrocyte adenine nucleotide levels regulate oxygen transport and, thereby, systemic metabolism. As ATP

is the currency of consumable energy for biochemical reactions in cellular processes, its production and consumption must be tightly regulated (Dzeja and Terzic, 2009). The energy charge of the adenine nucleotide pool, as reflected in the adenylate equilibrium, ATP + AMP <=> 2ADP, reflects the balance of energy production and consumption in a cell (Dzeja and Terzic, 2009). The ultimate availability of ATP depends on the level of the total adenine nucleotide pool (ATP + ADP + AMP), which in turn depends on the rates of synthesis and degradation of one component of this pool, AMP (Ataullakhanov and Vitvitsky, 2002). The intracellular catabolism of AMP is primarily carried out by AMPD in the erythrocyte (Daniels et al., 2013). The three known tissue-specific isoforms of the enzyme, AMPD1, AMPD2 and AMPD3, are expressed in muscle, liver, and erythrocytes, respectively (Mahnke-Zizelman and Sabina, 1992). AMPD3 is the only isoform present in erythrocytes and it is expressed in other tissues at low levels (Daniels et al., 2013). *Ampd3* expression is activated in response to energy imbalance (Chapman and Atkinson, 1993), oxidative stress (Tavazzi et al., 2001), or Ca^{2+}-calmodulin signaling (Mahnke and Sabina, 2005). Unlike cells of other tissues, erythrocytes have no salvage pathway that converts IMP back to AMP, because they are deficient in adenylosuccinate synthetase and lyase (Lowy and Dorfman, 1970). Thus, catabolism of AMP by AMPD3 in erythrocytes results in an irreversible loss of this nucleotide from the adenine nucleotide pool. Therefore, blocking AMP's main catabolic pathway, by targeted gene disruption of *Ampd3*, could result in an enlarged pool of adenine nucleotides. The cellular adenylate equilibrium preferentially maintains the majority of the adenine nucleotide pool as ATP (Hardie et al., 1998). As expected, humans lacking AMPD3 have a large increase in ATP levels in their erythrocytes, as do

mice deficient in AMPD3 (Ogasawara et al., 1987; Cheng et al., 2012; Daniels et al., 2013).

In order to further understand how erythrocyte AMP levels regulate systemic metabolism, we generated mice deficient in the two major intra- and extracellular AMP catabolic enzymes, the *Ampd3*$^{-/-}$/*Cd73*$^{-/-}$ model. Having shown that mice respond to an increase in AMP by entering AIHM (Daniels et al., 2010), we expected these mice to have a decrease in activity when compared to the wild type mice. Unexpectedly, we observed that the level of wheel running by *Ampd3*$^{-/-}$/*Cd73*$^{-/-}$ mice was on average 3-fold higher than wild type or *Cd73*$^{-/-}$ mice, and about 1.5-fold higher than *Ampd3*$^{-/-}$ mice (Figure 6). This differential in wheel running was consistent with the double knockout mice's elevated daily VO_2 and food intake compared to those of wild type, *Cd73*$^{-/-}$, or *Ampd3*$^{-/-}$ mice. These observations suggest that the metabolic regulatory pathways of extracellular CD73 and intra-erythrocyte AMPD3 are physiologically linked. Interestingly, when the mice did not have access to exercise (i.e., no wheel in cage), the basal metabolic activities among the four genotypes were comparable. This suggests that much of the increase in VO_2 of the *Ampd3*$^{-/-}$/*Cd73*$^{-/-}$ mice was driven by increased muscle activity during exercise and not by a general increase in basal metabolic state. We suspected that erythrocytes of the *Ampd3*$^{-/-}$/*Cd73*$^{-/-}$ mice were able to deliver greater levels of oxygen to working muscles thereby supporting more sustained periods of wheel running and leading to greater levels of oxygen consumed. To provide for the larger energy consumption during exercise, the *Ampd3*$^{-/-}$/*Cd73*$^{-/-}$ mice on average ate more food (Figure 7).

The results above raised the question of just how the loss of both CD73 and AMPD3 results in erythrocytes delivering greater amounts of oxygen to muscle during

exercise. We suspected that this effect stems from the fact that the two enzymes together regulate the erythrocyte adenine nucleotide pool, acting at different cellular locations. When erythrocyte adenine nucleotides were measured in mice of the four genotypes (Figure 9), the total levels of adenine nucleotides in AMPD3 deficient mice (both *AMPD3*$^{-/-}$ and *Ampd3*$^{-/-}$/*Cd73*$^{-/-}$) were about three-fold higher than those from wild type or *Cd73*$^{-/-}$ mice. Remarkably, the ratio of ATP:ADP:AMP was still maintained close to 100:10:1 in the *Ampd3*$^{-/-}$ erythrocytes, presumably by the adenylate equilibrium system. Consequently, the majority of the increase in adenine nucleotides in the *Ampd3*$^{-/-}$ erythrocytes came from the increase in ATP levels. When comparing the levels of ATP and ADP in *Ampd3*$^{-/-}$/*Cd73*$^{-/-}$ versus *Ampd3*$^{-/-}$ erythrocytes, the levels in the former were significantly elevated suggesting CD73 has an additive contribution to the increase of intracellular levels of adenine nucleotides in erythrocytes. Taken together, these data suggest that the increase in the adenine nucleotides is partly responsible for allowing the erythrocytes to deliver more oxygen in AMPD3 deficient mice (both *AMPD3*$^{-/-}$ and *Ampd3*$^{-/-}$/*Cd73*$^{-/-}$).

These findings of the increase in adenine nucleotide levels in the AMPD3 deficient mice led to the question of how the change in erythrocyte adenine nucleotide levels results in an increase in systemic metabolism. We reasoned that erythrocytes' regulation of metabolism likely involves regulation of the erythrocytes' main biological function, namely oxygen transport. When comparing erythrocytes from the 4 genotypes of mice (Figure 8), those from mice deficient in AMPD3 had p50 values that were on average about 6 mmHg higher compared with those from mice with functional AMPD3, indicating that the loss of AMPD3 is the main contributor to the observed increase in the p50 values. Intriguingly, whereas the average p50 value of *Ampd3*$^{-/-}$/*Cd73*$^{-/-}$

erythrocytes was noticeably higher than that from the *Ampd3*$^{-/-}$ genotype, the p50 values of *CD73*$^{-/-}$ erythrocytes were similar to those of wild type. These observations suggest that the role of CD73 in regulating erythrocyte adenine nucleotides becomes more prominent in the absence of AMPD3 while suggesting that the increase in ATP levels in the mice without functional AMPD3 was directly resulting in the increase in systemic metabolism as measured by the wheel running activity from figure 6.

We then examined how changes in adenine nucleotide levels affect the p50 of Hb. Do they act as direct modulators or do they act indirectly via changes in 2,3-BPG or pH? We found erythrocyte 2,3-BPG levels among mice of the four genotypes were similar (Figure 8). Furthermore, erythrocyte intracellular pH values of all 4 genotypes of mice were well within the established pH range of normal erythrocytes (Funder and Wieth 1966). Based on these findings, we conclude that the increase in p50 values observed in *Ampd3*$^{-/-}$ erythrocytes was not driven by increased 2,3-BPG levels or decreased intracellular pH. We then tested whether adenine nucleotides can regulate the p50 of Hb either directly or through another mechanism. Hb's affinity for oxygen can be regulated by many types of organic phosphates (Benesch and Benesch, 1967), so we examined the effects of adenine nucleotides on the p50 values of purified Hb-A. Consistent with findings from Benesch and Benesch (1967), we observed that ATP and ADP increased purified Hb-A p50 values (Figure 10). We observed a linear correlation between increasing concentrations of ATP or ADP with increases in p50 values of Hb-A. Consistent with previous findings, we observed that AMP has only a weak effect on purified Hb-A affinity for oxygen (Lo and Schimmel, 1969). While ADP can significantly alter Hb affinity for oxygen and increase its p50 value, the concentration required to shift the p50 by about 6 mmHg was estimated to be about 5 mM based on the

correlation between p50 values and ADP concentration shown in Figure 10D. Given that the physiological concentration of intracellular ADP in wild type erythrocytes is between 0.1-0.2 mM, a three-fold increase in this concentration cannot account for the observed *Ampd3*$^{-/-}$ erythrocytes' increase in p50 values. The concentration of ATP in wild type erythrocytes is between 1-2.5 mM (Benesch and Benesch, 1967, Miseta et al., 1993). We observed that ATP at this concentration can potently increase Hb's p50 value. Our present study shows that the loss of AMPD3 results in about a three-fold increase in ATP levels compared with wild type erythrocytes. This would put the estimated ATP concentration in AMPD3 deficient erythrocytes at between 3-7.5 mM, comparable to the reported K_d (2.55 mM) of ATP binding to the Hb-A (Benesch and Benesch, 1974). Based on the correlation between ATP concentration and Hb p50 value, we estimate this increase in *Ampd3*$^{-/-}$ erythrocyte ATP levels would generate an increase of between 4 to 9 mmHg in Hb p50 values, in line with the increase observed in *Ampd3*$^{-/-}$ erythrocytes. Thus, it is reasonable to conclude that accumulation of ATP in erythrocytes contributes to the majority of the increase in p50 values of AMPD3-deficient over normal erythrocytes.

Our studies identify AMPD3 as a major regulator of the adenine nucleotide pool in the erythrocytes. While the loss of CD73 itself appears to have little impact on the erythrocytes' p50 value, we can only speculate on the impact of extracellular AMP influx into erythrocytes deficient in AMPD3 *in vivo*. We reason that AMP influx must exert a dynamic and significant impact on the erythrocytes' ability to release oxygen, since systemic metabolism and the total adenine nucleotide pool are significantly elevated in *Ampd3*$^{-/-}$*/Cd73*$^{-/-}$ compared to *Ampd3*$^{-/-}$ mice.

It has been argued that Hb binding of oxygen is too tight in the absence of

organic phosphate to be physiologically useful (Garby et al., 1969). Hb binding of 2,3-BPG lowers the Hb affinity for oxygen to a range where H^+, CO_2, and other organic phosphates that occur at lower physiological concentrations could then fine tuned Hb affinity for oxygen. Since 2,3-BPG is the metabolite that can be synthesized without perturbing the adenylate ratios, the possible role of the adenine nucleotides in modulating Hb affinity for oxygen has not been considered important (Garby et al., 1969). By contrast, other studies have implicated the importance of ATP in regulating Hb affinity for oxygen (Weber and Lykkeboe 1978). In some ectothermic species, such as fish, ATP has been shown to be a major mediator of Hb's affinity for oxygen (Gupta et al., 1978). Our present studies indicate that the mammalian erythrocyte ATP levels are a major modulator of Hb affinity for oxygen, similar to ectothermic species.

Previous studies have demonstrated that both ATP and 2,3-BPG bind to Hb with comparable affinity (Benesch and Benesch, 1974, Weber and Lykkeboe, 1978, Gupta et al., 1979). Here, we have carried out measurements of ATP's effects on Hb-A p50 values in the absence and presence of 2,3-BPG (Figure 11). The p50 values obtained in the presence and absence of 2,3-BPG over a range of ATP concentrations were nearly parallel suggesting that the effects of 2,3-BPG and ATP on Hb-A p50 values are additive. Since both of these organic phosphates occur in erythrocytes at physiological concentrations in the millimolar range, it is likely that the Hb p50 value is regulated in part by the total intracellular levels of 2,3-BPG and ATP. Thus, we propose that a change in erythrocyte ATP levels during metabolic activities could be a mechanism to achieve finer dynamic control of oxygen delivery to tissues.

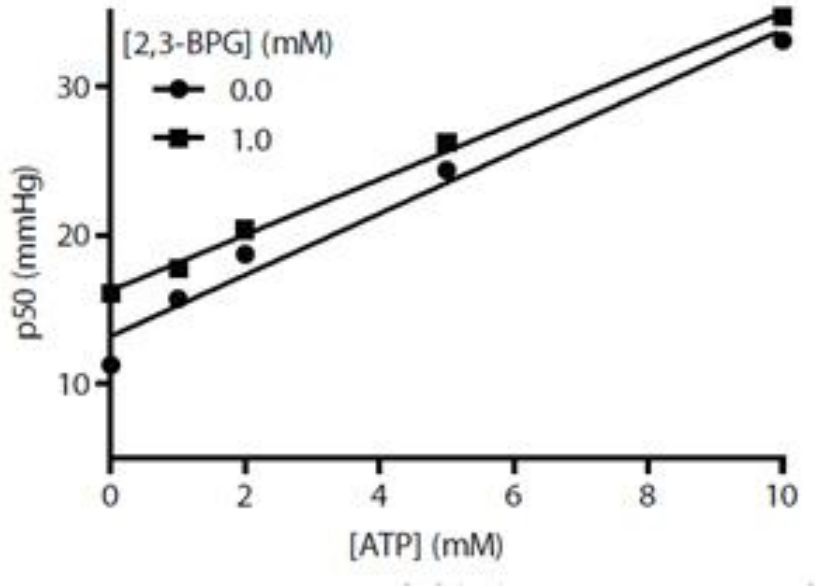

Figure 11. ATP's efficacy on p50 shift of HbA in the presence and absence of 2,3-BPG. ATP titration against HbA in the presence and absence of 1mM 2,3-BPG.

4. Unraveling the mechanism of 5'-AMP induced hypometabolism in mouse models

4.1. Results

4.1.1. Analysis of AIHM and torpor response in mice with deficiency in CD73 and AMPD3.

Having analyzed the physiological impact of deficiency in both AMPD3 and CD73, we next investigated how these mice would respond to AIHM compared to wild type or mice deficient in either AMPD3 or CD73. First, we measured and compared the length of time mice remain in AIHM or induced torpor, in response to a sub-obtimal dose of AMP (0.2 mg/gw) to see if the *Ampd3*$^{-/-}$/*Cd73*$^{-/-}$ mice were more sensitive to AMP. Throughout this experiment, the mice were kept in a Comprehensive Lab Animal Monitoring System (CLAMS) with the ambient temperature (T_a) set at 15°C and the VO_2 of individual animals was recorded. For the analysis of this experiment, we considered an animal to be in a torpor state when its VO_2 dropped below 1200 mL/kg/h. We previously have shown that mice deficient in either CD73 or AMPD3 stayed in AIHM longer than wild type mice when given a lower dose of AMP (Daniels et al., 2010, Daniels et al., 2013). Here, we observed that mice deficient in both CD73 and AMPD3 remained in AIHM for an average length of 9h, while wild type mice failed to enter the AIHM state with VO_2 levels staying above 1200 mL/kg/h after AMP injection (Figure 12). The VO_2 of most of the *Ampd3*$^{-/-}$ mice dropped below 1200 mL/kg/h for an average length of 2 h. The *Cd73*$^{-/-}$ mice responded more severely than the *Ampd3*$^{-/-}$ mice, typically staying in the AIHM for an average length of 6 h. Next, we compared the length of AIHM of the different genotypes upon receiving the optimal dosage of AMP (0.5 mg/gw). At this dosage all the mice in these studies entered deep AIHM after 2

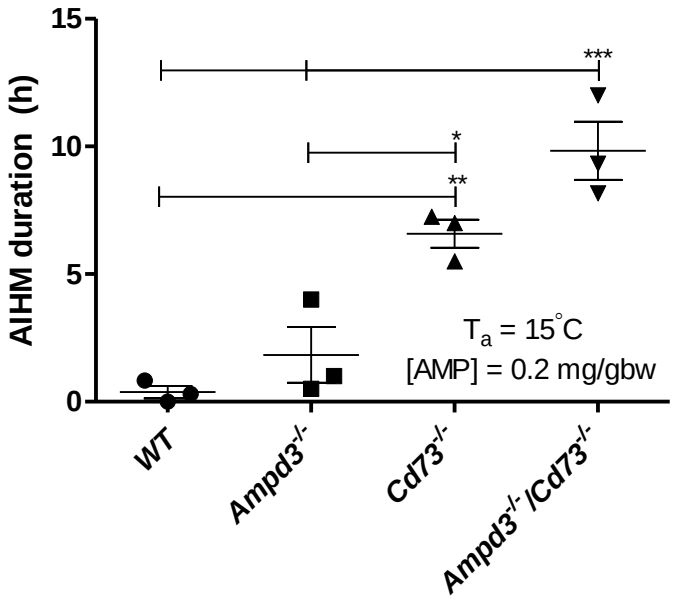

Figure 12. Loss of AMPD3 and CD73 impact on AIHM under sub-optimal AMP dose. Mice from each genotype (N=3) were injected with a sub-maximal dose of AMP (0.2 mg/gbw) and placed at an ambient temperature of 15°C. The amount of time in AIHM was calculated from injection to when they increase their VO_2 to 1200 mL/kg/h or, in the case of the wild type mice, until their VO_2 starts to increase. P values = * < .05, ** < .005, and *** < .0001.

hours following administration of AMP. The cohort of wild type mice had the shortest average length of AIHM (Figure 13 A and E). Over 90% of wild type mice had already aroused from AIHM 10 h following AMP administration. In contrast, at 10 h, over 60% of *Ampd3*$^{-/-}$ mice and about 95% of *Cd73*$^{-/-}$ and *Ampd3*$^{-/-}$/*Cd73*$^{-/-}$ mice were still in AIHM (Figure 13 B, C, D, and E). The difference between *Cd73*$^{-/-}$ and *Ampd3*$^{-/-}$/*Cd73*$^{-/-}$ mice became apparent 12 h after AMP administration when about 65% of *Cd73*$^{-/-}$ mice remained in AIHM but no change was observed for *Ampd3*$^{-/-}$/*Cd73*$^{-/-}$ mice. After 14 h, when the experiment was terminated as required by our AWC protocol, the number of *Ampd3*$^{-/-}$/*Cd73*$^{-/-}$ mice that remained in the AIHM state had not changed. Together, these data demonstrate that CD73 and AMPD3 regulate the potency and length of AIHM.

4.1.2. Manipulation of Extracellular AMP modulates erythrocyte p50.

The above findings raise the question of how CD73 and AMPD3 could regulate the efficacy of 5'-AMP in mediating AIHM and the subsequent effects of torpor. Given the above findings that the AMPD3 deficient erythrocytes naturally displayed increased p50 values as a result of a physiological increase in adenine nucleotide levels, we reasoned that the observed increased response to AMP in inducing the AIHM state could be due to a direct or indirect effect of AMP affecting the p50 value of erythrocytes. Figures 8 and 9 showed that the double deficiency of CD73 and AMPD3 led to changes in levels of erythrocyte adenine nucleotides, which shifted the Hb p50 values. Here, we ask whether the addition of extracellular AMP could shift the erythrocyte p50. We have estimated that an IP injection of 0.5 mg/gw of AMP would result in an extracellular AMP concentration of about 14.4 mM based on an estimated blood volume of 10% of the body weight. To investigate the effect of AMP on the p50

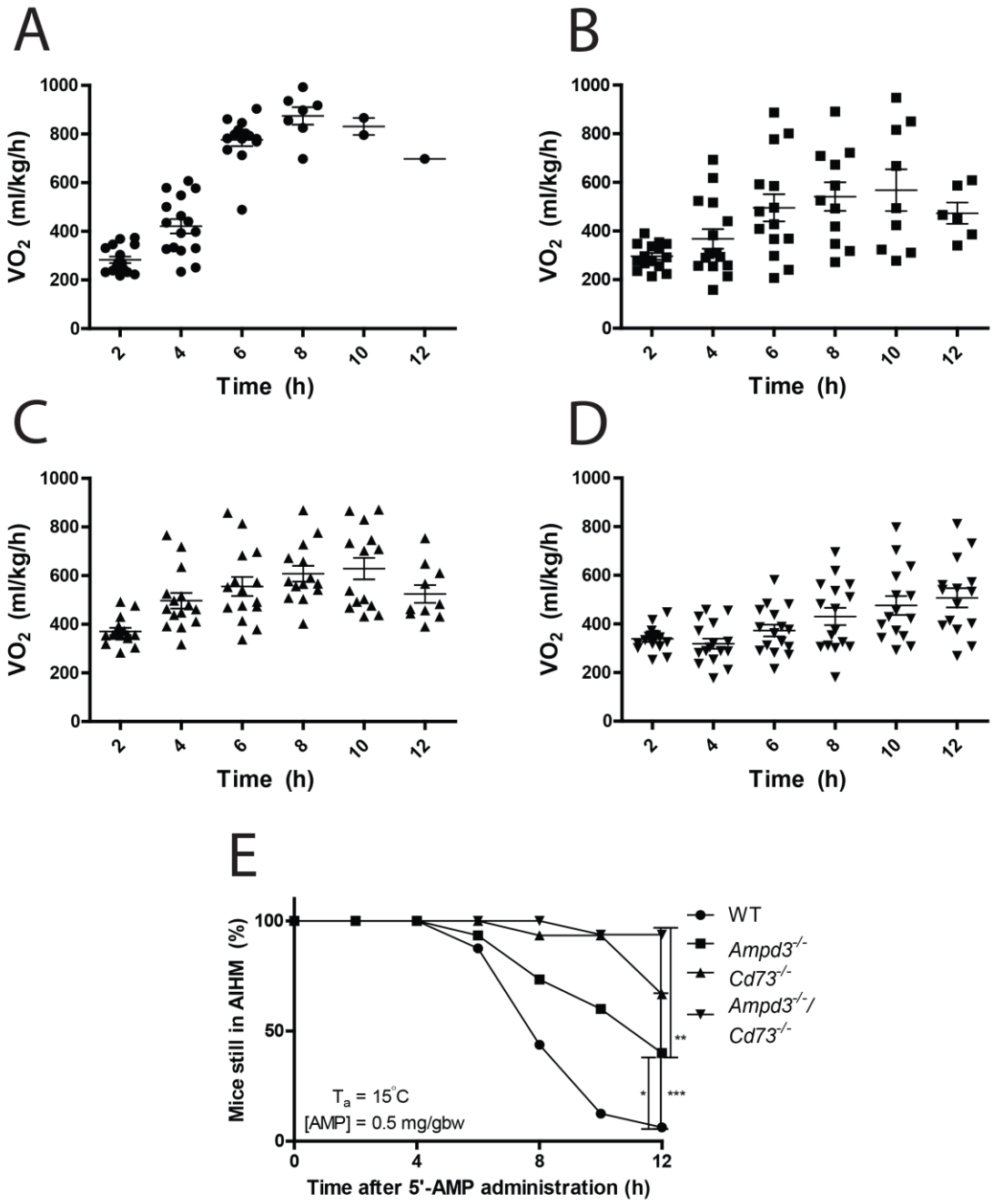

Figure 13. Loss of AMPD3 and CD73 impact on AIHM under optimal dose. (A-D) Mice from each genotype (A: wild type (N=16), B: *Ampd3*$^{-/-}$ (N=15), C:*Cd73*$^{-/-}$ (N=15), and D: *Ampd3*$^{-/-}$/*Cd73*$^{-/-}$ (N=16)) were injected with the optimal dose of AMP (0.5 mg/gbw) and placed at an ambient temperature of 15°C. The length of time each mouse stayed in AIHM was calculated from injection to when their VO_2 return to above 1200 mL/kg/h. E) Graphical representation of all four genotypes and the percent of injected animals over time. Sampling of animals in AIHM were taken every 2 h. P values = * < .05, ** < .005, and *** < .0001.

of the erythrocytes, we first tested a lower concentration of AMP (2 mM) on isolated mouse *Ampd3*$^{-/-}$/*Cd73*$^{-/-}$ erythrocytes (Figure 14 A and B); we observed a significant increase in p50 and a rightward shift in the oxygen saturation curve suggesting that AMP is lowering the erythrocytes' affinity for oxygen. The *Ampd3*$^{-/-}$/*Cd73*$^{-/-}$ erythrocytes were used to exclude the possibility of an indirect effect of AMP via dephosphorylation to adenosine. In addition, we carried out similar experiments with the same concentration of adenosine (2 mM) on isolated *Ampd3*$^{-/-}$/*Cd73*$^{-/-}$ erythrocytes. Compared to the vehicle solution, the addition of adenosine did not alter the erythrocytes' p50 significantly (Figure 14 C). This result further excluded the possibility that this shift in p50 was due to adenosine. Among all four genotypes, the isolated erythrocyte responses to AMP-induced p50 shifts were comparable (Figure 14 D).

Next, we wanted to test the response of the erythrocytes closer to the AIHM-inducing concentration, estimated at about 15 mM. We observed that the oxygen dissociation curve of the isolated mouse erythrocytes was shifted to the right by extracellular concentrations of 2-20 mM AMP with a linear (r^2=0.992) increase in p50 (Figure 14 E and F). Interestingly, despite the large shift in p50 induced by high AMP concentrations, the Hill co-efficient of the erythrocytes in the p50 experiments was not altered (Figure 14 G), indicating that the change in cooperativity of the Hb was not responsible for the large shift in p50 values.

These studies clearly demonstrate that extracellular AMP, not adenosine, modulates intact erythrocyte's p50 values. The p50 shift induced by extracellular 5'-AMP could either act indirectly via a previously unrecognized AMP-receptor mediated mechanism or directly after being taken up by erythrocytes (Daniels et al., 2010). We

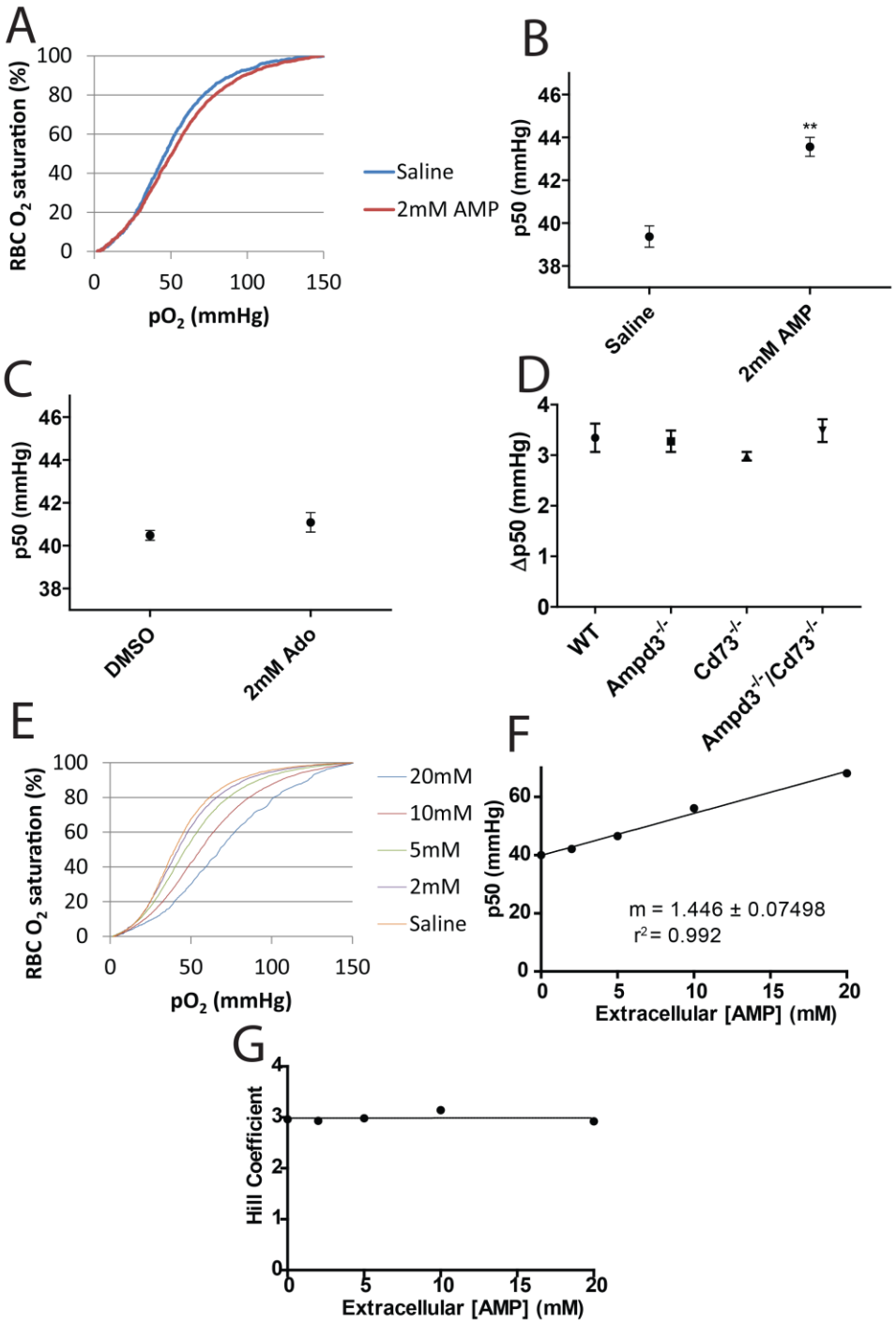

Figure 14. Effect of AMP on the p50 of intact erythrocytes. A) Erythrocytes oxygen saturation curve after addition of 2 mM AMP. B) Average erythrocytes p50 values in saline and 2 mM AMP (N=3). C) Average erythrocytes p50 values in vehicle and 2 mM Adenosine (N=3). D) Shift of p50 after 2 mM AMP incubation in the four genotypes (N=3). E) Erythrocytes oxygen saturation curves in response to extracellular AMP concentration. F) Plot of p50 values from E. G) Plot of the Hill coefficients from E. P values = ** < .005.

reasoned that a receptor based mechanism depends on the integrity of the cell. Therefore, if extracellular AMP depends on receptor-mediated mechanism to induce p50 shift, then this response should be abolished when erythrocytes were lysed. Double freeze-thawed *Ampd3*$^{-/-}$/*Cd73*$^{-/-}$ whole erythrocyte lysate was used to investigate this possibility. Evidence of the erythrocytes having undergone lysis was marked by the baseline change in p50 value in the absence of AMP. Intact mouse erythrocytes' p50 is approximately 40 mmHg. In contrast, lysate of mouse erythrocytes gave a baseline p50 of about 20 mmHg (Figure 15 A). Titration of the erythrocytes' lysate against different AMP concentrations revealed a linear p50 shift that correlates with AMP concentration and is independent of the erythrocytes lysate volume used (Figure 15 B and C). In addition, we observed that the level of p50 increase induced by AMP, whether in isolated *Ampd3*$^{-/-}$/*Cd73*$^{-/-}$ erythrocytes or its lysed counterpart, were comparable (Figure 15 D). The slopes (m) measured as the change in p50 as a function of AMP concentration were m=1 for whole erythrocytes and m=0.89 for the lysates. Together, these data show that the AMP-induced erythrocyte's p50 increase was not altered by disruption of the erythrocyte cell membrane suggesting against a receptor mediated mechanism.

4.1.3. Direct uptake of AMP by erythrocytes.

The above finding is consistent with our previous observations that erythrocytes can uptake AMP directly (Daniels et al., 2010). Although uptake of AMP by erythrocytes had been independently observed (Mathews et al., 2005), the characteristics and kinetics of this uptake remain unclear. We wanted to further investigate the mechanism of AMP uptake. Erythrocytes have equilibrative nucleoside transporters (ENTs) that readily uptake adenosine, which can be rephosphorylated into AMP by adenosine

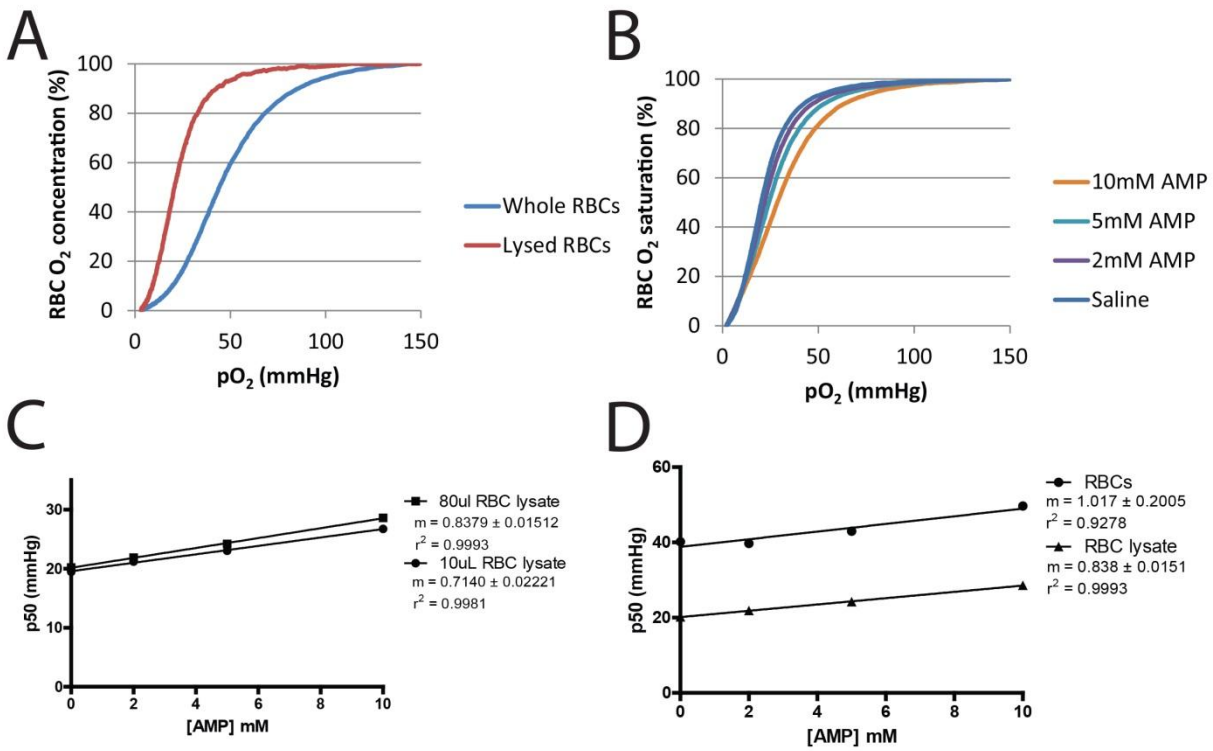

Figure 15. Effect of AMP on lysed erythrocytes and intact erythrocytes. A) Oxygen saturation curve of intact and lysed erythrocytes showing both a shift in baseline p50 value after lysis and a change in the curve shape. B) Oxygen saturation curve of erythrocyte lysate incubated with various concentrations of AMP. C) Plot of the change in p50 values in response to an AMP titration with different amounts of lysate. D) Plot of the change in p50 values in response to an AMP titration in intact and lysed erythrocytes.

kinase intracellularly. An experiment was designed to investigate whether the AMP was taken up directly or indirectly as a result of rephosphorylated adenosine. First, we verified that the dephosphorylation of AMP to adenosine by CD73 is truly absent in *Cd73*$^{-/-}$ mouse blood, using wild type mouse blood as a control. The cell lysates and supernatants, from a time-course of incubation of [^{14}C]-AMP with whole blood from the two genotypes, were profiled by thin-layer chromatography (TLC) (Figure 16 A). Interestingly, in cell fractions of both genotypes, the TLC displayed detectable levels of [^{14}C]-AMP, even at 5 min incubation, suggesting that AMP had already entered the erythrocytes. In addition, some ADP has formed from [^{14}C]-AMP through adenylate equilibrium, similar to our earlier observation (Daniels et al., 2011). The TLC analysis further revealed that the majority of [^{14}C]-AMP was already catabolized in wild type whole blood supernatant after a 15 min incubation at 37°C. By contrast, the majority of [^{14}C]-AMP remained intact in the supernatant of *Cd73*$^{-/-}$ whole blood even after 1h of incubation at 37°C. These findings are consistent with CD73 being the major extracellular catabolic enzyme for AMP (Castrop et al., 2004) and give confidence that studies using tissues deficient in CD73 would significantly eliminate dephosphorylation of AMP into adenosine.

Next, we investigated whether isolated erythrocytes would dephosphorylate AMP into adenosine, addressing the question of whether CD73 or other AMP catabolic enzymes are directly associated with erythrocytes. The isolated and washed erythrocytes were incubated with [^{14}C]-AMP over a time course spanning 5 h at 37°C. Cell and supernatant fractions were separated and analyzed by TLC (Figure 16 B). Both isolated erythrocytes from wild type and *Cd73*$^{-/-}$ mice did not catabolize [^{14}C]-AMP significantly even after 5 h of incubation at 37°C. In addition, the uptake of [^{14}C]-AMP

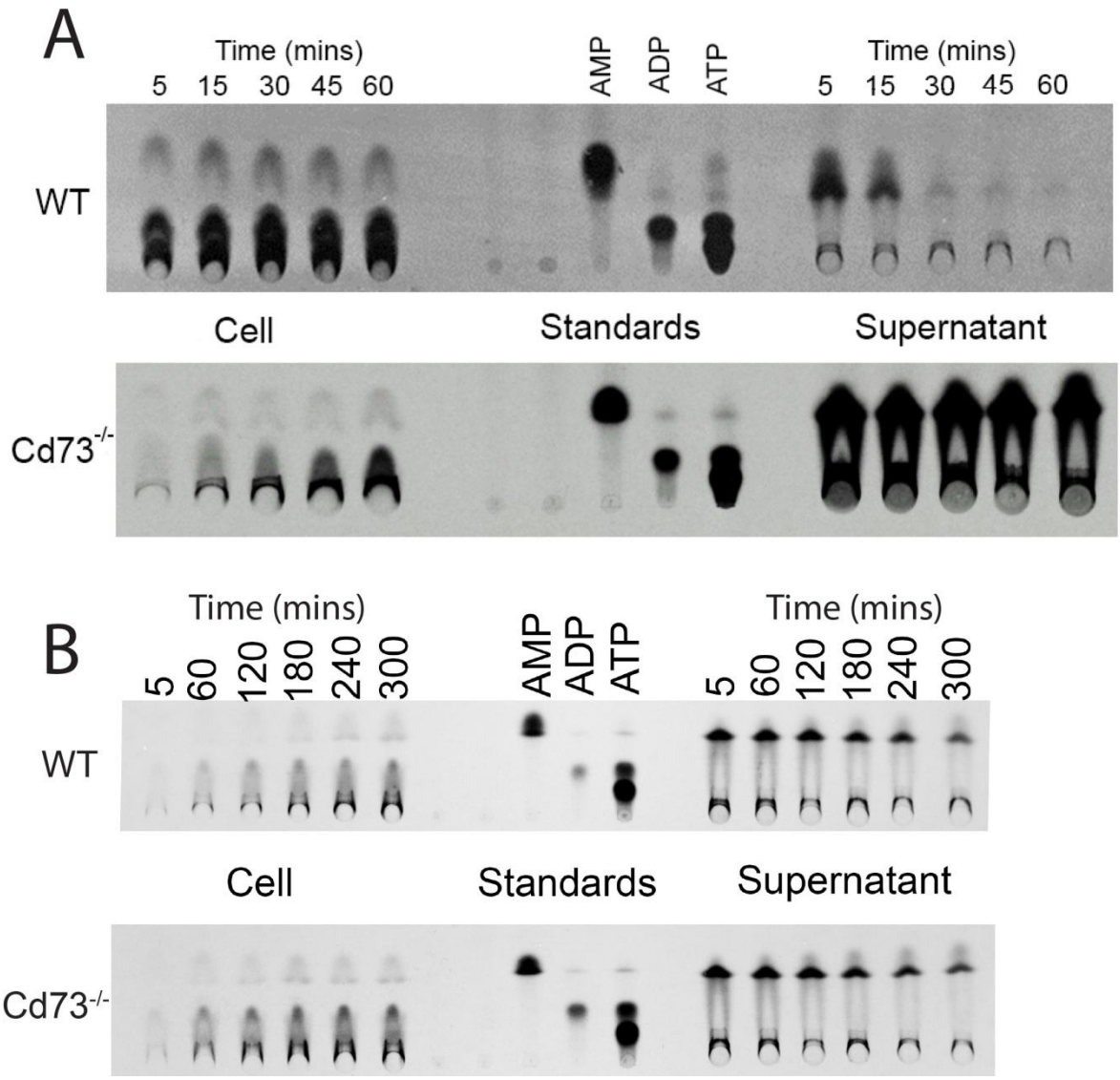

Figure 16. Stability of extracellular AMP in whole blood and in isolated erythrocytes. A) Whole blood incubation of [^{14}C] AMP from wild type and *Cd73*$^{-/-}$ mice. B) Isolated erythrocyte incubation of [^{14}C] AMP from wild type and *Cd73*$^{-/-}$ mice Note: x-ray film exposure time was selected to favor signals in the supernatant.

into the erythrocytes was comparable between the two genotypes. These studies demonstrated that uptake of [^{14}C]-AMP by erythrocytes can be direct and that CD73 is not associated directly with erythrocytes.

Finally, we investigated whether erythrocytes could also directly uptake other adenine nucleotides. Since it has been demonstrated that CD39/ATPase would convert ATP into ADP and then into AMP extracellularly (Wang and Guidotti, 1996), we investigate whether [^{14}C]-ADP would be taken up directly. Isolated *CD73*$^{-/-}$ erythrocytes were incubated with [^{14}C]-ADP over a 3 h time course. Cell and supernatant fractions were then separated at specific time points of incubation and analyzed by TLC (Figure 17). From the supernatant fraction, we observed that a significant levels of [^{14}C]-ADP had already been dephosphorylated into [^{14}C]-AMP after 5 min of incubation with isolated erythrocytes at 37°C. In the cell fraction, within the first 5 min we observed [^{14}C]-AMP but no apparent levels of [^{14}C]-ADP. No significant level of [^{14}C]-ADP was detected in the cells even after 30 min of incubation. By this time, the majority of the supernatant [^{14}C]-ADP had already been dephosphorylated to [^{14}C]-AMP. After 1 h, both [^{14}C]-AMP and [^{14}C]-ADP were detected inside the erythrocytes but the increase in [^{14}C]-ADP coincided with decreases in [^{14}C]-AMP levels suggesting that the rise in [^{14}C]-ADP could be a result of the erythrocytes adenylate equilibrium rebalancing the cellular adenine nucleotides ratio rather than via ADP uptake by the erythrocytes. Together, these studies suggest that the outer membrane of erythrocytes contained CD93/ATPase but not CD73, or another 5'-nucleotidase, and that erythrocytes readily uptake AMP but not ADP.

4.1.4. Kinetics of AMP uptake by erythrocytes.

To better understand the uptake of AMP by erythrocytes, we investigated the

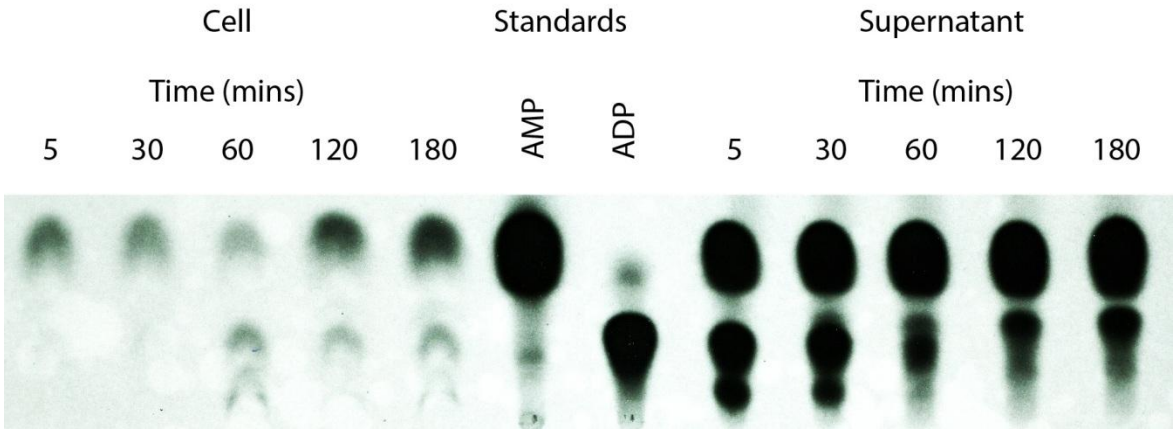

Figure 17. Kinetics of ADP metabolism by isolated erythrocytes. A suspension of washed erythrocytes (150 x 10^6 cells in 15 µl) was incubated with 1 mM [^{14}C] AMP at 37°C for the indicated lengths of time before the nucleotide products inside (cells) or outside (supernatant) the erythrocytes were extracted and analyzed by TLC.

kinetics of this uptake process. We reasoned that if this uptake was enzymatically mediated, we should be able to calculate the K_m and V_{max} of the corresponding protein. Radiolabelled [^{14}C]-AMP was incubated with isolated wild type mouse erythrocytes at 37°C. At specific time points of this incubation, aliquots of the reaction mixture were separated by centrifugation into cell and supernatant fractions. The cell fraction was further washed 3 times with 1ml PBS, and the supernatant of the initial wash was kept. The levels of radioactivity in the cell, supernatant, and first wash fractions were then determined with a scintillation counter. The percentages of the radioactivity from the three fractions were plotted against the time of incubation (Figure 18 A). We observed that the percentage of radioactivity in the wash fraction was constant over the entire time course. The supernatant fractions have the highest percentage of radioactivity at the beginning of the time course, but the levels declined over time. Corresponding to this decline, the radioactivity in the cell fraction, which was lowest at the beginning of the time course, now increased over time. We observed a reciprocal inversion of radioactivity between cell and supernatant fractions, which was linear during the initial 2 h of the incubation.

Based on conditions established in the experiment above, the amount of AMP uptake was measured against the extracellular AMP using a 45 m incubation period at 37°C. We observed that erythrocytes' uptake of AMP was linearly related (r^2= 0.97) to the extracellular concentration of AMP, up to 10 mM for isolated wild type (Figure 18 B) and *Cd73*$^{-/-}$ erythrocytes (Figure 18 C). There was no major difference between wild type and *Cd73*$^{-/-}$ erythrocytes at extracellular AMP concentrations above 1 mM. However, within the concentration range below 1 mM, we observed a "saturable" component from wild type but not in *CD73*$^{-/-}$ erythrocytes (Figure 18 D and E). We

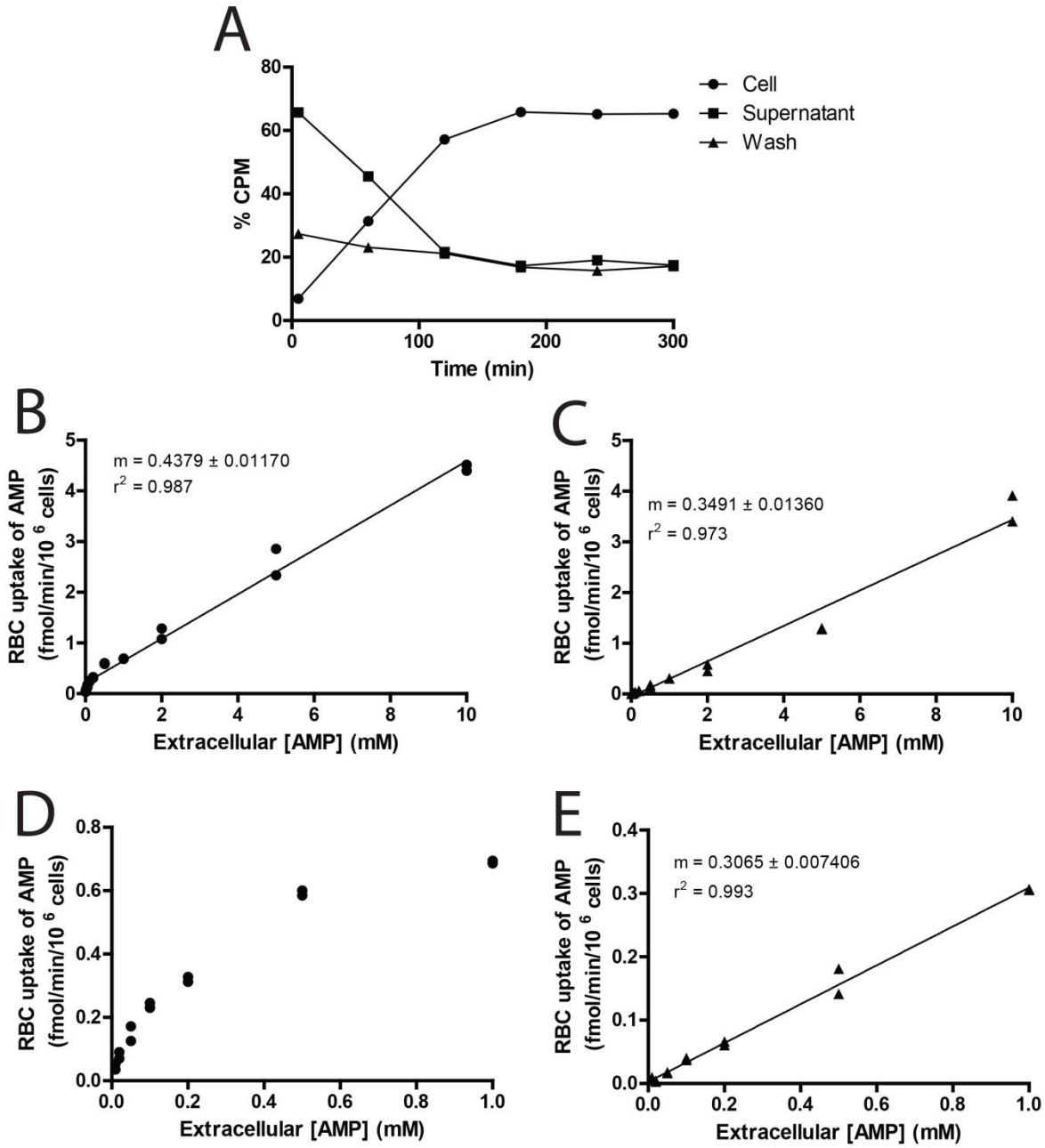

Figure 18. Concentration dependence of AMP uptake by erythrocytes. A) The fractions of total added radioactivity in the supernatant, erythrocyte, and wash fractions at the indicated times after adding [^{14}C]-AMP (1 mM) to suspended erythrocytes (150 x 10^6 cell/ 15 µl) at 37°C. Uptake of AMP by wild type (B) and *Cd73*$^{-/-}$ (C) erythrocytes up to 10 mM extracellular AMP. Plots of up take in the range of 0 - 1 mM extracellular AMP concentrations in wild type (D) and *Cd73*$^{-/-}$ (E) erythrocytes.

reasoned that wild type samples have trace amounts of CD73, likely from the low level of white blood cells that were not completely removed when the erythrocytes were isolated. The CD73 dephosphorylates the extracellular AMP to adenosine, which can then enter the erythrocytes via the ENTs. This small adenosine uptake due to the trace amount of CD73 “contamination” in the wild type isolated erythrocytes. Above 0.1 mM extracellular concentration, the AMP uptake was linear, as such the K_m and V_{max} values could not be determine. Together, these findings suggest that erythrocytes have a very large relative capacity to uptake extracellular AMP, presumably through a pore or channel.

As mentioned above, we surmised that this uptake could be based on membrane pores or specific channels. However, there is no known channel(s) for transporting AMP across the erythrocyte membrane. There are known adenine nucleotides transporters, ATP-ADP translocase (ANT), which are members of the solute carrier family 25 (slc25) proteins in the mitochondria (SLC25a 4-6 and 31) and peroxisomes (SLC25a17). The mitochondria but not the peroxisomes ANT’s are sensitive to carboxyatractyloside (CAT) inhibition (Guitierrez-Aguilar and Baines, 2013). Therefore, we carried out an uptake study to determine if CAT had an impact on AMP uptake by the erythrocytes. We observed that the erythrocytes’ uptake of AMP was not significantly affected by the addition of CAT (Figure 19 A).

Erythrocytes express ENT1 that mediates the uptake of adenosine. Could ENT1 also mediate the uptake of AMP? Since ENT1 is sensitive to inhibition by dipyridamole, we examined the AMP uptake of erythrocytes in the presence of 10 µM dipyridamole. We found that the AMP uptake was not significantly affected by the addition of dipyridamole (Figure 19 B).

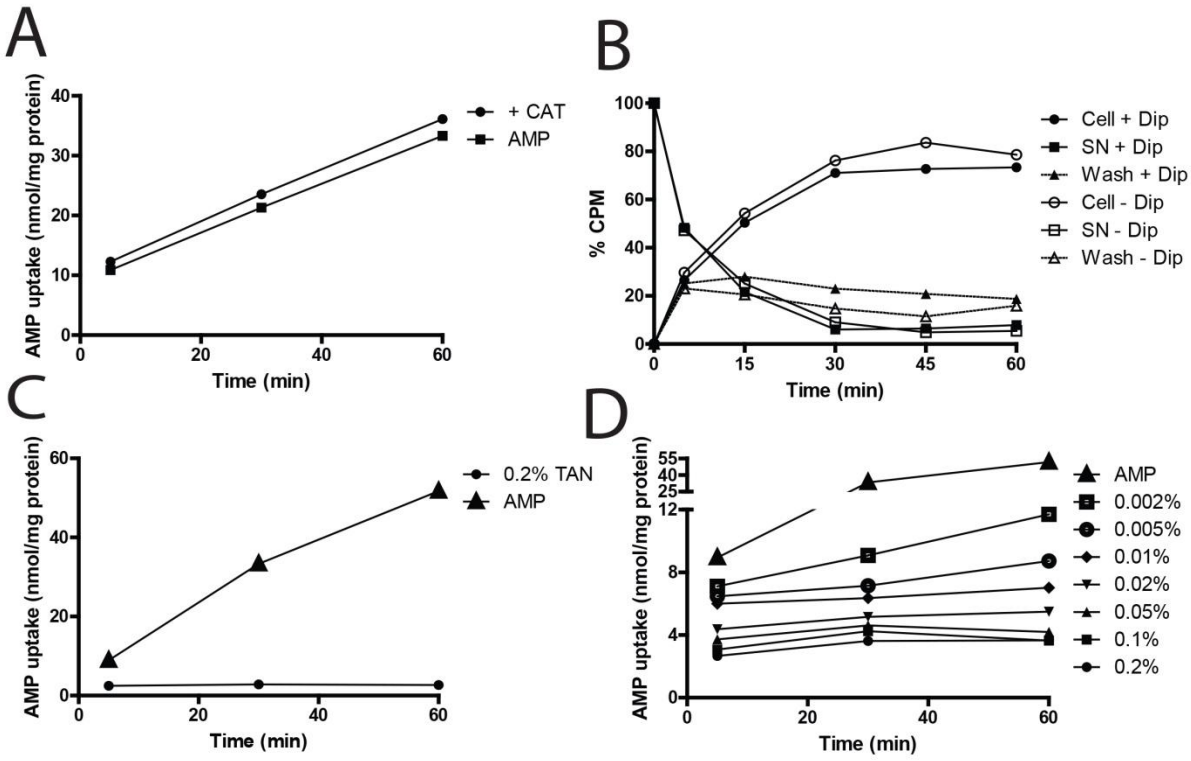

Figure 19. Inhibitors of AMP uptake by erythrocytes. A) CAT effect on erythrocytes AMP uptake. B) Dipyridamole (Dip) effect on erythrocytes AMP uptake. C) Tannic Acid (TAN), inhibition of erythrocytes AMP uptake. D) Titration of TAN concentration against erythrocytes AMP uptake.

Next, we investigated whether chloride channel inhibitor Tannic Acid (TAN), which has been shown to be a highly effective inhibitor of adenine nucleotide transporter (SLC25a family) and Ca^{2+} and Cl^- ion channels (Namkung et al., 2010), had an effect on AMP uptake. We observed a strong inhibitory effect on erythrocytes' uptake of radiolabeled [^{14}C]-AMP by 0.2% of TAN, a commonly used dose (Figure 19 C). Next, we carried out a titration for the effective dose of TAN on inhibition of AMP uptake (Figure 19 D). We observed that the amount of AMP uptake by the erythrocytes was significantly reduced when the concentration of TAN decreased to below 0.01%. We could conclude that AMP uptake was sensitive to TAN interaction with the erythrocytes. Together, these studies suggest that uptake of AMP by erythrocytes is insensitive to CAT inhibition but is sensitive to TAN inhibition.

Next, we investigate if the erythrocytes' AMP uptake is competively inhibited by cellular metabolites. We examined various common cellular metabolites including ATP, ADP, adenosine, cAMP, CMP, GMP, glucose, lactate, and urea. The uptakes of [^{14}C]-AMP by wild type erythrocytes with and without 1 mM of the competing metabolite were compared (Figure 20 A). We observed that glucose, urea, lactate, and adenosine had minimal effect on AMP uptake by erythrocytes. While all nucleotides tested show some level of inhibition of or competition with [^{14}C]-AMP uptake, cAMP is the least effective one, followed by CMP. The inhibition effect of ATP was as strong as unlabeled AMP, while ADP was only slightly less effective. Interestingly, GMP appeared comparable to ADP in inhibiting uptake or in competing with AMP for uptake by erythrocytes. We further characterized this putative inhibition by GMP on AMP uptake by the erythrocytes by comparing the effect of increasing extracellular AMP in the presence and absence of 1 mM GMP (Figure 20 B). We observed that the rate of AMP uptake

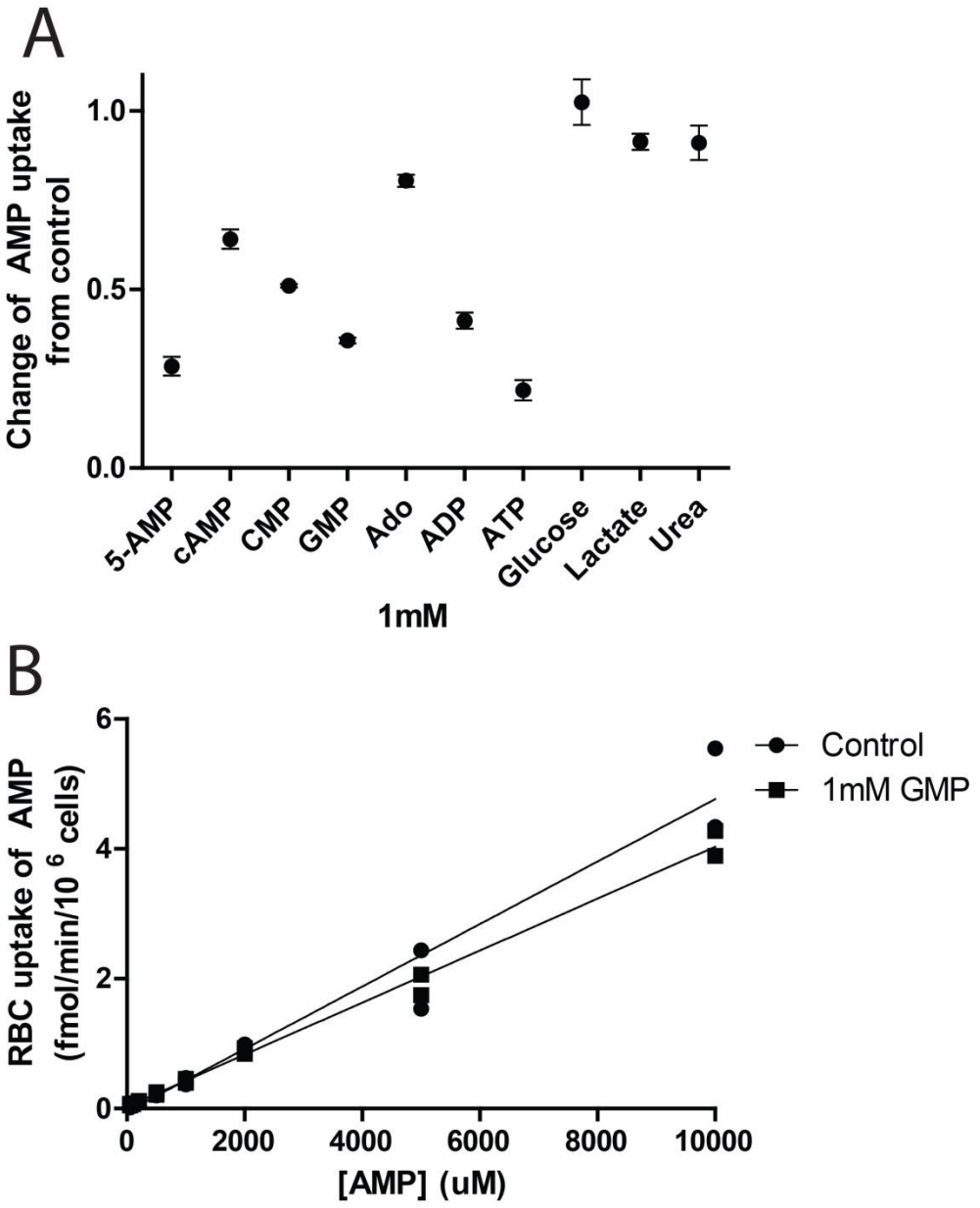

Figure 20. Competitive nucleotide inhibitors of AMP uptake by erythrocytes. A) AMP uptake inhibition assay using common metabolites and nucleotides/nucleoside. B) Examining GMP inhibition of AMP uptake under increasing concentration of extracellular AMP.

was driven by the extracellular concentration and was not inhibited by GMP. Together these studies suggest that the putative channel/pore for AMP uptake by erythrocytes has some level of specificity to adenine nucleotides.

4.1.5. AMP uptake leads to change in intracellular adenine nucleotide levels.

Physiological AMP levels in the wild type erythrocytes have been estimated to be about 25 µM. The above findings that erythrocytes' uptake of AMP was linear, even when the extracellular AMP level was 20 mM, raises the question as to its impact on the erythrocyte adenylate pool and its link to the large p50 increase observed. To obtain measurements of intracellular adenine nucleotide levels correlated to various levels of extracellular AMP, isolated erythrocytes from each of the genotypes were incubated with varying concentrations of extracellular AMP, up to 20 mM at 37°C. After 15 min, the cells were separated from the supernatant, washed, and the cell's nucleotides were extracted using acid extraction methods. The neutralized cell extracts were analyzed by HPLC. Based on ATP, ADP, and AMP standards and their absorbance spectra, the levels of each of these adenine nucleotides in the respective erythrocyte samples were determined. Here we show the data obtained from erythrocytes from each genotype (Figures 21, 22, 23). Even though the levels of erythrocyte adenine nucleotides were 3 times higher in the *AMPD3*$^{-/-}$ genotypes, the erythrocytes from all the genotypes in these studies show similar correlative trends as described below.

Similarly to the AMP uptake experiments using [^{14}C]-AMP, the HPLC approaches also revealed a linear uptake of AMP into the cell that is driven by the concentration of extracellular AMP (Figure 21). At 20 mM extracellular AMP, the intracellular AMP has increased over 30-fold from the physiological level. The HPLC

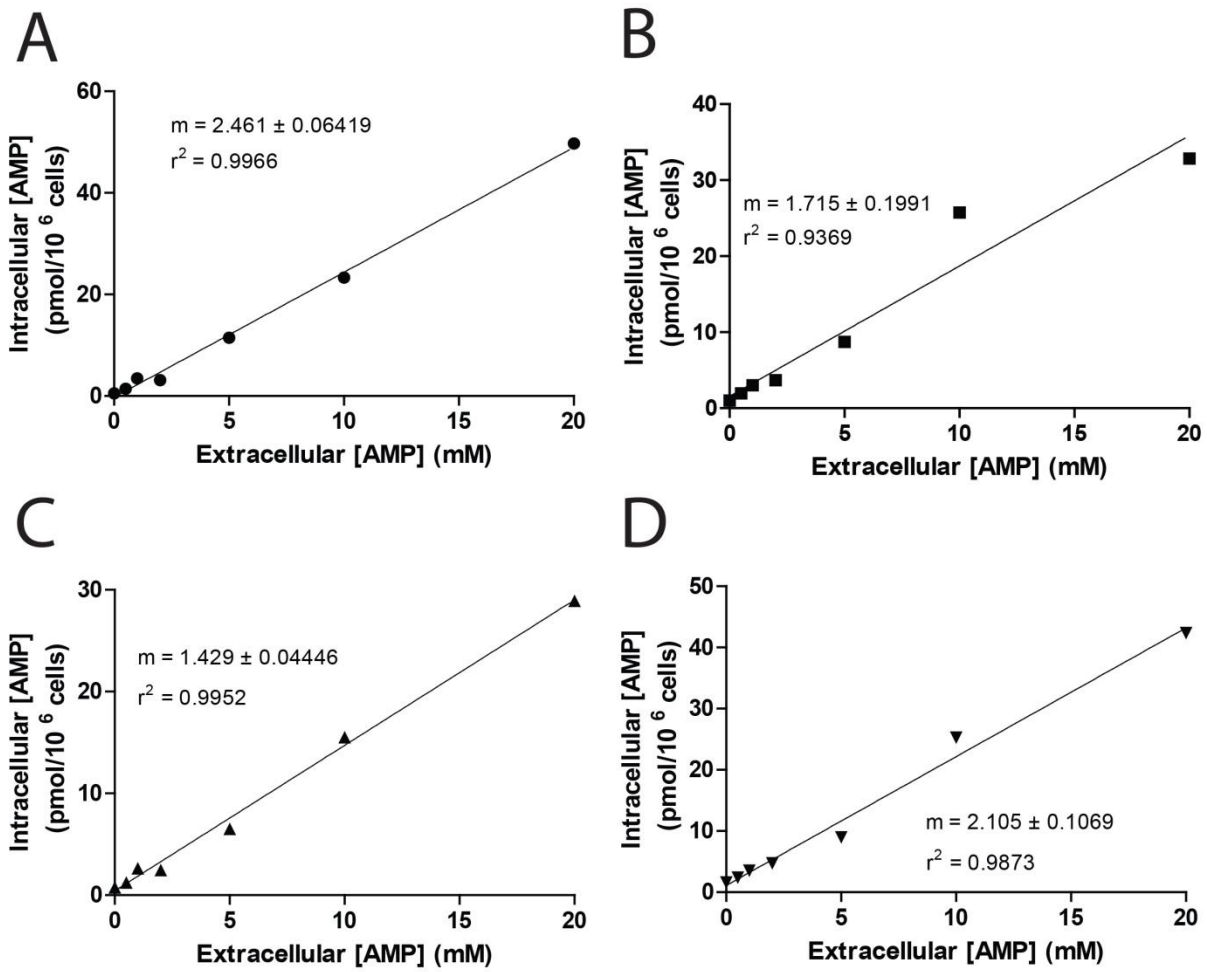

Figure 21. Erythrocytes intracellular AMP after incubation with increasing extracellular AMP concentration A-D) Erythrocytes intracellular levels of AMP in each of the four genotypes after extracellular AMP incubation (A: wild type, B: *Ampd3*$^{-/-}$, C: *Cd73*$^{-/-}$, and D: *Ampd3*$^{-/-}$/ *Cd73*$^{-/-}$).

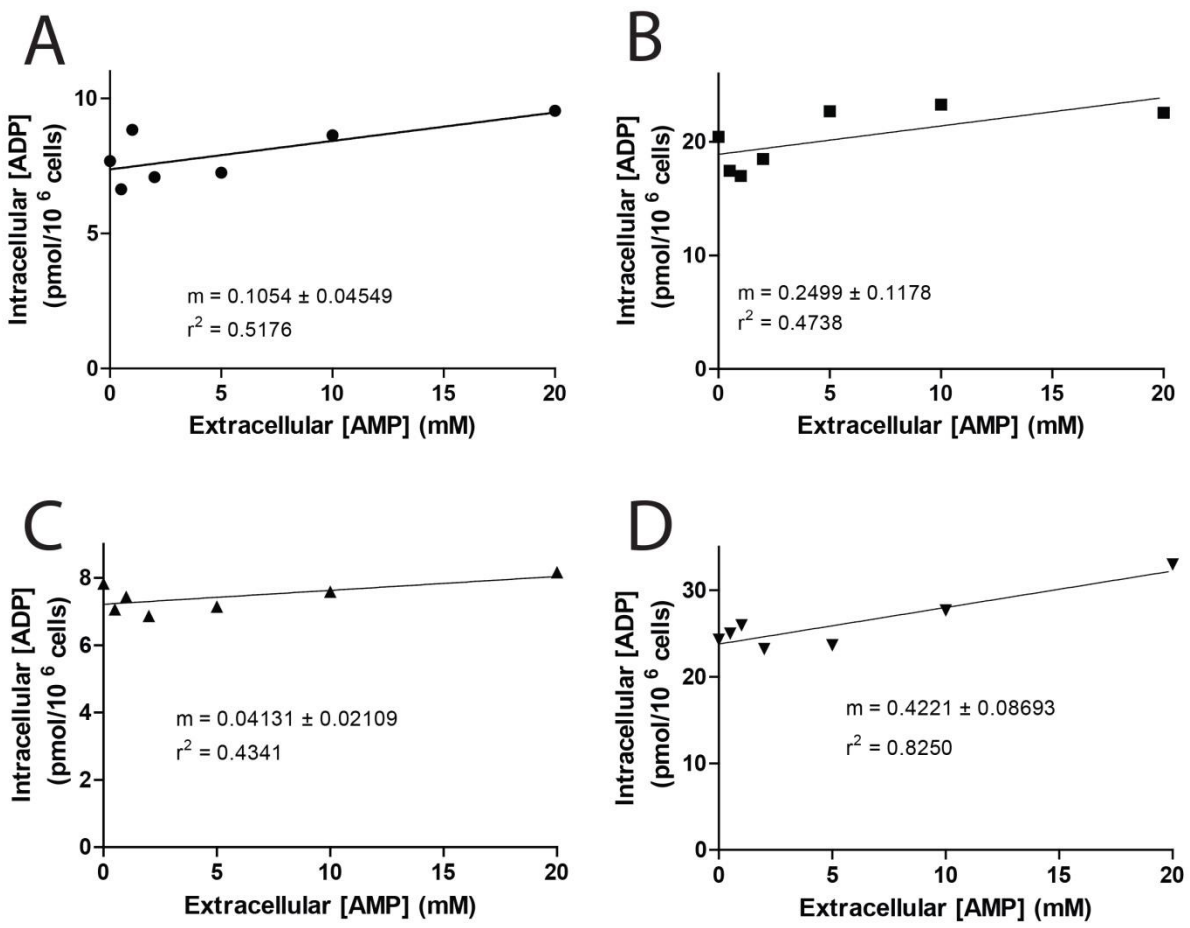

Figure 22. Erythrocytes intracellular ADP after incubation with increasing extracellular AMP concentration A-D) Erythrocytes intracellular levels of ADP after extracellular AMP incubation in each of the four genotypes (A; wild type, B; *Ampd3*$^{-/-}$, C; *Cd73*$^{-/-}$, and D; *Ampd3*$^{-/-}$/ *Cd73*$^{-/-}$).

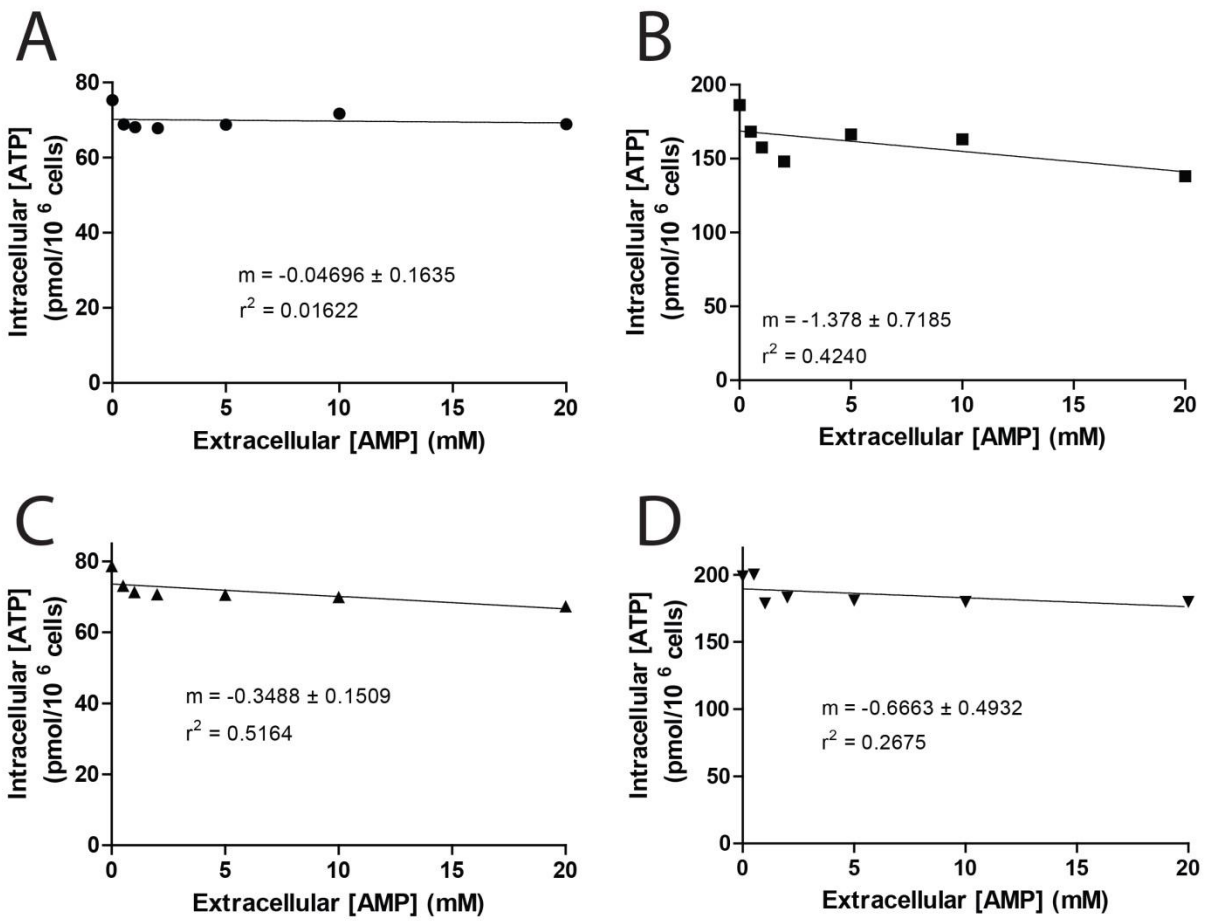

Figure 23. Erythrocytes intracellular ATP after incubation with increasing extracellular AMP concentration A-D) One plot for erythrocytes of each of the four genotypes (A; wild type, B; *Ampd3*$^{-/-}$, C; *Cd73*$^{-/-}$, and D; *Ampd3*$^{-/-}$/ *Cd73*$^{-/-}$). [Tre, see if you can plot the inverse trace of the initial ATP decreased]

analysis revealed relatively small changes to intracellular ADP despite large increases in AMP (Figure 22). The level of intracellular ATP initially decreased rapidly when erythrocytes were incubated with extracellular AMP below 2 mM. At higher extracellular AMP levels, there was little change to the levels of intracellular ATP levels (Figure 23).

These findings were somewhat surprising since we would have expected the ratio of the three nucleotides to be regulated by the adenylate equilibrium, AMP + ATP ⇔ 2 ADP. When we plot the ATP:AMP ratio relative to the extracellular AMP concentration, we observed that the drop in the ATP:AMP ratio is inversely exponential (r^2=0.991) to extracellular AMP concentrations (Figure 24). Our analysis revealed a smaller change to intracellular AMP result in a large drop in intracellular ATP levels, especially when extracellular AMP is below 1 mM. However, further increased in intracellular AMP do not generate corresponding decreased the intracellular ATP levels.

In addition, we also plot the ATP:ADP ratio against extracellular AMP, we observed that the ATP:ADP ratio is inversely linear (r^2=0.977) to the concentration of extracellular AMP (Figure 25). Since the cellular levels of ADP remained relative constant, the large drop in ATP as a result of a smaller increase in AMP is rather perplexing. The ratio of ATP:AMP induced by the influx of AMP into the erythrocytes appears inconsistent with the rebalancing of the adenylate equilibrium controlling ratio of ATP:ADP:AMP. This ratio is approximately 100:10:1 observed in a wild type physiological state. At a 1 mM extracellular AMP concentration, the erythrocytes' intracellular ATP:AMP ratio has dropped from over 100:1 to 25:1, a 4-fold change. Given that the intracellular ADP concentration appeared relatively constant, it suggests that either a significant amount of the ATP is rapidly degraded or is somehow lost from

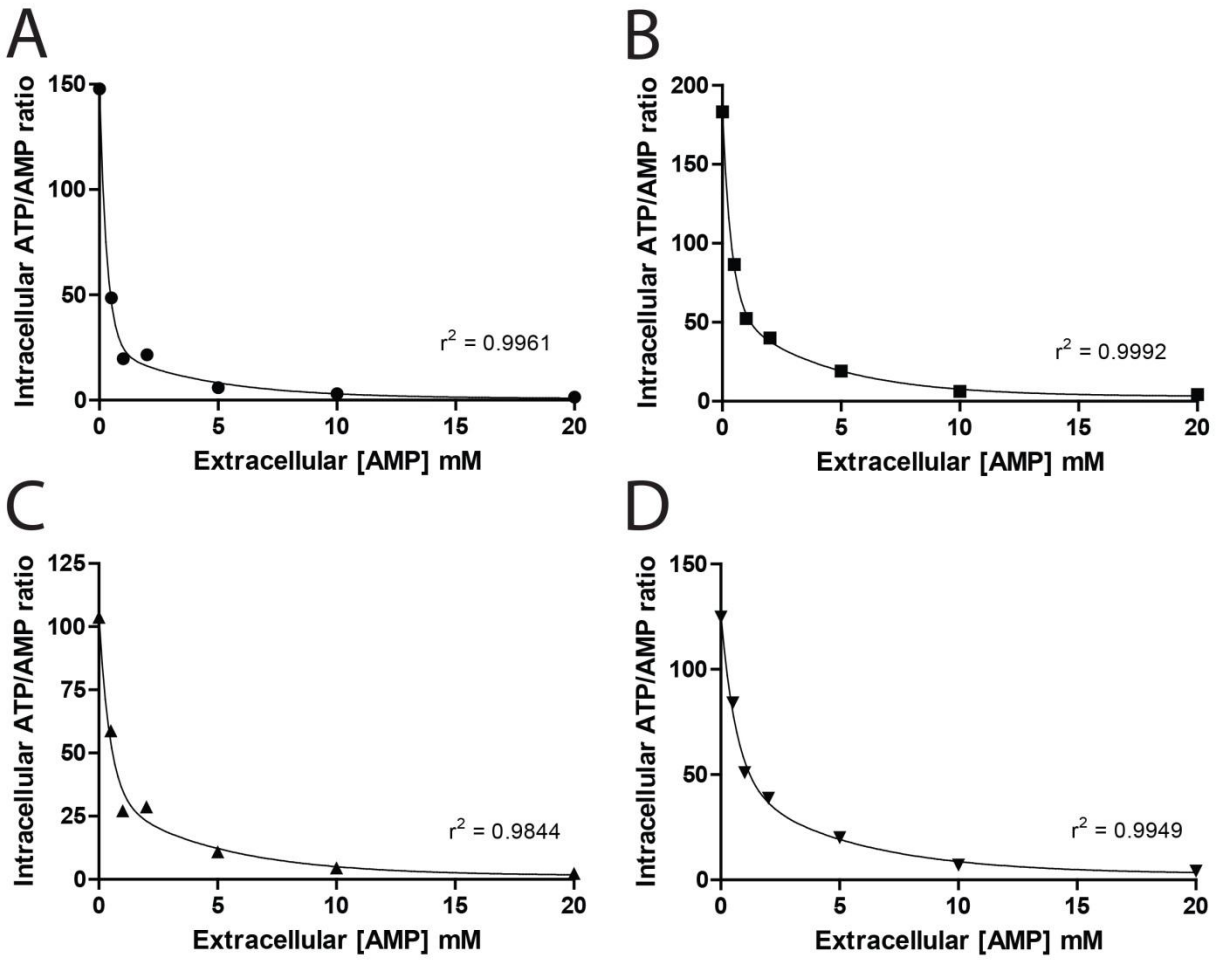

Figure 24. Erythrocytes intracellular ATP:AMP ratio after incubation with increasing extracellular AMP concentration. A-D) One plot for erythrocytes of each of the four genotypes: (A; wild type, B; *Ampd3*$^{-/-}$, C; *Cd73*$^{-/-}$, and D; *Ampd3*$^{-/-}$/*Cd73*$^{-/-}$).

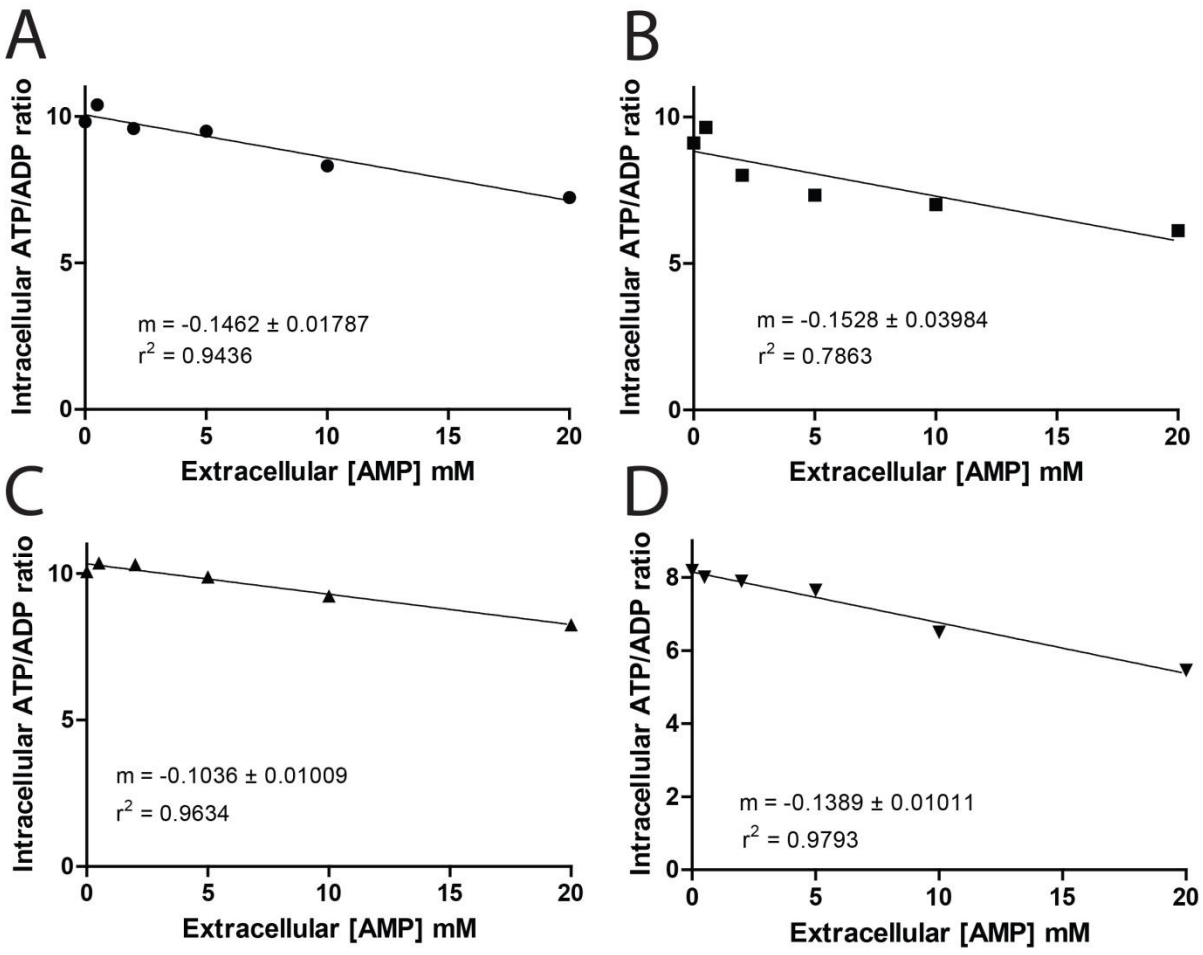

Figure 25. Erythrocytes AMP uptake and its correlation with intracellular ATP:ADP ratio. A-D) One plot for erythrocytes of each of the four genotypes (A; wild type, B; *Ampd3*$^{-/-}$, C; *Cd73*$^{-/-}$, and D; *Ampd3*$^{-/-}$/*Cd73*$^{-/-}$).

.

the erythrocytes. Together, these findings indicate that the influx of AMP into the erythrocytes can occur at non-physiological levels, which then alters the adenine nucleotide ratios inconsistently with the established adenylate equilibrium.

4.1.6. Influx of AMP induces ATP Release from erythrocytes.

We were surprised by the observations that the intracellular ATP:AMP ratio decreased only during the initial incubation with extracellular AMP and that it does not change much after this initial rapid drop even when extracellular AMP concentrations increased significantly. We reasoned that this initial loss of ATP is not a result of rising intracellular AMP concentration driving ATP catabolism. Since there is no corresponding large increase in ADP, the dephosphorylated product of ATP, we investigated the possibility that the intracellular ATP could have been released by the erythrocytes during the initial influx of AMP.

Given the possibility that extracellular ATP can be quickly degraded by ATPase's that are associated with erythrocytes, a luminometer, Lumicycle (Actimetrics, IL, USA), was used to monitor the ATP release with an ATP-activated luciferase assay in real-time. Induced ATP release from isolated erythrocytes was measured when the erythrocytes were incubated with saline (control), 5'-AMP, other nucleotides (3'-AMP, 5'-CMP, 5'-GMP, IMP, and 5'-3'-cAMP), or adenosine at 1 mM concentrations (Figure 26 A). Interestingly, responses above the PBS control levels of ATP activated luciferase activities were observed for 5'-AMP and, to a small extent, 3'-AMP but not for the other nucleotides and nucleosides tested (Figure 26 A and B). Again, adenosine, unlike 5'-AMP, was no more effective in inducing ATP release from erythrocytes than PBS (Figure 26 C). Together, these studies demonstrate that influx of AMP into erythrocytes was accompanied by efflux of ATP, which could explained the absence of

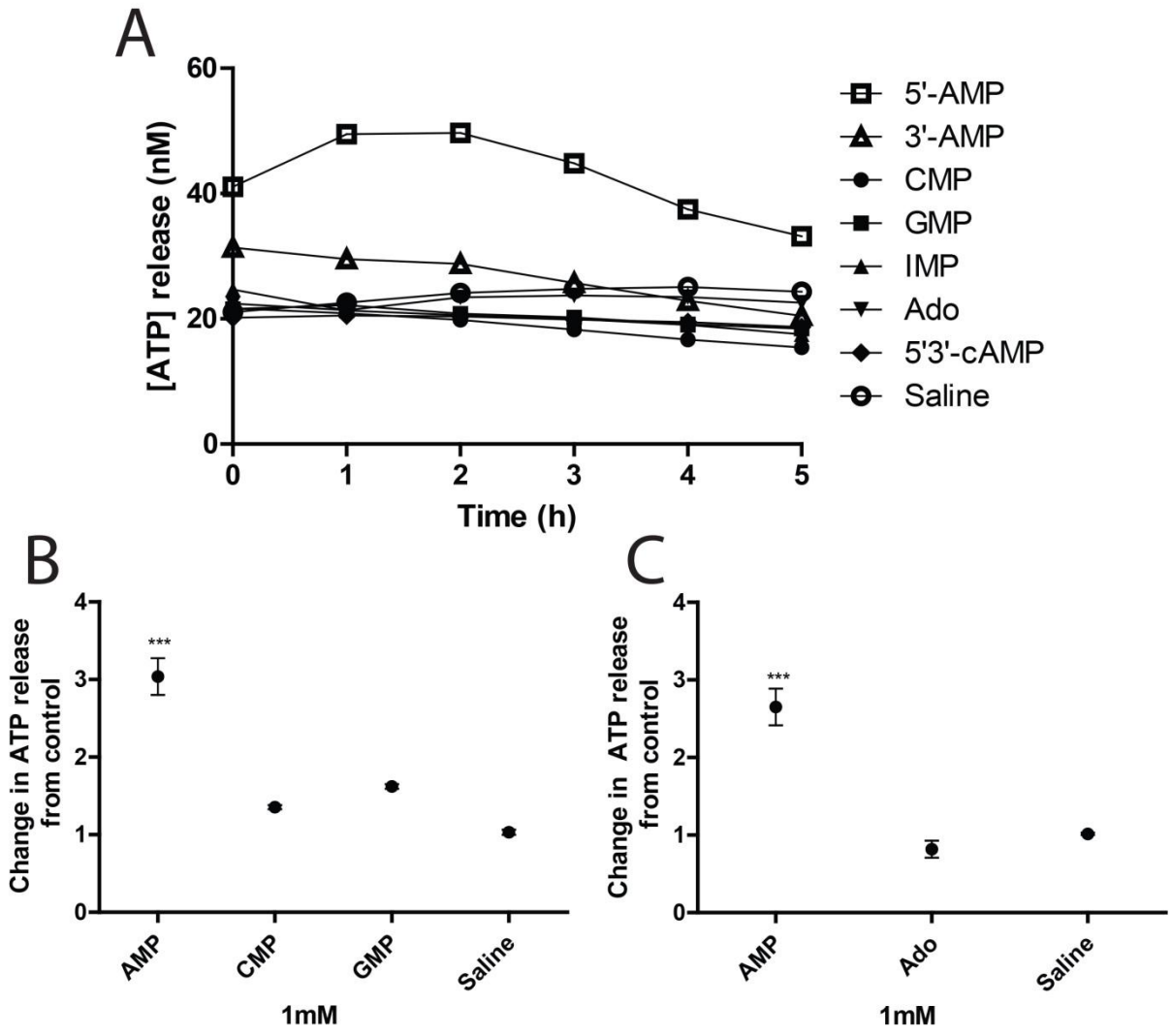

Figure 26. Nucleotides' induction of ATP release by erythrocytes. A) ATP luciferase time course after addition of nucleotides and adenosine. B) Quantification of multiple samples of various nucleotides (N=3). C) Quantification of multiple samples of AMP and adenosine (N=3). P values = *** < .0001.

ADP increase predicted under the adenylate equilibrium control.

Next, we investigated whether the efflux of ATP from the erythrocytes that was stimulated by AMP influx could be inhibited by ion channels blockers. Considering the earlier observation that tannic acid blocks AMP uptake, we first investigated whether tannic acid could block ATP release. We observed that tannic acid could potently inhibit ATP released by erythrocytes, but further characterization of this activity revealed that tannic acid may directly inhibit the luciferase enzyme rendering these findings ambiguous.

Studies have reported that ATP released by erythrocytes was mediated by the pannexin channel, PANX1, which is sensitive to blockage by carbenoxolone (10 µM) (Montalbetti et al., 2011). Therefore, we investigated whether ATP released by erythrocytes induced by AMP uptake could be blocked by carbenoxolone. ATP release by erythrocytes induced by AMP was measured in the absence or presence of 1 µM, 10 µM and 100 µM carbenoxolone (Figure 27 A). We observed that AMP-induced release of ATP from erythrocytes was not blocked by carbenoxolone. If anything, at the highest carbenoxolone concentration, we observed some level of additional AMP-mediated ATP release.

In another independent study, it was reported that the voltage-dependent anion channel (VDAC) inhibitor TRO19622 could inhibit ATP release from erythrocytes (Sridharan et al., 2012). Therefore, we undertook studies to investigate whether AMP mediated ATP release by erythrocytes could be blocked by TRO19622. ATP released by erythrocytes stimulated by 1 mM AMP was titrated against increasing concentrations of TRO19622 (Figure 27 B). We observed that the erythrocytes' ATP release stimulated by AMP was sensitive to inhibition by TRO19622 above 1 µM. These

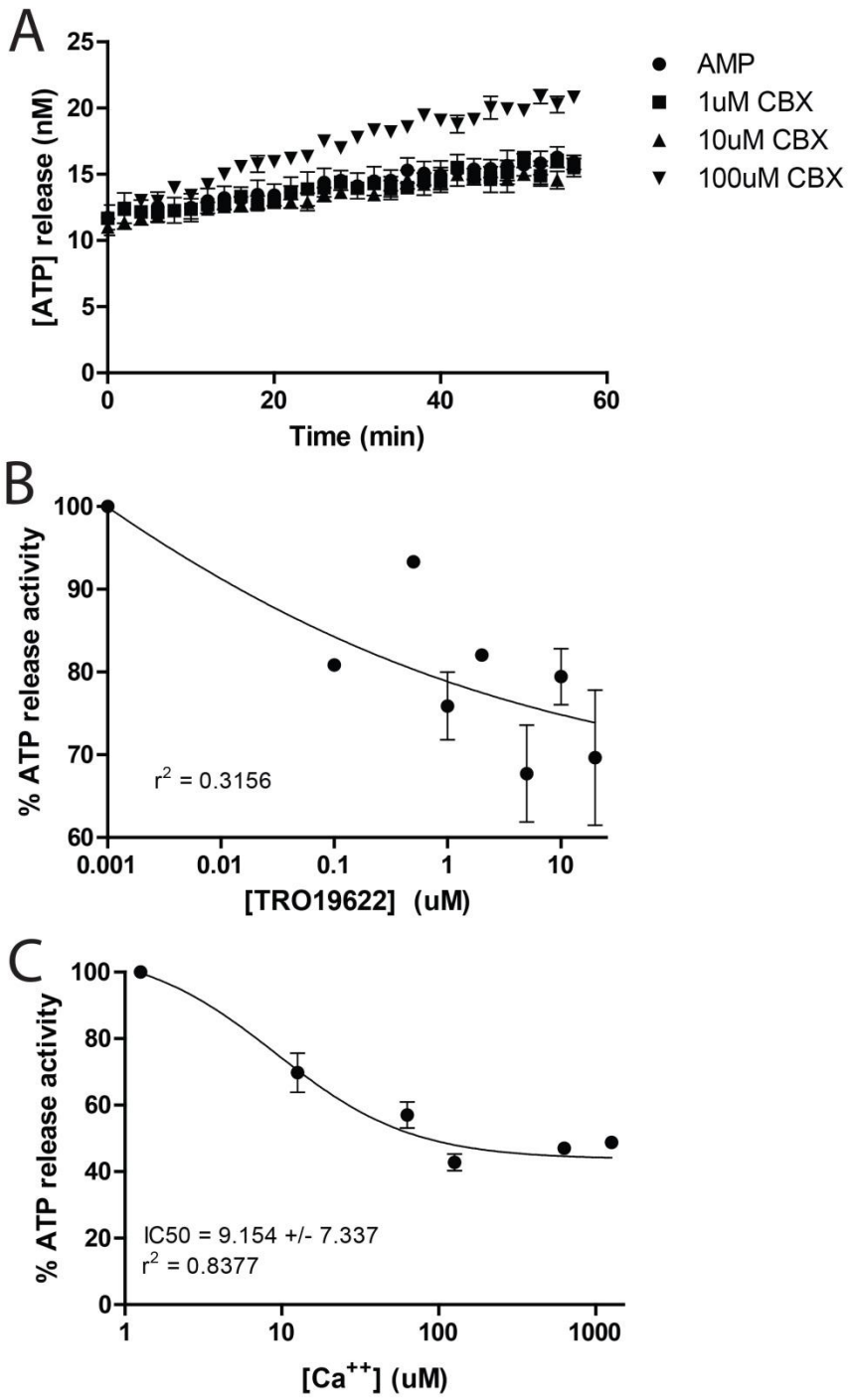

Figure 27. Inhibitors of ATP release by erythrocytes. A) Effect of CBX on ATP release stimulated by AMP. B) Effect of TRO19622 on ATP release stimulated by AMP. C) Effect of Ca^{2+} on ATP release stimulated by AMP.

observations suggest that the channel that is mediating AMP influx and/or ATP efflux could be a member of the VDAC family. Since VDAC is implicated in the ATP export process by TRO19662 and VDAC is known to be a major calcium exporter during apoptosis, we investigated whether calcium could modulate the AMP mediated ATP released from erythrocytes (Figure 27 C). We observed a correlation between increased calcium concentrations up to 100 µM and the inhibition of AMP-mediated ATP release from erythrocytes with an IC_{50} value of ~9 µM. In addition to calcium, we investigated another divalent ion, magnesium. Unlike calcium, we observed that magnesium stimulated luciferase activity but had no effect on AMP-mediated ATP release by erythrocytes. These findings suggest that the AMP-mediated ATP release by erythrocytes is regulated by calcium. Together these studies demonstrate that the AMP mediated release of ATP by the erythrocytes is likely mediated by an ion channel/pore that is sensitive to inhibition by TRO196222 and calcium cations.

4.1.7. Modulation of erythrocyte p50 by acute changes in levels of adenine nucleotides.

Finally, we wanted to gain insight into how are the changes in intracellular adenine nucleotide levels as a result of AMP uptake correlated with changes in erythrocytes' oxygen saturation, presented as changes in p50? First we plot the p50 values against increases in intracellular erythrocytes' AMP, ADP, and ATP levels (Figures 28, 29, 30). There was a clear linear correlation between the rise in intracellular AMP and the increase of the erythrocytes' p50 with an average $r^2 = 0.96$ among the genotypes (Figure 28). However, there was no apparent correlation between the changes in the erythrocytes' p50 and the intracellular ATP or ADP levels (Figure 29 and 30). Given our previous observation that the ATP:ADP ratio was

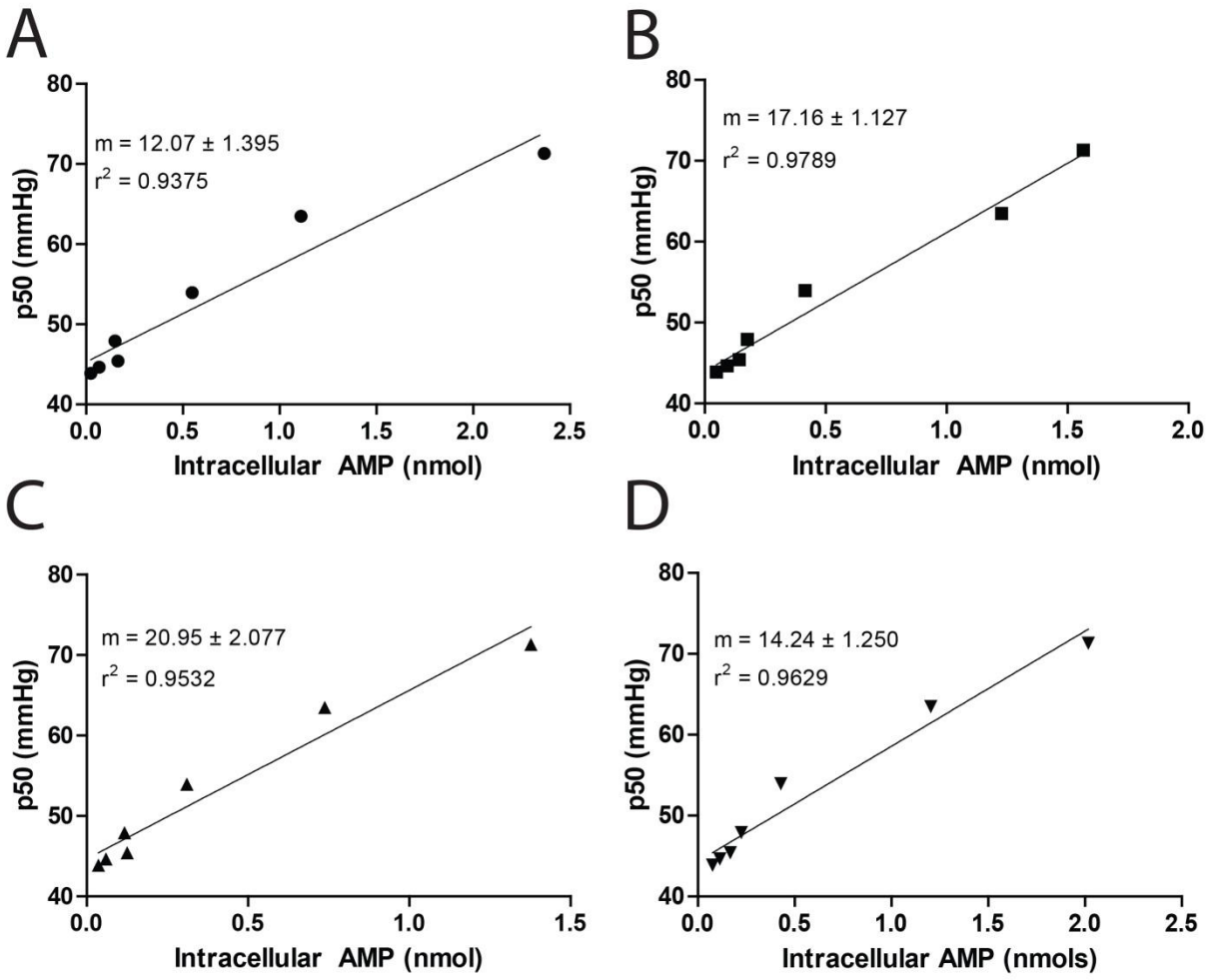

Figure 28. Correlation of p50 shift with intracellular change of AMP as a result of AMP incubation. A-D) Plot of p50 change vs. change in intracellular AMP of the four genotypes. (A; wild type, B; *Ampd3*$^{-/-}$, C; *Cd73*$^{-/-}$, and D; *Ampd3*$^{-/-}$/*Cd73*$^{-/-}$).

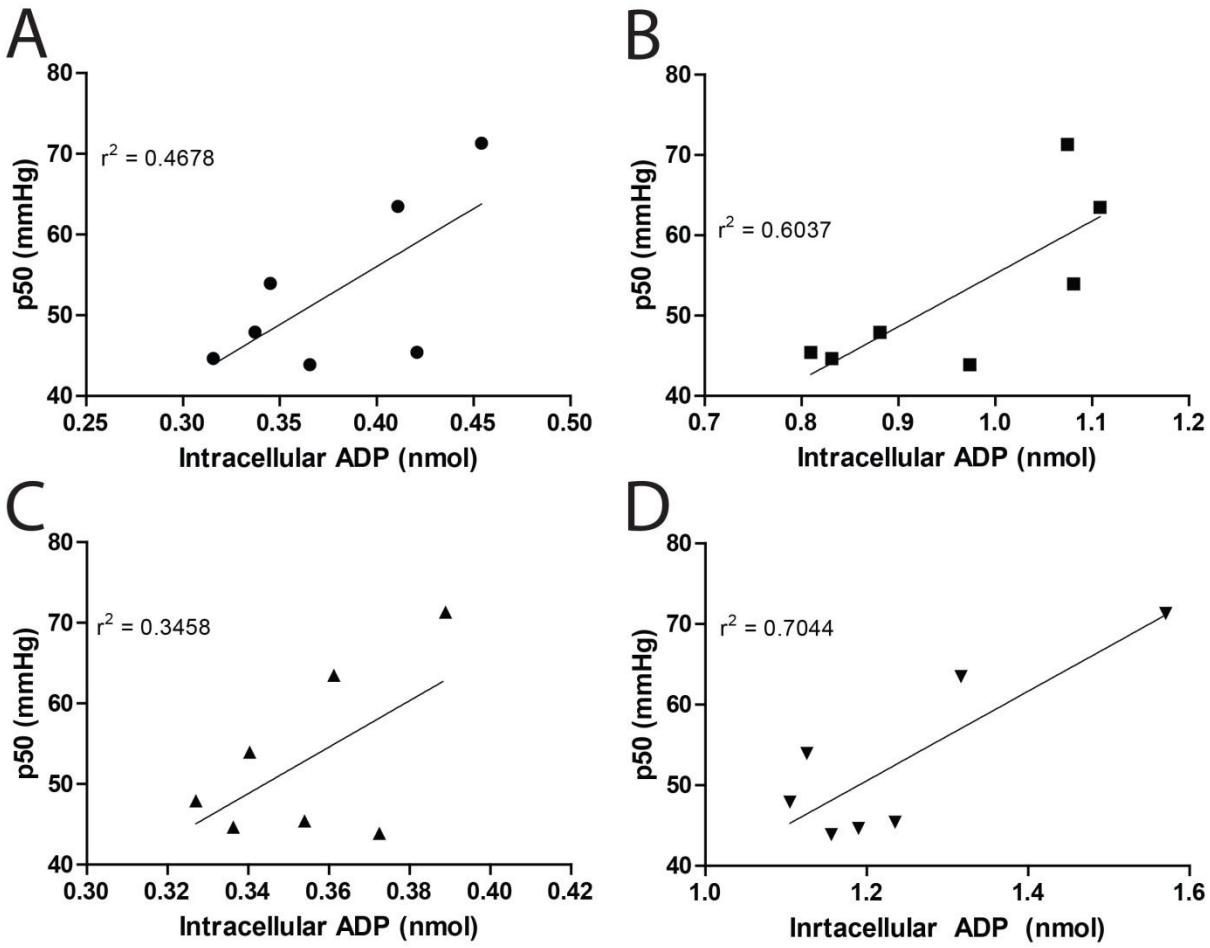

Figure 29. Correlation of p50 shift with intracellular change of ADP as a result of AMP incubation. A-D) Plot of p50 change vs. change in intracellular ADP of the four genotypes. (A; wild type, B; *Ampd3*$^{-/-}$, C; *Cd73*$^{-/-}$, and D; *Ampd3*$^{-/-}$/*Cd73*$^{-/-}$).

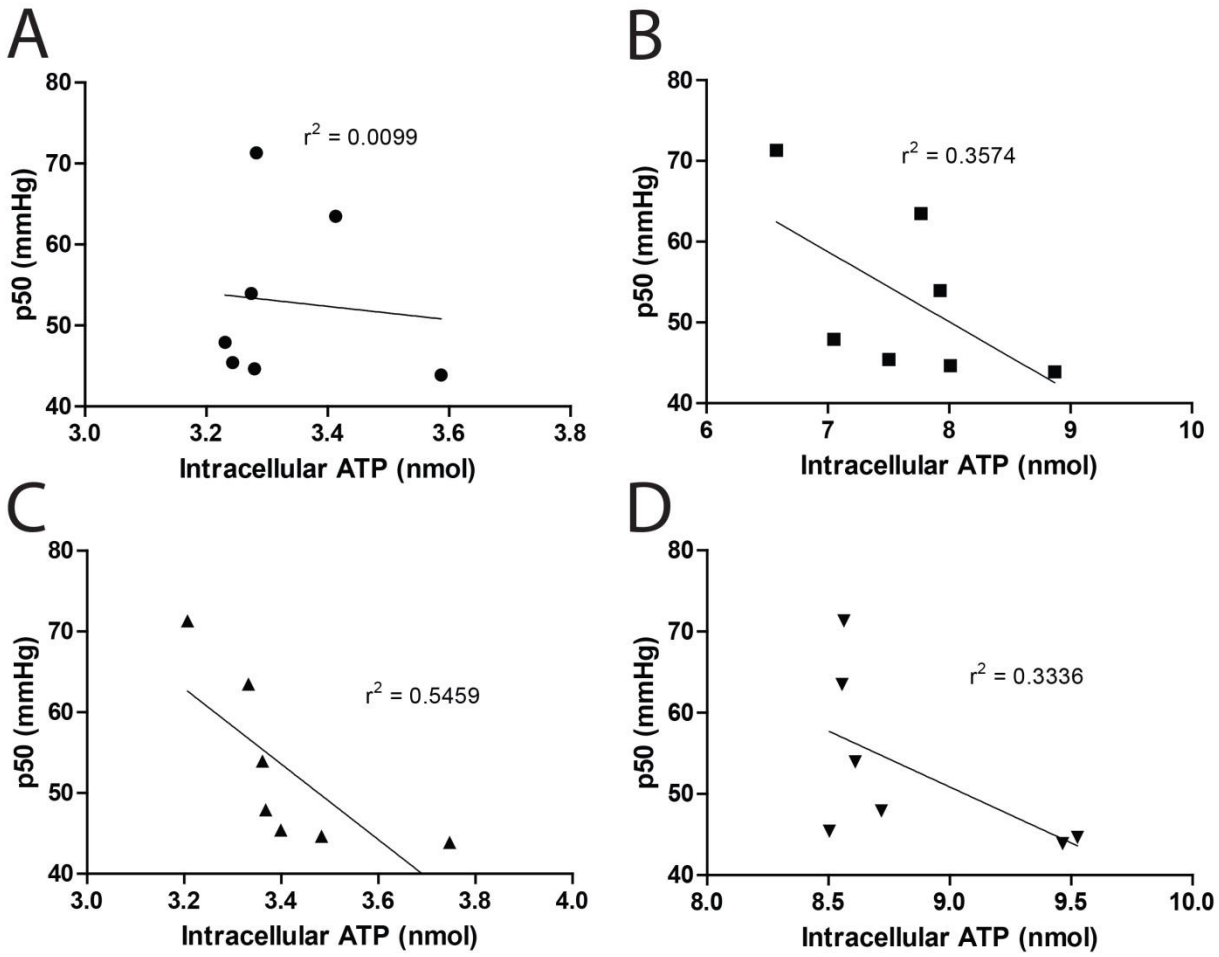

Figure 30. Correlation of p50 shift with intracellular change of ATP as a result of AMP incubation. A-D) Plot of p50 change vs. change in intracellular ATP of the four genotypes. (A; wild type, B; *Ampd3*$^{-/-}$, C; *Cd73*$^{-/-}$, and D; *Ampd3*$^{-/-}$/*Cd73*$^{-/-}$).

inversely correlated with extracellular AMP levels (Figure 25), the plot of the erythrocytes' p50 against the intracellular ATP:ADP ratio revealed that they are also inversely related with an $r^2 = 0.82$ (Figure 31).

While the direct correlation of p50 with acute intracellular AMP uptake is clear, our earlier studies (Fig 10 A and B) showed that AMP's effect on purified human Hb-A p50 is weak. One possibility is that the effect of AMP on erythrocytes' p50 is indirectly mediated by factors or processes absent in the purified human Hb-A preparation. As shown in Figure 15D, the p50 increases as a function of AMP concentration was comparable in isolated mouse erythrocytes (m= 1.0 +/- 0.2) and lysed erythrocytes (m= 0.83 +/- 0.01).

Another possibility for the discrepancy in observations is the species difference between human and mouse Hb, as it has been shown that p50 values among hemoglobin from different animal species is different (Weber and Campbell, 10). To investigate this possibility, we compared the p50 shift of isolated mouse and human erythrocytes as a function of extracellular AMP concentration (Figure 32 A). While the rate of p50 increase with respect to AMP levels of isolated erythrocytes from mouse (m= 1.00 +/- 0.13) and human (m= 0.87 +/- 0.03) was not significantly different, the baseline p50 reading for human versus mouse erythrocytes' p50 is 28 versus 40, respectively. These observations suggest that the weak p50 shift induced by AMP using purified human Hb-A needed to be further examined. Given that purified mouse Hb-A was not available commercially, we chose to examine whether the p50 shift of human erythrocytes' lysate in response to AMP is comparable to purified human Hb-A. Using isolated human erythrocytes, which had been freeze-thawed twice at -80°C, we

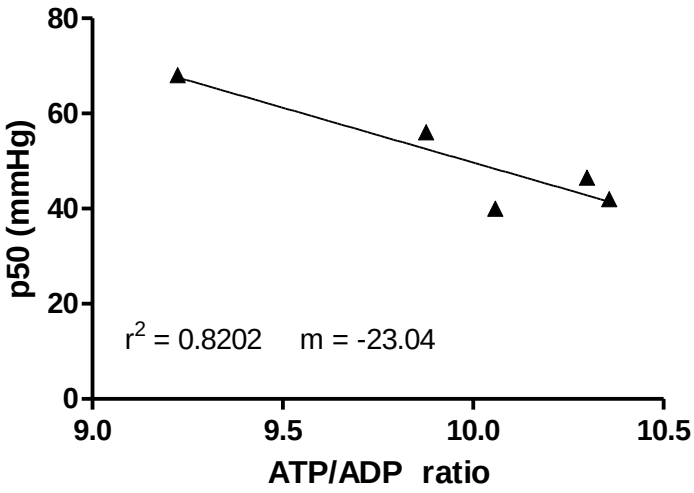

Figure 31. Correlation of p50 shift with intracellular change of ATP:ADP ratio as a result of AMP incubation. Correlation of the change in p50 with the ATP:ADP ratio in response to AMP incubation.

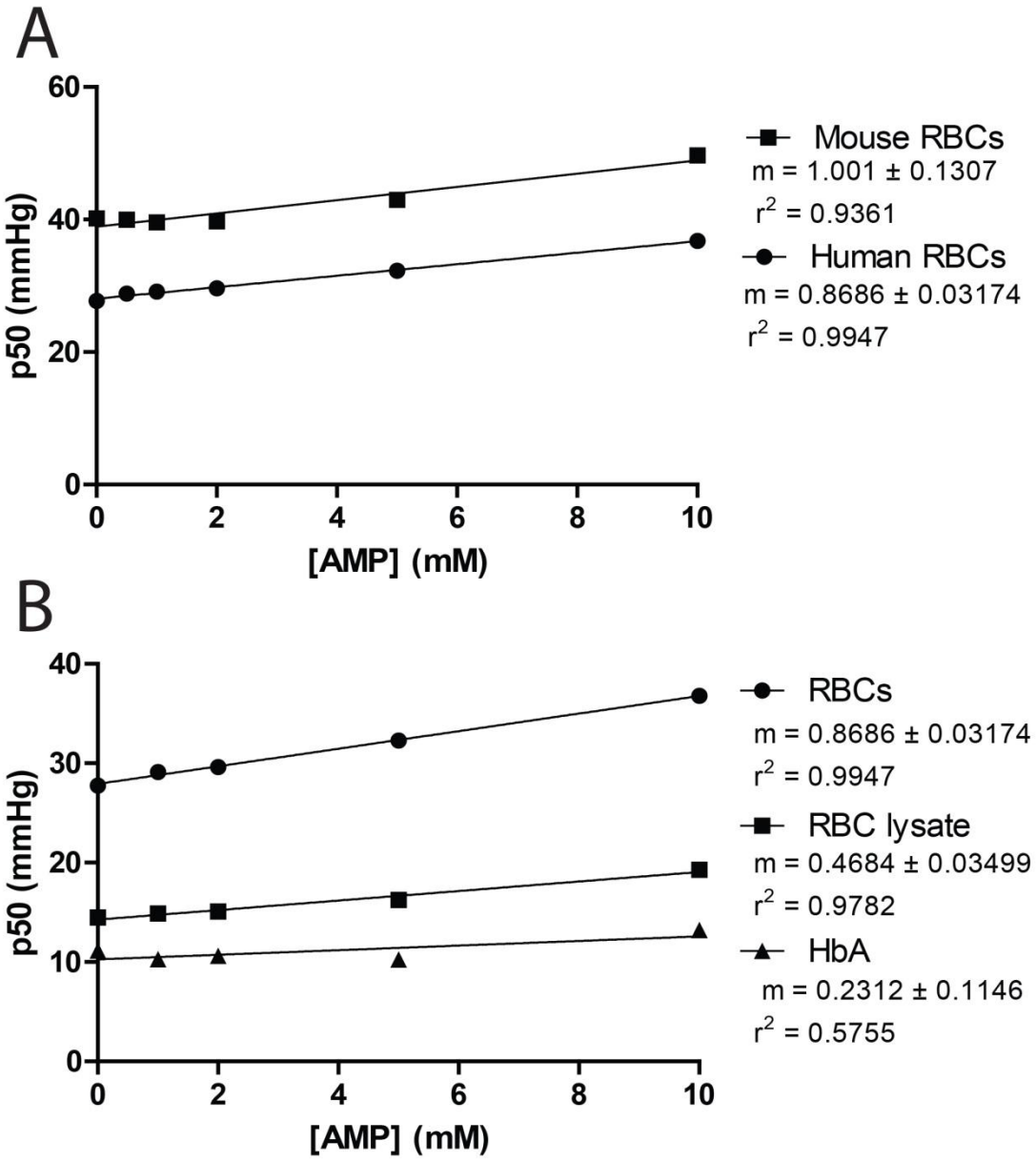

Figure 32. Comparison of human vs. mouse p50 in response to AMP. A) p50 values of intact erythrocytes from Mouse and Human in relation to extracellular AMP concentrations. B) Comparing p50 values of human erythrocytes, lysed erythrocytes, and purified Hb-A in respond to extracellular AMP concentrations.

measured the p50 shift induced by AMP as compared to isolated erythrocytes and purified human Hb-A (Figure 32 B). Unlike the mouse isolated erythrocytes and lysate, where the p50 shift induced by AMP was comparable, the p50 shifts induced by AMP were much stronger in intact human erythrocytes than in lysate. The p50 shift induced by AMP in the lysate was more than twice that from the purified Hb-A. We surmise that the differences in p50 baselines (starting point) among intact erythrocytes, lysates, and purified Hb-A could possibly be due to the presence of co-factor(s), that gets diluted in the lysate and is absent in purified Hb-A. Known co-factors present in intact erythrocytes and crude lysate include 2,3-BPG and ATP that regulate hemoglobin p50. However, given that the Hemox-reaction mixture is 4 mL and that the added lysate volume is 50 µL, an 80 times dilution, the concentration of these lysate co-factors would be in the µM range. Neither 2,3-BPG nor ATP, would have significant effects on Hb-A p50 oxygen saturation at such concentration. This raises the question of whether another “co-factor” may exists that could have mediated the AMP induced p50 shift in the lysate and in intact erythrocytes.

4.2. Discussion

The importance of CD73 and AMPD3 in modulating the response of the animal to AIHM was evident when comparing the responses from mice deficient in both CD73 and AMPD3 to those from wild type and the single gene mutant mice. Applying a sub-optimal dosage of AMP to differentiate the responses from various strains of mice, we observed the longest length of torpor was in *Ampd3*$^{-/-}$*/Cd73*$^{-/-}$ mice, then *Cd73*$^{-/-}$, followed by *Ampd3*$^{-/-}$ mice. Meanwhile, the wild type mice largely failed to enter torpor for any significant length of time under a T_a of 15°C. These observations were further confirmed when the optimal dosage of AMP was administered, when mice of all four

genotypes underwent torpor successfully. Here we observed the earliest arousal from torpor were wild type mice, followed by *Ampd3*$^{-/-}$, then *Cd73*$^{-/-}$, and finally *Ampd3*$^{-/-}$ */Cd73*$^{-/-}$ mice. At 12 h after AMP administration, about 95% of *Ampd3*$^{-/-}$/*Cd73*$^{-/-}$ remained in torpor. In contrast, 95% of wild type mice had aroused from torpor. Interestingly, loss of CD73 generated a stronger AIHM response than the loss of AMPD3, suggesting that extracellular catabolism of AMP by CD73 is a major regulatory step in preventing AIHM. The observations that the absence of AMPD3 further enhanced the AIHM response suggest that the uptake of AMP and its effect on the erythrocyte's function is fundamental in understanding the mechanistic process of AIHM.

Given that a major function of erythrocytes is oxygen transport to tissues, we investigated whether AMP could alter the p50 of intact erythrocytes. To eliminate the complication of extracellular dephosphorylation of AMP by CD73, we used *Cd73*$^{-/-}$ erythrocytes for these studies. We observed that incubation of isolated intact erythrocytes with 2 mM AMP consistently induced a p50 increase of about 4 mmHg. We also observed that adenosine, at a similar concentration, gave p50 values that were insignificant to those from PBS or vehicle buffer. The increase in p50 induced by AMP was comparable among the erythrocytes from all four genotypes, further confirming that dephosphorylation of AMP is not essential for mediating the p50 shift. A titration of extracellular AMP concentrations up to 20 mM against erythrocytes' p50 value revealed a linear ($r^2 = 0.99$) correlation between these two parameters. Despite a large increase in p50 induced by 20 mM extracellular AMP, the Hill coefficient, which measures hemoglobin's co-operative binding of oxygen, remained constant and is within its known values of 2.3-3.0 (Perutz, 1970). These observations suggest that the

erythrocytes hemoglobin co-operative oxygen binding function were change by being expose to non-physiological concentrations of AMP. Thus, it suggests that the erythrocytes' function in oxygen transport inherently has a large capacity to respond to extracellular AMP. Observing comparable rates of p50 increase from intact and lysed mouse erythrocytes as a function of extracellular AMP concentration, we concluded that the effect of AMP on hemoglobin is not mediated via a receptor based mechanism.

Our previous studies have suggested that AMP can be directly taken up by the erythrocytes, though the nature of this uptake process is poorly understood. While studying the stability and fate of extracellular AMP in the whole blood of wild type and *Cd73*$^{-/-}$ mice, we observed that AMP was rapidly taken up by both wild type and *Cd73*$^{-/-}$ erythrocytes. The extracellular AMP was also rapidly catabolized by wild type but not *Cd73*$^{-/-}$ whole blood, validating conclusion that CD73 is the major extracellular catabolic enzyme for AMP (Castrop et al., 2004). In contrast to the whole blood, incubation of AMP with isolated erythrocytes resulted in minimal degradation of AMP, indicating that CD73 is not associated with the outer membrane of erythrocytes. As ATP and ADP can be dephosphorylated extracellularly by ATPase (CD39) into AMP, we investigated whether ADP could also enter intact erythrocytes. Our studies revealed that extracellular ADP was rapidly dephosphorylated into AMP within minutes of incubation with isolated erythrocytes. The appearance of ADP inside the erythrocytes after about 1 h of incubation could have been converted from AMP taken up by erythrocytes via the adenylate equilibrium. These observations indicate that ADP likely does not enter the erythrocytes directly. The rapid conversions of ADP into AMP by the isolated erythrocytes suggest that the ATPase is likely associated with the extracellular

membrane, which is consistent with studies showing that Mg^{2+} and Ca^{2+} dependent ATPase have been purified from erythrocytes membrane (Wang and Guidotti, 1996).

Using radiolabeled AMP, we measured AMP uptake by *Cd73*$^{-/-}$ erythrocytes initially to exclude the possibility of uptake via adenosine. We observed a direct correlation between increases of radioactivity in cellular fraction with decreases of radioactivity in extracellular supernatant over a 2 h incubation period. In addition, we observed a linear (r^2 = 0.99) correlation between AMP uptake and extracellular AMP concentration from 0.01 to 10 mM suggesting that the uptake rate is driven by an AMP concentration gradient across the erythrocyte's membrane. These observations are consistent with the p50 findings where increases in p50 have a linear correlation with extracellular AMP concentrations. Examining the AMP uptake in wild type erythrocytes, we observed a "saturable" component at about 0.1 – 0.8 mM of extracellular AMP, not observed in *Cd73*$^{-/-}$ erythrocytes. We reasoned that the saturable component is likely contributed by adenosine uptake via ENT1 due to residual levels of white blood cells that express CD73 in the isolated wild type erythrocytes. To characterize the involvement of adenosine in AMP uptake, we examined the effect of dipyridamole, a specific blocker of ENT1, on the uptake of AMP by *Cd73*$^{-/-}$ erythrocytes. We found that the erythrocyte uptake of AMP was unaffected by dipyridamole. We were able to replicate this result in wild type whole blood, showing that the uptake of AMP was unaffected by dipyridamole. These observations indicate that ENT1 is not a transporter for AMP uptake, and that the uptake of AMP was not the result of a conversion to adenosine entering the erythrocyte via ENT1. Our observation verified a previous report that AMP uptake by erythrocytes is unaffected by dipyridamole (Mathews et al., 05).

Among the few membrane proteins that had been shown to be permeable to adenine nucleotides, ADP/ATP translocases (ANT) have been characterized for mitochondria and peroxisomes (Guitierrez-Aguilar and Baines, 2013). The ANT is known to transport ATP out of the mitochondrial matrix in exchange for ADP from the inner-membrane space. One study has suggested that isolated ANT was able to transport AMP (Fiermonte et al., 2009). Interestingly, an earlier proteomics study showed that ANT1 was expressed in reticulocytes, the immature erythrocyte (Prenni et al., 2012), while another study suggested the expression of ANT in mature erythrocytes (Bouyer et al., 2011). Therefore, we investigated whether similar players were involved in AMP uptake of the erythrocytes. Carboxyatractyloside (CAT) was previously shown to inhibit ANT nucleotide transport in the mitochondria (Vignais, 1976). We found that the AMP uptake by the erythrocytes was not blocked by CAT. These observations suggest that the uptake of AMP by erythrocytes is not mediated by an ATP-ADP translocase.

Tannic acid (TAN) is a large molecular inhibitor of various channels and transporters including the SLC25 transporter proteins (Guitierrez-Aguilar and Baines, 2013). Using a dose of 0.2% TAN, we observed a greatly reduced AMP uptake compared to control. Even at 0.002% of TAN, we observed a significant reduction in AMP uptake by erythrocytes. This inhibitory effect of TAN on the AMP uptake suggests that the channel responsible for AMP uptake is either directly inhibited by TAN or that the presence of the large molecular TAN complex passively blocks the channel. Given the broad target of TAN on many channels and transporters, the identity of the AMP channel/transporter remains unclear.

In addition to pharmacological blockers, we further investigated whether there were natural nucleotides or metabolites that could modulate the AMP uptake activity, presumably through competitive inhibition. We found that common metabolites such as glucose, lactate and urea did not inhibit AMP uptake by erythrocytes at the similar concentration to extracellular AMP. Nucleosides, such as adenosine, also did not inhibit AMP uptake by erythrocytes indicating that the uptake of adenosine and AMP likely occurs through separate channels. These observations are consistent with the dipyridamole studies described earlier. We observed that the three adenine nucleotides and GMP were all able to reduce uptake of AMP by erythrocytes. However, a titration of AMP uptake against GMP as an antagonist demonstrates that AMP uptake was not significantly altered. In the uptake studies, the inhibition of AMP uptake by ADP and ATP is not surprising given that our studies and others have demonstrated the presence of ATPase (CD39) associated with the membrane of erythrocytes (Wang and Guidotti, 1996). It is possible that the ATP and ADP are rapidly degraded to unlabeled AMP, which acts as a competitor to the radiolabeled AMP.

As demonstrated in the physiological studies in Chapter 3, the ratios between adenine nucleotides in the erythrocytes are maintained by the adenylate equilibrium despite differential levels of these nucleotides in the respective genotypes. As previously discussed, adenylate kinase maintains a tight regulation of adenine nucleotides by facilitating the reversible reaction of AMP + ATP ←→ 2ADP. However, will the adenylate equilibrium be maintained when erythrocytes are challenged with an acute increase of extracellular AMP? Using HPLC, we quantified the adenine nucleotide levels in erythrocytes from all the genotypes after AMP incubation. The response to extracellular AMP on the intracellular AMP was consistent with the ^{14}C-

AMP uptake experiments demonstrating a linear correlation with respect to extracellular AMP concentration. However, the change of the ADP and ATP levels was not as predicted by the adenylate equilibrium. We observed that intracellular ATP did decline but not in a linear fashion that matched the uptake of AMP. Rather, the decline displayed an inverse exponential profile with respect to extracellular AMP concentration. It showed that an initial increase in intracellular AMP resulted in a rapid decline in intracellular ATP. However, this decline in ATP then plateaued beyond about 1 mM extracellular AMP. The other unexpected finding was the intracellular ADP levels were relatively constant despite significant changes in intracellular AMP and ATP levels. Based on the adenylate equilibrium equation, we would have predicted that ADP should increase when ATP decreases and as AMP increases. These observations suggest that the adenine nucleotide ratios are not successfully maintained by adenylate kinase in response to the rapid influx of AMP, or that the process to restore the equilibrium through adenylate kinase requires a much longer time frame for the erythrocytes. In addition, there are other enzymes in the erythrocytes such as AMP kinase that could be activated by the influx of AMP, or the decrease in ATP may have activated other pathways.

Studies have shown that erythrocytes export ATP as a result of stress signals, one of which is low oxygen saturation similar to what we are seeing in our AIHM mice (Goldman et al., 2012). The above consideration led us to investigate whether erythrocytes' ATP release can be triggered by uptake of AMP, while using responses to other nucleotides and adenosine for comparison. Among the panel of nucleotides and nucleosides tested, including 5'-CMP, 5'-GMP, 5'-3'-cAMP, 5'-IMP, adenosine and 5'-

AMP, only 5'-AMP consistently induces ATP release from the erythrocytes. Addition of 3'-AMP could also result in a release of ATP slightly greater than the saline control.

In efforts to find out the possible transporter for ATP release, we tested if TAN would also inhibit the erythrocyte ATP release, knowing that AMP uptake can be inhibited by TAN. A strong decline in ATP release was observed following the addition of the TAN, but the result was compromised by the observation that TAN was inhibitory on the luciferase reaction, even at low doses. Another study reported that ATP released by erythrocytes was mediated by PANX1 and that a PANX1 specific inhibitor, carbenoxolone (CBX), could block ATP release by erythrocytes (Goldman et al., 2012). However, we observed that CBX did not prevent AMP induced ATP released by the erythrocytes. In addition, we also observed that CBX did not alter the AMP induced p50 increase in isolated erythrocytes. Thus, PANX1 is likely not involved in ATP release induced by AMP uptake. Other studies have reported that the voltage dependent anion changer (VDAC) is known to exchange ATP for ADP in the inner mitochondrial membrane and it has been suggested a similar protein is on the membrane of the erythrocytes (Sridharan et al., 2012). We found that TRO19622, a VDAC inhibitor, was effective in partially inhibiting the ATP release that was induced by extracellular AMP. This finding suggests that a VDAC type protein might be responsible for this ATP release induced by AMP. However the inhibition level by TRO19622 was about 30% of the control values, suggesting that other channels/pore could also be involved.

These observations led us to investigate the properties of VDAC. VDAC is known to be inhibited by Ca^{2+}, having divalent cation binding sites on the external interface of the protein (Shoshan-Barmatz et al., 2010). Since TRO19622 inhibition implicated VDAC as a potential transporter for the ATP release, we investigated

whether divalents, namely Mg^{2+} and Ca^{2+}, were able to inhibit the ATP release. Mg^{2+} was unable to impact the ATP release when added to the buffer, however, Ca^{2+} was able to inhibit ATP release significantly. By measuring ATP release against a titration of Ca^{2+} concentrations, we found that the maximal inhibition occurred around 100 μM, with an IC_{50} of ~10 μM. These data suggest that a voltage dependent channel could be responsible for releasing ATP that is induced by AMP uptake by erythrocytes.

Evidence from our studies further suggests that erythrocytes, which do not have *de novo* purine biosynthesis, regulate their intracellular adenine nucleotide levels via its ability to uptake AMP and released ATP. The ATP released by erythrocytes into the extracellular matrix has been reported to be triggered by stress signals such as hypoxia and exercise (Goldman et al., 2012). It has been shown that extracellular ATP has important biological functions, such as activating the P2Y family of receptors which help control vascular tissue relaxation and blood pressure (Ellsworth et al., 2009). We surmised that the extracellular enzymes, such as CD73 and ATPase/CD39, are part of the regulatory control on the movement of adenine nucleotides into the erythrocytes. While releasing energy to drive various cellular activities, ATP and ADP undergo dephosphorylation by erythrocyte-associated ATPase to AMP. The AMP, in turn, is either taken up by erythrocytes, which then moderates Hb p50 values in modulating tissue oxygen consumption. Alternatively, the AMP could be dephosphorylated extracellularly by CD73 into adenosine that could be utilized by adenosine receptors, while the excess adenosine is rapidly degraded by adenosine deaminase. Hence, our studies would suggest that the erythrocytes, which utilize glycolysis as an ATP regenerator, are a power source for extracellular matrix function, a somewhat parallel role to the mitochondria in intracellular function of nucleated cells.

Having demonstrated that the intracellular AMP levels correlate linearly to extracellular AMP uptake, it is not surprising to see that there is a direct positive correlation of p50 increase with intracellular AMP, but not ATP or ADP concentrations. A linear correlation between increases in intracellular AMP and p50 has an r^2 of ~0.96, which is close to a perfect correlation value of 1.0. In contrast, those of ADP and ATP concentrations against p50 increases had r^2 of ~0.5 and ~0.4, respectively.

Having observed an inverse linear shift in ATP:ADP ratio corresponding to extracellular AMP concentrations, we examined the correlation between ATP:ADP ratio and the p50 increase. An inverse correlation between ATP:ADP and p50 shift present itself with an r^2 value of about 0.82, suggesting that ATP:ADP ratio and p50 increased are likely linked. This inverse correlation between the ATP:ADP ratio with p50 values was observed in erythrocytes from all genotypes indicating that the differential in adenine nucleotides levels between AMPD3 deficient and proficient cells did not alter this correlation. In contrast, the ATP:AMP ratio had no correlation to the p50 values. Together, these observations suggest that the p50 increase could be a result of either the increasing intracellular AMP levels or is mediated indirectly via pathways controlled by AMP dependent enzymes such as AMPK. Alternatively, the possibility of enzymatic pathways modulating Hb oxygen saturation being activated or inhibited after sensing the change in the ATP:ADP ratio cannot be excluded. The exact mechanism of how non-physiological AMP modulates p50 increases remains to be addressed.

Our observation that AMP has a weak effect on purified human hemoglobin (Hb-A) p50 suggests several possibilities. One possibility is that mouse and human hemoglobin may have different responses to AMP. To address this possibility, we compared p50 values in intact isolated erythrocytes from human and mouse blood in

response to AMP. We found that the human erythrocytes similarly experience an AMP-induced p50 shift to the mouse erythrocytes. The rate of p50 increase with respect to extracellular AMP concentration gave slopes (m value) of 0.87 and 1, for human and mouse, respectively. Next we compared mouse intact erythrocytes and their lysed counterpart in p50 shift as a function of AMP concentration. We observed comparable rates of p50 increases as a function of AMP concentration for mouse erythrocytes and their lysates with slopes of 1.0 and 0.84, respectively. However, when we compared intact human erythrocytes to lysed human erythrocytes and purified Hb-A, we observed a great differential with the rate of change from intact erythrocytes (m=0.87) giving the biggest rate of change in p50 compared to lysed erythrocytes (m=0.47) and purified Hb-A (m=0.23) in response to AMP. To provide a rationale for these observations, we reasoned that modulators of Hb-A oxygen saturation were present in the intact erythrocytes that were diluted in the lysate but were absent in the purified Hb-A. Given that the lysates were diluted approximately 100 fold in the lysate studies, the observation will rule out common modulators of p50 such as 2,3-BPG and ATP. The possibility of novel co-factors that could modulate AMP effects on Hb p50 cannot be ruled out.

5. Summary

In order to further our understanding of the role of adenine nucleotides in erythrocyte function, we created a mouse model that was deficient in both AMPD3 and CD73, the key intracellular and extracellular AMP catabolic enzymes, respectively. The current studies demonstrate that this enzymatic deficiency significantly alters the physiological (steady state) regulation in erythrocytes' function and enhances the animals' sensitivity to AIHM, without altering the mechanism of how erythrocytes respond to acute changes in extracellular AMP levels.

Our investigations on the physiological impact of the double deficiency suggest that regulation of erythrocytes' affinity for oxygen could regulate systemic metabolism. We show that increased adenine nucleotide levels, ATP in particular, correlate with increases in erythrocyte p50 values. We demonstrate using purified Hb *in vitro* that physiological ATP and ADP concentrations can directly modulate Hb p50 at a value consistent with observed erythrocyte p50 values *in vivo*. A rise in the ATP concentration leads to increased Hb p50 values and to erythrocytes' reduced affinity for oxygen. Such a decrease in affinity results in release of oxygen at a faster rate to working muscle and other tissues, accounting for the enhanced metabolism observed in *Ampd3*$^{-/-}$*/Cd73*$^{-/-}$ mice during wheel running.

The observations from the studies on how erythrocytes respond to non-physiological extracellular AMP levels suggest that, while erythrocytes readily take up AMP, it releases ATP in a process of re-establishing a new balance among AMP, ADP and ATP. Our findings suggest that erythrocytes have a previously uncharacterized capability of regulating their own adenylate pool, and an extracellular supply of adenine

nucleotide and nucleoside by uptake extracellular AMP and release ATP. These observations bring new insight that the lack of *de novo* purine biosynthesis and the absence of IMP salvage in erythrocytes could be compensated by the adenine nucleotide uptake and release mechanisms. We also found that acute changes in intracellular AMP levels lead to a linear decrease in the ATP:ADP ratio, and a linear increase (right shifts) in erythrocyte p50 values. Thus, changes in extracellular AMP directly regulate erythrocyte p50 and consequently their oxygen transport function.

6. Future directions

Our investigations lead to new understandings of the role of adenine nucleotides in erythrocyte function and regulation, while raising additional questions to be answered. First, is AMP uptake mediated by the same channel/transporter(s) responsible for ATP efflux? What are the identities of the associated transporters? One of the first transporters that calls for further investigation is VDAC. Our preliminary studies showed that a VDAC inhibitor partially inhibited ATP release; whether it also blocks AMP uptake has not been tested. VDAC has been shown to be non-selective in what it transports (Shoshan-Barmatz et al., 2010). Since VDAC is a gated pore instead of a selective channel, it is possible that AMP and ATP could both be using the same pore to pass through the membrane. Therefore, we plan on testing both of the VDAC inhibitors that showed an effect on inhibiting ATP release, TRO19622 and Ca^{2+}, on their effects of AMP uptake and shifting the p50 value of the erythrocytes. Another observation that may aid our future studies is the fact that TAN inhibits AMP uptake at low concentration. Currently, there is no report of TAN directly inhibiting VDAC. However, as mentioned above, TAN could be a steric hindrance to pores due to the size of the molecule as opposed to a direct interaction.

Considering VDAC inhibitor could only block the ATP release partially, additional untested transporters that are expressed in erythrocytes will be evaluated. The selected transporters will be studied for their possible involvement in AMP uptake and/or ATP release by erythrocytes.

Another important question pertains to the response mechanism of hemoglobin and erythrocytes to AMP. Studies from decades ago show contrasting data; some

reported that hemoglobin responds to AMP while others do not. We observed that the difference seems to lie in whether the experiments were done with purified hemoglobin or erythrocyte cell lysate. In our own experiments, the p50 of purified hemoglobin was weakly responsive to changes in AMP levels. However, we observed a similar p50 shift to AMP in erythrocyte lysate to that in erythrocytes. This observation suggests that there is(are) endogenous “modulator(s)”, no longer present with the purified Hb, that interact with Hb in the erythrocytes and allow Hb to be responsive to AMP. To test the assumption that the modifier is a heat-stable metabolite and not a protein, we plan to examine if the p50 of purified human Hb can be shifted by AMP upon addition of boiled human erythrocyte lysate. Further, to examine if the modifier is a protein, we plan on homing in on the protein, initially by sized fractions of the lysate, and then testing candidate proteins in the positive fraction.

7. Bibliography

Adair GS. A critical study of the direct method of directly measuring the osmotic pressure of haemoglobin. *Proc. R. Soc. Lond. Ser. A*, 108A, 627–637 (1925).

Albert V and Hall MN. mTOR signaling in cellular and organismal energetics. *Curr Opin Cell Biol*. Dec 30;33C:55-66.(2014).

Andrews MT. Advances in molecular biology of hibernation in mammals. *Bioessays.* May;29(5):431-40 (2007).

Andrews MT, Squire TL, Bowen CM, Rollins MB. Low-temperature carbon utilization is regulated by novel gene activity in the heart of a hibernating mammal. *Proc. Natl. Acad. Sci*. U.S.A., 95, pp. 8392–8397 (1998).

Antonini E and Brunori M. Hemoglobin and myoglobin in their reactions with ligands. *Frontiers of Biology*. North Holland Publishing Co. (Vol 21) 1971.

Aslami H, Schultz MJ, Juffermans NP. Potential applications of hydrogen sulfide-induced suspended animation. *Curr Med Chem* 16:1295–1303 (2009).

Ataullakhanov FI and Vitvitsky VM. What determines the intracellular ATP concentration. *Biosci. Rep.* 22, 501–11 (2002).

Baranowska-Bosiacka I, Hlynczak AJ, Wiszniewska B, Marchlewicz M. Disorders of purine metabolism in human erythrocytes in the state of lead contamination. *Pol J of Env Studies*. Vol 13. No. 5. 467-476 (2004).

Benesch R and Benesch RE. The effect of organic phosphates from the human erythrocyte on the allosteric properties of hemoglobin. *Biochem. Biophys. Res. Commun.* 26, 162–7 (1967).

Benesch RE and Benesch R. The mechanism of interaction of red cell organic phosphates with hemoglobin. *Adv. Protein Chem.* 28, 211–37 (1974).

Benesch R, Benesch RE, Enoki Y. The interaction of hemoglobin and its subunits with 2,3-diphosphoglycerate. *Proc. Natl. Acad. Sci. U. S. A.* 61, 1102–6 (1968).

Bergfeld GR and Forrester T. Release of ATP from human erythrocytes in response to a brief period of hypoxia and hypercapnia. *Cardiovasc. Res*., 26, pp. 40–47 (1992).

Bhatt DP, Chen X, Geiger JD, Rosenberger TA. A sensitive HPLC-based method to quantify adenine nucleotides in primary astrocyte cell cultures. *J Chromatogr B Analyt Technol Biomed Life Sci.* Mar 15;889-890:110-5 (2012).

Blackstone E. H2S induces a suspended animation-like state in mice. *Science* 308:518 (2005).

Bouma HR, Verhaag EM, Otis JP, Heldmaier G, Swoap SJ. Induction of torpor: mimicking natural metabolic suppression for biomedical applications. *J Cell Physiol*. Apr;227(4):1285-90 (2012).

Bouyer G, Cueff A, Egée S, Kmiecik J, Maksimova Y, Glogowska E, Gallagher PG, Thomas SL. Erythrocyte peripheral type benzodiazepine receptor/voltage-dependent anion channels are upregulated by Plasmodium falciparum. *Blood*. Aug 25;118(8):2305-12 (2011).

Braulke LJ, Klingenspor M, DeBarber A, Tobias SC, Grandy DK, Scanlan TS, Heldmaier G. 3-Iodothyronamine: A novel hormone controlling the balance between glucose and lipid utilisation. *J Comp Physiol B* 178:167–177 (2008).

Buttgereit F and Brand MD. A hierarchy of ATP-consuming processes. *Biochem. J*., 312, pp. 163–167 (1995).

Calvert JW, Coetzee WA, Lefer DJ. Novel insights into hydrogen sulfide-mediated cytoprotection. *Antioxid Redox Signal*12:1203–1217 (2010).

Carey HV, Andrews MT, Martin SL. Mammalian hibernation: cellular and molecular responses to depressed metabolism and low temperature. Physiol Rev 83:1153–1181 (2003).

Castrop H, Huang Y, Hashimoto S, Mizel D, Hansen P, Theilig F, Bachmann S, Deng C, Briggs J, Schnermann J. Impairment of tubuloglomerular feedback regulation of GFR in ecto-5'-nucleotidase/CD73-deficient mice. *J Clin Invest.* Sep;114(5):634-42 (2004).

Chapman AG and Atkinson DE. Stabilization of adenylate energy charge by the adenylate deaminase reaction. *J. Biol. Chem.* 248, 8309–12 (1973).

Coletta M, Condò SG, Scatena R, Clementi ME, Baroni S, Sletten SN, Brix O, Giardina B, Condo SG. Synergistic modulation by chloride and organic phosphates of hemoglobin from bear (*Ursus arctos*). *J Mol Biol* 236, 1401–1406 (1994).

Coll AP and Yeo GSH. The hypothalamus and metabolism: integrating signals to control energy and glucose homeostasis. *Curr Opin in Pharm*. 13:970-976 (2013).

Daan S, Barnes BM, Strijkstra AM. Warming up for sleep?—ground squirrels sleep during arousals from hibernation. *Neurosci Lett* 128:265–268 (1991).

Daniels IS, O Brien WG 3rd, Nath V, Zhao Z, Lee CC. AMP deaminase 3 deficiency enhanced 5'-AMP induction of hypometabolism. *PLoS One*. Sep 16;8(9):e75418 (2013).

Daniels IS, Zhang J, O'Brien WG 3rd, Tao Z, Miki T, Zhao Z, Blackburn MR, Lee CC. A role of erythrocytes in adenosine monophosphate initiation of hypometabolism in mammals. *J Biol Chem*. Jul 2;285(27):20716-23 (2010).

Dausmann KH, Glos J, Ganzhorn JU, Heldmaier G. Hibernation in the tropics: lessons from a primate. *J Comp Physiol B*. Apr;175(3):147-55 (2005).

Duling BR. Oxygen sensitivity of vascular smooth muscle. II. *In vivo* studies. *Am. J. Physiol*., 227, pp. 42–49 (1974).

Dzeja P, Terzic A. Adenylate kinase and AMP signaling networks: metabolic monitoring, signal communication and body energy sensing. *Int J Mol Sci.* Apr 17;10(4):1729-72 (2009).

Ellsworth ML. The red blood cell as an oxygen sensor: what is the evidence? *Acta Physiol. Scand.*, 168, pp. 551–559 (2000).

Ellsworth ML, Ellis CG, Goldman D, Stephenson AH, Dietrich HH, Sprague RS. Erythrocytes: oxygen sensors and modulators of vascular tone. *Physiology (Bethesda*). Apr;24:107-16 (2009).

Ellsworth ML, Ellis CG , Popel AS, Pittman RN. Role of microvessels in oxygen supply to tissue. *News Physiol. Sci.*, 9, pp. 119–123 (1994).

Ellsworth ML and Pittman RN. Arterioles supply oxygen to capillaries by diffusion as well as by convection. *Am. J. Physiol.*, 258, pp. H1240–H1243 (1990).

Else PL and Hulbert AJ. Comparison of the “mammal machine” and the “reptile machine”: energy production. *Am. J. Physiol*., 240, pp. R3–R9 (1981).

Lovatt EC. The toxicity of hydrogen sulphide and other sulphides. Experimental Physiology, 52. (1967).

Felig P and Wahren J. Fuel homeostasis in exercise. *N Eng J Med*. Nov 293: 1078-1084 (1975).

Fiermonte G, Paradies E, Todisco S, Marobbio CM, Palmieri F. A novel member of solute carrier family 25 (SLC25A42) is a transporter of coenzyme A and adenosine 3',5'-diphosphate in human mitochondria. *J Biol Chem*. Jul 3;284(27):18152-9 (2009).

Formato M, Masala B, De Luca G. The levels of adenine nucleotides and pyridine coenzymes in red blood cells from the newborn, determined simultaneously by HPLC. *Clin. Chim. Acta.* 189, 131–7 (1990).

Funder J and Wieth JO. Chloride and hydrogen ion distribution between human red cells and plasma. *Acta Physiol. Scand.* 234–245 (1966).

Gadalla MM, Snyder SH. Hydrogen sulfide as a gasotransmitter. *J Neurochem* 113:14–26 (2010).

Garby L, Gerber G, De Verdier CH. Binding of 2,3-diphosphoglycerate and adenosine triphosphate to human haemoglobin A. *Eur. J. Biochem.* 10, 110–5 (1969).

Geiser F and Ruf T. Hibernation versus daily torpor in mammals and birds: physiological variables and classification of torpor patterns. *Physiol. Zool*., 68, pp. 935–966 (1995).

Goldman D, Fraser GM, Ellis CG, Sprague RS, Ellsworth ML, Stephenson AH. Toward a multiscale description of microvascular flow regulation: O(2)-dependent release of ATP from human erythrocytes and the distribution of ATP in capillary networks. *Front Physiol.* Jul 16;3:246 (2012).

Gomes AP, Blenis J. A nexus for cellular homeostasis: the interplay between metabolic and signal transduction pathways. *Curr Opin Biotechnol*. Jan 3;34C:110-117 (2015).

Guarnone R, Centenara E, Barosi G. Performance characteristics of Hemox-Analyzer for assessment of the hemoglobin dissociation curve. *Haematologica*. Sep-Oct;80(5):426-30 (1995).

Gupta RK, Benovic JL, Rose ZB. Magnetic resonance studies of the binding of ATP and cations to human hemoglobin. *J. Biol. Chem.* 253, 6165–71 (1978).

Gupta RK, Benovic JL, Rose ZB. Location of the allosteric site for 2,3-bisphosphoglycerate on human oxy- and deoxyhemoglobin as observed by magnetic resonance spectroscopy. *J. Biol. Chem.* 254, 8250–5 (1979).

Gutiérrez-Aguilar M, Baines CP. Physiological and pathological roles of mitochondrial SLC25 carriers. *Biochem J.* Sep 15;454(3):371-86 (2013).

Hancock CR, Brault JJ, Terjung RL. Protecting the cellular energy state during contractions: role of AMP deaminase. *J Physio Pharm*. 57, suppl 10, 17-29 (2006).

Hardie DG, Carling D, Carlson M. The AMP-activated/SNF1 protein kinase subfamily: metabolic sensors of the eukaryotic cell? *Annu. Rev. Biochem*., 67, pp. 821–855 (1998).

Heldmaier G, Klingenspor M, Werneyer M, Lampi BJ, Brooks SPJ, Storey KB. Metabolic adjustments during daily torpor in the Djungarian hamster. *Am. J. Physiol*., 276, pp. E896–E906 (1999).

Heldmaier G, Ortmann S, Elvert R. Natural hypometabolism during hibernation and daily torpor in mammals. *Respir Physiol Neurobiol*. Aug 12;141(3):317-29 (2004).

Heldmaier G, Ortmann S, Körtner G. Energy requirement of hibernating alpine marmots. In: Carey C, Florant GL, Wunder BA, Horwitz B. (Eds.), *Life in the Cold—Ecological, Physiological, and Molecular Mechanisms.* Westview Press, Boulder. pp. 175–183 (1993).

Heldmaier G and Ruf T. Body temperature and metabolic rate during natural hypothermia in endotherms. *J. Comp. Physiol. B*, 162, pp. 696–706 (1992).

Heller HC, Colliver GW, Beard J. Thermoregulation during entrance into hibernation. *Pflügers Arch*., 369, pp. 55–59 (1977).

Hester RL. Uptake of metabolites by postcapillary venules: mechanism for the control of arteriolar diameter. *Microvasc. Res*., 46, pp. 254–261(1993).

Horman S, Hussain N, Dilworth SM, Storey KB, Rider MH. Evaluation of the role of AMP-activated protein kinase and its downstream targets in mammalian hibernation. *Comp Biochem Physiol B Biochem Mol Biol.* Dec;142(4):374-82 (2005).

Houston DA, Burnstock G, Vanhoutte PM. Different P2-purinergic receptor subtypes of endothelium and smooth muscle in canine blood vessels. *J. Pharmacol Exp Ther.* May;241(2):501-6 (1987).

Humphries MM, Thomas DW, Kramer DL. The role of energy availability in mammalian hibernation: a cost-benefit approach. *Physiol Biochem Zool* 76:165–179 (2003).

Hunter AR, Jefferson LS. Role of adenosine monophosphate in regulation of metabolic pathways of perfused rat liver. *Biochem J*. Feb;111(4):537-45 (1969).

Ikeda, S. Exsanguination cooling. *Tohoku J. Exp. Med.* 87, 185–98 (1965).

Isaacks RE, Lai LL, Goldman PH, Kim CY. Studies on avian erythrocyte metabolism. XVI. Accumulation of 2,3-bisphosphoglycerate with shifts in oxygen affinity of chicken erythrocytes. *Arch Biochem Biophys.* Aug 15;257(1): 177-85 (1987).

Jackson WF. Arteriolar oxygen reactivity: where is the sensor. *Am. J. Physiol*., 253, pp. H1120–H1126 (1987).

Jagger JE, Bateman RM, Ellsworth ML, Ellis CG. Role of erythrocyte in regulating local O_2 delivery mediated by hemoglobin oxygenation. *Am. J. Physiol. Heart Circ. Physiol*., 280, pp. H2833–H2839 (2001).

Jelkmann W. Functional significance of erythrocytes. F Lang, M Föller (Eds.), *Erythrocytes*, Imperial College Press, London 1-56 (2012).

Kanaori K, Tajiri Y, Tsuneshige A, Ishigami I, Ogura T, Tajima K, Neya S, Yonetani T. T-quaternary structure of oxy human adult hemoglobin in the presence of two allosteric effectors, L35 and IHP. *Biochim. Biophys. Acta*, 1807, 1253–1261 (2011).

Kennedy C, Delbro D, Burnstock G. P2-purinoceptors mediat both vasodilation (cia the endothelium) and vasoconstriction of the isolated rat femoral artery. *Eur J Pharmacol.* Jan 2;107(2): 161-8 (1985).

Krogh A. The number and distribution of capillaries in muscles with calculations of the oxygen pressure head necessary for supplying the tissue. *J. Physiol*., 52, pp. 409–415 (1919).

Lang E, Qadri SM, Lang F. Killing me softly - suicidal erythrocyte death. *Int J Biochem Cell Biol*. Aug;44(8):1236-43 (2012).

Leibman KC, Heidelberger C. The metabolism of P32-labeled ribonucleotides in tissue slices and cell suspensions. *J Biol Chem*. Oct;216(2):823-30 (1955).

Levin BE and Sherwin RS. Peripheral glucose homeostasis: does brain insulin matter? *J. Clin. Invest.* 121, 3392–3395 (2011).

Lo HH and Schimmel PR. Interaction of human hemoglobin with adenine nucleotides. *J. Biol. Chem.* 244, 5084–6 (1969).

Lowy B and Dorfman BZ. Adenylosuccinase activity in human and rabbit erythrocyte lysates. *J. Biol. Chem.* 245, 3043–6 (1970).

Lovegrove BG, Lawes MJ, Roxburgh L. Confirmation of plesiomorphic daily torpor in mammals: the rounded-eared elephant shrew *Macroscelides proboscideus*. *J. Comp. Physiol. B*, 169, pp. 453–460 (1999).

Lundby C, Robach P, Saltin B. The evolving science of detection of “blood doping”. *Br. J. Pharmacol.* 165, 1306–15 (2012).

Mahnke DK and Sabina RL. Calcium activates erythrocyte AMP deaminase [isoform E (AMPD3)] through a protein-protein interaction between calmodulin and the N-terminal domain of the AMPD3 polypeptide. *Biochemistry* 44, 5551–9 (2005).

Mahnke-Zizelman DK and Sabina RL. Cloning of human AMP deaminase isoform E cDNAs. Evidence for a third AMPD gene exhibiting alternatively spliced 5’-exons. *J. Biol. Chem.* 267, 20866–77 (1992).

Marion DW, Leonov Y, Ginsberg M, Katz LM, Kochanek PM, Lechleuthner A, Nemoto EM, Obrist W, Safar P, Sterz F, Tisherman SA, White RJ, Xiao F, Zar H. Resuscitative hypothermia. *Crit. Care Med.* 24, S81–9 (1996).

Martin I, Vinas O, Mampel T, Iglesias R, Villarroya F. Effects of cold environment on mitochondrial genome expression in the rat—evidence for a tissue- specific increase in the liver, independent of changes in mitochondrial gene abundance. *Biochem J* 296:231–234 (1993).

Mathews WB, Nakamoto Y, Abraham EH, Scheffel U, Hilton J, Ravert HT, Tatsumi M, Rauseo PA, Traughber BJ, Salikhova AY, Dannals RF, Wahl RL. Synthesis and biodistribution of [11C]adenosine 5'-monophosphate ([11C]AMP). *Mol Imaging Biol*. May-Jun;7(3):203-8 (2005).

Meghji P, Pearson JD, Slakey LL. Kinetics of extracellular ATP hydrolysis be microvascular endothelial cells from rat heart. *Biochem J.* Jun 15;308(Pt 3):725-31 (1995).

Miki T, Matsumoto T, Zhao Z & Lee CC. p53 regulates Period2 expression and the circadian clock. *Nat. Commun.* 4, 2444 (2013).

Miseta A, Bogner P, Berényi E, Kellermayer M, Galambos C, Wheatley DN, Cameron IL. Relationship between cellular ATP, potassium, sodium and magnesium

concentrations in mammalian and avian erythrocytes. *Biochim. Biophys. Acta* 1175, 133–9 (1993).

Montalbetti N, Leal Denis MF, Pignataro OP, Kobatake E, Lazarowski ER, Schwarzbaum PJ. Homeostasis of extracellular ATP in human erythrocytes. *J Biol Chem*. Nov 4;286(44):38397-407 (2011).

Motte S, Pirotton S, Boeynaems JM. Heterogeneity of ATP receptors in aortic endothelial cells. Involvement of P2y and P2u receptors in inositol phosphate response. *Circ Res.* Mar;72(3):504-10 (1993).

Mulquiney PJ and Kuchel PW. Model of 2,3-bisphosphoglycerate metabolism in the human erythrocyte based on detailed enzyme kinetic equations: computer simulation and metabolic control analysis. *Biochem J.* Sep 15; 342 (pt 3): 597-604 (1999).

Namkung W, Thiagarajah JR, Phuan PW, Verkman AS. Inhibition of Ca2+-activated Cl- channels by gallotannins as a possible molecular basis for health benefits of red wine and green tea. *FASEB J*. Nov;24(11):4178-86 (2010).

Nasrallah CM and Horvath TL. Mitochondrial dynamics in the central regulation of metabolism. *Nature Reviews Endocrinology* 10, 650–658 (2014).

Ogasawara N, Goto H, Yamada Y, Nishigaki I, Itoh T, Hasegawa I, Park KS. Deficiency of AMP deaminase in erythrocytes. *Hum. Genet.* 75, 15–8 (1987).

Panas HN, Lynch LJ, Vallender EJ, Xie Z, Chen GL, Lynn SK, Scanlan TS, Miller GM. Normal thermoregulatory responses to 3-iodothyronamine, trace amines and amphetamine-like psycho stimulants in trace amine associated receptor 1 knockout mice. *J Neurosci Res*. Jul;88(9):1962-9 (2010).

Perutz MF. Stereochemistry of cooperative effects in haemoglobin. *Nature*, 228, 726–739 (1970).

Pittman RN and Duling BR. Oxygen sensitivity of vascular smooth muscle. *Microvasc. Res.*, 6, pp. 202–211 (1973).

Pocai A, Obici S, Schwartz GJ, Rossetti L. A brain–liver circuit regulates glucose homeostasis. *Cell Metab.* 1, 53–61 (2005).

Prenni JE, Vidal M, Olver CS. Preliminary characterization of the murine membrane reticulocyte proteome. *Blood Cells Mol Dis*. 2012 Aug 15;49(2):74-82 (2012).

Pries AR, Secomb TW, Gaehtgens P. Biophysical aspects of blood flow in the microvasculature. *Cardiovasc Res*. Oct;32(4):654-67 (1996).

Pritlove DC, Gu M, Boyd CA, Randeva HS, Vatish M. Novel placental expression of 2,3-bisphosphoglycerate mutase. *Placenta*. 27 (8): 924-7 (2006).

Revel FG, Herwig A, Garidou ML, Dardente H, Menet JS, Masson-Pévet M, Simonneaux V, Saboureau M, Pévet P. The circadian clock stops ticking during deep_hibernation in the European hamster. *Proc Natl Acad Sci USA*. Aug 21;104(34):13816-20 (2007).

Rumi E, Passamonti F, Pagano L, Ammirabile M, Arcaini L, Elena C, Flagiello A, Tedesco R, Vercellati C, Marcello AP, Pietra D, Moratti R, Cazzola M, Lazzarino M. Blood p50 evaluation enhances diagnostic definition of isolated erythrocytosis. *J Intern Med*. Feb;265(2):266-74 (2009).

Salhany JM, Elliot RS, Mizukami H. The effect of 2,3-diphosphoglycerate on the kinetics of deoxygenation of human hemoglobin. *Biochem. Biophys. Res. Commun*., 39, 1052–1057 (1970).

Schaedel ML, Waldvogel MJ, Schlenk F. The specificity of adenosine deaminase and purine nucleosidase. *J Biol Chem.* 171: 135-141 (1947).

Shoshan-Barmatz V, De Pinto V, Zweckstetter M, Raviv Z, Keinan N, Arbel N. VDAC, a multi-functional mitochondrial protein regulating cell life and death. *Mol Aspects Med*. Jun;31(3):227-85 (2010).

Siepka SM & Takahashi JS. Methods to record circadian rhythm wheel running activity in mice. *Methods Enzymol.* 393, 230–9 (2005).

Sprague RS, Stephenson AH, Ellsworth ML. Red not dead: signaling in and from erythrocytes. *Trends Endocrinol Metab*. Nov;18(9):350-5 (2007).

Sridharan M, Bowles EA, Richards JP, Krantic M, Davis KL, Dietrich KA, Stephenson AH, Ellsworth ML, Sprague RS. Prostacyclin receptor-mediated ATP release from erythrocytes requires the voltage-dependent anion channel. *Am J Physiol Heart Circ Physiol*. Feb 1;302(3):H553-9 (2012).

Stadtman ER. Allosteric regulation of enzyme activity. *Adv Enzymol Relat Areas Mol Biol.*;28:41-154 (1966).

Stein JC and Ellsworth ML. Capillary oxygen transport during severe hypoxia: role of hemoglobin oxygen affinity. *J. Appl. Physiol*., 75, pp. 1601–1607 (1993).

Stocchi V, Cucchiarini L, Magnani M, Chiarantini L, Palma P, Crescentini G. Simultaneous extraction and reverse-phase high-performance liquid chromatographic determination of adenine and pyridine nucleotides in human red blood cells. *Anal Biochem.* Apr;146(1):118-24 (1985).

Strijkstra AM, Hut RA, de Wilde MC, Stieler J, Van der Zee EA. Hippocampal synaptophysin immunoreactivity is reduced during natural hypothermia in ground squirrels. *Neurosci Lett* 344:29–32 (2003).

Strijkstra AM, Koopmans T, Bouma HR, De Boer SF, Hut RA, Boerema AS. On the dissimilarity of 5’-AMP induced hypothermia and torpor in mice. Eds. Ruf TH, Bieber C, Arnold W, Millesi E. Living in a Seasonal World. Springer-Verlag Berlin Heidelberg. 351-362 (2012).

Swoap SJ, Rathvon M, Gutilla M. AMP does not induce torpor. *Am J Physiol Regul Integr Comp Physiol.* Jul;293(1):R468-73 (2007).

Tao Z, Zhao Z, Lee CC. 5'- Adenosine monophosphate induced hypothermia reduces early stage myocardial ischemia/reperfusion injury in a mouse model. *Am J Transl Res*. Aug 15;3(4):351-61 (2011).

Tavazzi B, Amorini AM, Fazzina G, Di Pierro D, Tuttobene M, Giardina B, Lazzarino G. Oxidative stress induces impairment of human erythrocyte energy metabolism through the oxygen radical-mediated direct activation of AMP-deaminase. *J. Biol. Chem.* 276, 48083–92 (2001).

Thompson LF, Eltzschig HK, Ibla JC, Van De Wiele CJ, Resta R, Morote-Garcia JC, Colgan SP. Crucial role for ecto-5’-nucleotidase (CD73) in vascular leakage during hypoxia. *J Exp Med*. 200(11):1395-405 (2004).

Thomson LF, Ruedi JM, Glass A, Moldenhauer G, Moller P, Low MG, Klemens MR, Massaia M, Lucas AH. Production and characterization of monoclonal antibodies to the glycosyl phosphatidylinositol-anchored lymphocyte differentiation antigen ecto-5'-nucleotidase (CD73). *Tissue Antigens*. Jan;35(1):9-19 (1990).

Vignais PV. Molecular and physiological aspects of adenine nucleotide transport in mitochondria. *Biochim. Biophys. Acta* 456, 1–38 (1976).

Wang TF and Guidotti G. CD39 is an ecto-(Ca2+,Mg2+)-apyrase. *J Biol Chem*. Apr 26;271(17):9898-901 (1996).

Weber RE and Campbell KL. Temperature dependence of haemoglobin-oxygen affinity in heterothermic vertebrates: mechanisms and biological significance. *Acta Physiol (Oxf)*. Jul;202(3):549-62 (2011).

Weber RE and Lykkeboe G. Respiratory adaptations in carp blood. Influences of hypoxia, red cell phosphates, divalent cations and CO2 on hemoglobin-oxygen affinity. *J Comp Physiol* 127–137 (1978).

Williams KW and Elmquist JK. From neuroanatomy to behavior: central integration of peripheral signals regulating feeding behavior. *Nat. Neurosci.* 15,1350–1355 (2012).

Wilz M and Heldmaier G. Comparison of hibernation, estivation and daily torpor in the edible dormouse. *J. Comp. Physiol. B*, 170, pp. 511–521(2000).

Wullschleger, S., Loewith, R., Hall, M.N. TOR signaling in growth and metabolism. *Cell*, 124 (3), pp. 471–484 (2006).

Yonetani T, Kanaori K. How does hemoglobin generate such diverse functionality of physiological relevance? *Biochim Biophys Acta.* Sep;1834(9):1873-84 (2013).

Zhang B. CD73: a novel target for cancer immunotherapy. *Cancer Res.* Aug 15; 70(16): 6407-6411 (2010).

Zhao Z, Miki T, Van Oort-Jansen A, Matsumoto T, Loose DS, Lee CC. Hepatic gene expression profiling of 5'-AMP-induced hypometabolism in mice. *Physiol Genomics*. Apr 12;43(7):325-45 (2011).

Zhao Z, Van Oort A, Tao Z, O'Brien WG 3rd, Lee CC. Metabolite profiling of 5’-AMP-Induced Hypometabolism. *Metabolomics*. Feb 1;10(1):63-76 (2014).

8. Vita

William G. O'Brien III (Tre') was born in Lake Jackson, Texas on December 19, 1984 to W. Gerry O'Brien Jr. and Patricia A. Jackson. After completing his work at Elkins High School in Missouri City, Texas in 2003, he enrolled at University of Miami in Coral Gables, Florida. He received the degree of Bachelor of Science with a major in biochemistry from Miami in May, 2007. Upon graduation, he enrolled in the Master of Science program at University of Texas Graduate School of Biomedical Sciences at Houston where he studied until completion in December, 2009. He enrolled in the Ph.D. program at the same school immediately after in January, 2010.